EVALUATING THE *IN VITRO* ANTI–METASTATIC EFFECTS OF SILVER(I) PHOSPHINE COMPLEXES ON MALIGNANT BREAST CANCER CELL LINES

by

Mizán Ferreira

(2340915)

Thesis

Submitted in fulfilment of the requirements for the degree

Philosophiae Doctor

in

Molecular and Cell Biology

in the Faculty of Science, University of the Witwatersrand, Johannesburg, South Africa

Supervisor: Prof. Marianne Jacqueline Cronjé

Co-supervisor: Dr. Zelinda Engelbrecht

August 2023

Declaration

I, **Mizán Ferreira (2340915)**, am a student registered for the degree of **PhD** in the academic year **2023**.

I hereby declare the following:

• I am aware that plagiarism (the use of someone else's work without their permission and/or without acknowledging the original source) is wrong.

• I confirm that the work submitted for assessment for the above degree is my own unaided work except where explicitly indicated otherwise and acknowledged. In this context, I understand that the use of editing services is considered aided work and must be declared.

• I have not submitted this work before for any other degree or examination at this or any other University.

• The information used in the Thesis **HAS** been obtained by me while employed by, or working under the aegis of, any person or organisation other than the University.

• I have followed the required conventions in referencing the thoughts and ideas of others.

• I understand that the University of the Witwatersrand may take disciplinary action against me if there is a belief that this is not my own unaided work or that I have failed to acknowledge the source of the ideas or words in my writing.

22 day of **August 2023** signed at **Johannesburg**

Abstract

Breast cancer is the most diagnosed cancer type among females worldwide. Metastasis, the spread of cancer cells from the primary tumour and establishment of macroscopic secondary tumours, is regarded as the most dangerous characteristic of cancer cells as it is responsible for over 90% of cancer-related deaths. Globally there is a lack of drugs available to specifically target or prevent either the dissemination of cells from the primary tumour or the establishment of distant metastases. The purpose of this study was to ascertain whether a series of silver(I) phosphine complexes, which have previously been shown to display anti-cancer properties *in vitro*, are also effective as anti-metastatic compounds. The migration, invasion and adhesive abilities of two malignant breast cancer cell lines, MCF-7 and MDA-MB-231, in response to silver(I) phosphine treatment were evaluated. In addition, the colony-forming abilities of cells under both anchorage-dependent and -independent conditions were investigated. Furthermore, the effects of silver(I) phosphine treatment on the expression and activities of key metastatic proteins, matrix metalloproteinases (MMPs), were studied. Of the nine complexes evaluated, all of them showed the ability to reduce one or more metastatic steps namely cell migration, invasion through collagen towards a chemoattractant or adhesion to collagen. In addition, a selected number of complexes reduced the colony-forming abilities of MCF-7 and/or MDA-MB-231 cells in culture plates as well as in soft agar. Moreover, three of these complexes increased the *in vitro* invasion and colony formation of breast cancer cells. Further investigation into complexes showing anti-metastatic abilities revealed that, apart from one complex on MDA-MB-231 cells, anti-metastatic effects were not achieved through a reduction in MMP levels or activities. The findings presented here show the potential for silver(I) phosphine complexes to reduce the *in vitro* metastatic abilities of breast cancer cells, warranting further investigations into these complexes for their use as anti-metastatic drugs.

Dedication

TO MY MOTHER

Acknowledgements

- Prof. Marianne J. Cronjé and Dr. Zelinda Engelbrecht for their supervision and support throughout the duration of this study.

- The University of the Witwatersrand, Faculty of Science and School of Molecular and Cell Biology for the opportunity to complete the study.

- University of the Witwatersrand and the PV Tobias Educational Bursary for financial support.

- University of Johannesburg, Department of Chemical Sciences for supply and chemical characterisation of the silver(I) phosphine complexes.

- Dr. Vanessa Meyer and Dr. Eloise van der Merwe for support and technical assistance.

- Dr. Kim Roberts and Alisha Badal for their support and assistance.

- My family for emotional support

- All the researchers that participated in the development of the silver(I) phosphine complexes as a potential anti-cancer treatment without whom the development of this project would not have been possible.

Table of Contents

List of Figures

List of Tables

List of symbols

ºC – temperature in degrees Celsius

µg - microgram

µg/mL – microgram per millilitre

µl – microliter

µm – micrometre

µM – micromolar

List of abbreviations

1º – primary
2º – secondary
3D-CRT – three dimensional conformal radiotherapy

Ab - antibody
ADAMTS-4 – metalloproteinase with thrombospondinmotifs-4
AKT – protein kinase B
ALS – amyotrophic lateral sclerosis
AR – androgen receptor
ATCC – American Type Culture Collection
ATM – ataxia-telangiesctasia mutated
ATR – attenuated total reflectance

BC – breast cancer
BCS – breast-conserving surgery
BISSA – Breast Imaging Society of South Africa
BRAC1/2 – breast cancer gene 1 or 2
BRIP1 – gene encoding *BRAC1* interacting protein 1
BSA – bovine serum albumin

CAF – cancer associated fibroblast
CANSA – Cancer Association of South Africa
CDDP – *cis*-diamminedichloroplatinum II / cisplatin
CDH1 – gene encoding cadherin-1
CDH1 – E-cadherin
CDK – cyclin-dependent kinase
CHEK2 – checkpoint kinase 2
CLDN3 – claudin-3
COPD – chronic obstructive pulmonary disease
CSC – cancer stem cell
CTC – circulating tumour cell
CTLA-4 – cytotoxic T-lymphocyte associated protein-4
CV – crystal violet
CXCR2 – gene encoding C-X-C motif chemokine receptor 2
CXCR4 – C-X-C motif chemokine receptor 4

DDT - dichlorodiphenyltrichloroethane
DES – diethylstilbestrol
DMEM – Dulbecco's Minimal Essential Medium
DMS - dimethylsulfide
DMSO – dimethyl sulfoxide
DMSO-S – sulphur-bonded DMSO
DNA – deoxyribonucleic acid
DTC – disseminated tumour cell

ECM – extracellular matrix
EGFR – epidermal growth factor receptor
EMT – epithelial-to-mesenchymal transition
ER – estrogen receptor

FAK – focal adhesion kinase
FCS – foetal calf serum
FGF – fibroblast growth factor
FITC – fluorescein isothiocyanate
FT-IR – Fourier transform infrared

GLOBOCAN – Global Cancer Observatory
GLUT1 – glucose transporter 1

HBSS – Hanks Balanced Salt Solution
HER2 – human epidermal growth factor receptor 2
HIF – hypoxia inducible factor
HMEC – human mammary epithelial cells
HMSC – human bone marrow derived mesenchymal stem cells
HRP – horseradish peroxidase
HRT – hormone replacement therapy

IC_{50} – 50% inhibitory concentration
ICAM-1 – intercellular adhesion molecule-1
IGF-BP-1 – insulin-like growth factor-binding protein-1
IgG – immunoglobulin G
IMRT – intensity-modulated radiotherapy
IORT – intraoperative radiation therapy

---

kDa – kilodaltons
KP1019 – (indazolium *trans*-[tetrachlorobis(1*H*-indazole)ruthenate(III)])
KP1339 – sodium *trans*-[tetrachloridobis(1*H*-indazole)ruthenate(III)])

LAFCA – low adherence flow cytometry analysis
LARA – low adherence and re-attachment assay
LCIS – lobular carcinoma *in situ*
LOX – lysyl oxidase

MAPK – mitogen-activated protein kinase
mBC – metastatic breast cancer
MCT1 – mono-carboxylate transporter-1
MET – mesenchymal-to-epithelial transition
MMPs – matrix metalloproteinases
MRI – magnetic resonance imaging
MT-MMP – membrane type MMP
mTOR – mammalian target of rapamycin

NAMI-A – [imidazoleH][*trans*-RuCl4(dmso-S)(imidazole)]
NF-κB – nuclear factor kappa B
NSAIDs – non-steroidal anti-inflammatory drugs

PAH – polycyclic aromatic hydrocarbons
PALB2 – gene encoding partner and localiser of *BRCA2*
PARP – polyadenosine diphosphate-ribose polymerase
PET – polyester
PBS – phosphate buffered saline
PCB – polychlorinated biphenyl
PD-1 – programmed cell death protein-1
PD-L1 – programmed death-ligand-1
PET – polyethylene terephthalate
PI – propidium iodide
PI3k – phosphatidylinositol-3-kinase
PMA – phorbol 12-myristate 13-acetate
PR – progesterone receptor
PTEN – phosphatase and tensin homolog deleted on chromosome 10
PVDF – polyvinylidene difluoride
Pyk2 – proline-rich tyrosine kinase 2

RAPTA-C - (Ru(η6-p-cymene)Cl2(1,3,5-triaza-7-phosphaadamantane)]
RIPA - radioimmunoprecipitation assay
ROS – reactive oxygen species
RSSA – Radiological Society of South Africa
Rt – room temperature

SA – South Africa
SEM – standard error of the mean
SERM – selective estrogen receptor modulator
SFM – serum-free media
Slug – SNAI2
SM-TBS – skimmed milk in TBS
SNAI1 – snail family transcriptional repressor-1
Src – non-receptor tyrosine kinase
STK11 – gene encoding serine/threonine kinase 11

TAMs – tumour associated macrophages
TBS – tris buffered saline
TBS-T – TBS containing tween-20
TIMPs – tissue inhibitors of metalloproteinases
TLD1433 - [Ru(4,4′-dimethyl-2,2′-bipyridine)2(2-(2′,2″:5″,2‴-terthiophene)-imidazol[4,5f])]Cl_2
TNBC – triple-negative breast cancer
TNF – tumour necrosis factor
TP53 – gene encoding p53 protein
TrkB – tropomyosin receptor kinase B
TWIST – twist-related protein

UC – untreated control
UJ – University of Johannesburg
uPA – urokinase plasminogen activator
uPAR – uPA receptor

VC – vehicle control
VCAM – vascular cell adhesion molecule-1
VEGF – vascular endothelial growth factor

WNT2 – wingless-type MMTV integration site family member 2

---

x%M – DMEM supplemented with x% FCS (x=5 or 10)

ZEB – zinc finger E-box-binding homeobox-1

Introduction

Not only is cancer one of the primary causes of death worldwide but living with cancer has a tremendous impact on the quality of life and imposes serious financial and emotional constraints not only on those directly affected but also on their loved ones (Lukasiewicz *et al*., 2021). Globally and in South Africa, breast cancer (BC) is the most diagnosed cancer and one of the leading causes of cancer-related deaths among females (Cairncross *et al*., 2021; Sung *et al*., 2021).

Metastasis is often regarded as the most dangerous aspect of cancer since more than 90% of deaths owing to cancer are due to metastasis of the primary tumour (Anderson *et al*., 2019). Current chemotherapeutic strategies are mostly focussed on decreasing the size of the primary tumour; however, these treatment options are not adequate to prevent or treat metastases. Consequently, there is a lack of drugs that specifically target metastasis, creating an enormous market for research into these drugs (Anderson *et al*., 2019; Gandalovičová *et al*., 2017; Weber, 2013).

A novel class of silver(I) phosphine complexes have gained some recognition over the past decade for their ability to selectively induce apoptosis in several cancer types *in vitro* while causing minimal damage to non-malignant cells (Engelbrecht *et al*., 2018; Ferreira *et al*., 2015).

The aim of this study was to assess the feasibility of utilizing silver(I) phosphine complexes as anti-metastatic drugs for the treatment of metastatic BC. Silver(I) phosphine complexes were assessed on their ability to 1) prevent the dissemination of cells from the primary tumour by reducing cell migration, invasion and adhesion and 2) prevent the formation of secondary metastases through reducing colony formation. These assessments gave rise to a select few complexes with the ability to reduce more than one key step of metastasis in either minimally invasive MCF-7 or highly invasive MDA-MB-231 BC cells *in vitro*. Accordingly, an attempt was made to establish the anti-metastatic mechanism of action of these promising complexes by studying the expression and activity of matrix metalloproteinases (MMPs). Only one of these complexes seemingly exerts its effects by reducing gelatinase (MMP-2) and collagenase (MMP-8) activity in MDA-MB-231 cells, while the remaining complexes' mechanism of action is unclear. For these complexes, additional studies are required and are beyond the scope of this study.

It is important to note that metastatic cells possess a distinct set of characteristics that distinguish them from cells making up the primary tumour, necessitating unique treatment strategies for preventing or eliminating these cells (Welch and Hurst, 2019). Anti-metastatic drug development is therefore a crucial aspect of cancer research requiring more attention. Anti-metastatic drugs with low systemic toxicity could potentially form a part of future cancer therapy strategies where they may be used alongside current anti-cancer drugs.

The findings presented here are arguably limited to the abilities of a selected few silver(I) phosphine complexes to decrease the metastatic potential of BC cells *in vitro*, carried out on cell culture models of BC. On the other hand, it does introduce a new class of potential inhibitors of metastasis that seem to work independently of the commonly targeted MMPs. It also proposes an additional use for silver(I) phosphine complexes, not just as anti-cancer agents but also as anti-metastatic agents at low concentrations that deserve further investigation.

Chapter 1: Literature review

1.1 Cancer, a worldwide burden

1.1.1 Cancer statistics

Being one of the primary causes of death, cancer, the uncontrollable production of cells (Tynga *et al.*, 2013), is a global burden that continues to rise in cases each year (Lukasiewicz *et al.*, 2021). Cancer as a disease is recognised by a rapid and overwhelming proliferation of atypical cells capable of forming a mass, which leads to the disruption of organ and tissue functioning (Tynga *et al.*, 2013). Along with its ability to spread to distant sites within the organism, it can lead to systemic dysfunction and ultimately death (Lukasiewicz *et al.*, 2021). Apart from its effect on the physical health of an individual, cancer can also have detrimental repercussions on the mental and emotional state of those diagnosed with cancer as well as their friends and family members, not to mention the financial constraints (Feng *et al.*, 2018; Lukasiewicz *et al.*, 2021). Multiple different types of cancer exist (carcinomas, sarcomas, lymphomas etc.) affecting almost every known organ or tissue in the human body, each one having different characteristics and responding differently to available therapies (Lucaciu *et al.*, 2022). This heterogeneity not only between different types of cancers but also within the same type of cancer in different individuals as well as key differences between cells of the same tumour in one individual creates, even today, the need for the development of novel anti-cancer drugs with fewer side-effects and better selectivity (Lucaciu *et al.*, 2022).

According to statistics reported by GLOBOCAN for 2020, the number of newly diagnosed cases of cancer was just over 19 million, while the number of cancer-related deaths was just below 10 million (Sung *et al.*, 2021). Globally, the top five most diagnosed cancers are cancer of the female breast, lung, colon and rectum, prostate, and stomach. The top five causes of cancer-related deaths in 2020 worldwide were lung, colorectal, liver, stomach and female BC (Sung *et al.*, 2021). It was reported in 2020 that in South Africa (SA) the number of newly diagnosed cases of cancer was 110 000, while the number of cancer-related deaths was over 56 000 (Cairncross *et al.*, 2021). The top five most diagnosed cancers in SA in 2020 were cancers of the breast, prostate, cervix, lung and lastly the colon and rectum. Furthermore, the top five causes of cancer-related deaths in SA were lung, cervical and uterine, breast, prostate, and colorectal cancer (Cairncross *et al.*, 2021).

Predictions made for 2040 state that the number of newly diagnosed cancer cases will increase to over 28 million and 175 000 cases globally and in SA, respectively. Similarly, a rise in cancer-related deaths in 2040 is predicted to be up to 94 000 deaths in SA alone (Cairncross *et al.*, 2021; Sung *et al.*, 2021). Interestingly, it is predicted that the COVID-19 pandemic will increase the number of cancer-related deaths and diagnoses at more advanced stages which will only be noticeable in a few years. This is due to the immense burden the pandemic had on the global healthcare systems, causing a decrease in cancer screening programmes as well as in the access and distribution of treatment (Sung *et al.*, 2021).

Possibly what contributes to the difficulty in the eradication of cancer is that it has the ability to use our body's regular mechanisms crucial for cell survival, to its advantage to fuel its progression (Welch and Hurst, 2019). This then creates the problem of inhibiting or eradicating these mechanisms in malignant cells without adversely affecting normal cell functioning.

1.1.2 Hallmarks of cancer

Cells that have the potential to develop into cancer contain certain characteristics that distinguish them from normal functioning cells. The eight characteristics, most commonly known as the "Hallmarks of Cancer", defined in Hanahan and Weinberg (2000), Hanahan and Weinberg (2011) and Hanahan (2022) are:

i. *Independence on the environment for the production of growth-stimulating factors*

   In general, cells possess intricate intracellular signalling pathways which are activated by the binding of growth factors from the extracellular matrix (ECM) to transmembrane receptors, making them dependent on the environment to stimulate proliferation. In contrast, the ability to proliferate independently of these signals can be used by cells during cancer development. This can be achieved via the self-production of growth factors that can activate proliferation or stimulate the additional release of other growth-inducing factors from non-malignant cells in their immediate environment. Modification of the intracellular pathways or growth factor receptors making them more sensitive to extracellular signals may also contribute to an increase in proliferation (Hanahan and Weinberg, 2000; Leber and Efferth, 2009).

ii. *The capacity to undergo an infinite number of divisions*

With each cell division, there is a shortening of the caps of chromosome telomeres, resulting in the onset of genetic instability thereby limiting the number of cell divisions normal cells can undergo. By activating telomerase proteins or using a mechanism referred to as "alternative lengthening of telomeres", cancer cells can avoid this genetic instability allowing them to undergo an infinite number of divisions contributing to the development of cancer (Hanahan and Weinberg, 2000; Hanahan and Weinberg, 2011; Leber and Efferth, 2009).

iii. *Not responding to surrounding anti-proliferative signals*

Another factor contributing to controlled cell growth is the existence of anti-growth signalling molecules in a cell's environment to which cells respond by being driven into a post-mitotic or quiescent state. Cancer cells however can disrupt key intracellular signalling pathways that react to these anti-proliferative signals so that continued proliferation is made possible (Hanahan and Weinberg, 2000; Hanahan and Weinberg, 2011).

iv. *Circumvention of cell death*

There exist several checkpoints throughout the cell cycle that may, whenever a dysfunction or abnormality is encountered, induce apoptotic cell death. Mutations of these regulatory genes of which *TP53* is the most common, allows abnormal cells to avoid cell death and continue with proliferation, further increasing the number of cells in possession of such a mutation (Hanahan and Weinberg, 2000; Hanahan and Weinberg, 2011; Leber and Efferth, 2009).

v. *Induction of angiogenesis or access of vasculature to support tumour growth*

In order to sustain growth, especially uninhibited growth, cells need constant access to oxygen and nutrients while metabolic by-products are transported away. As proliferation continues and results in the formation of a tumour mass, the cells at the centre of the mass are farther away from essential vasculature to perform these functions. Therefore, cancer cells have developed the ability to produce certain factors including vascular endothelial growth factor (VEGF) or fibroblast growth factor (FGF) that encourage the production of blood vessels (pro-angiogenic factors) while

preventing the production of inhibitors involved in vascular formation (Hanahan and Weinberg, 2000; Hanahan and Weinberg, 2011; Leber and Efferth, 2009).

vi. The ability to metastasize

Often regarded as the most detrimental characteristic is the ability of cancer cells to escape their present environment, travel through the circulatory system and colonise secondary locations. This is achieved through an intricate process termed the metastatic cascade (Hanahan and Weinberg, 2000; Hanahan and Weinberg, 2011).

vii. An alteration in cellular energy metabolism

In order to fuel the multitude of divisions enabled by the abovementioned characteristics, cancer cells can alter metabolic pathways to use to their advantage. Normally within a cell, in order to produce energy, glucose is broken down to pyruvate in the cytoplasm, through glycolysis; where after carbon dioxide is produced in the mitochondria from the pyruvate along with metabolic energy. In a process referred to as the Warburg effect, owing to Otto Warburg, the first person to observe such a change in cancer cells, malignant cells may, even in the presence of adequate amounts of oxygen, rely mainly on glycolysis for energy production (Hanahan and Weinberg, 2011). This avoidance of the mitochondrial oxidative phosphorylation of pyruvate which normally produces the largest amount of energy might seem counterproductive. This however can be explained in part by the suggestion that it enables cancer cells to divert intermediate metabolites to other pathways responsible for synthesising proteins and organelles needed for the formation of additional cells (Hanahan and Weinberg, 2011). The Warburg effect is achieved mainly by an up-regulation of enzymes participating in glycolysis as well as glucose transporters including GLUT1, thus explaining the increased consumption of glucose observed in multiple cancer types. This increase in glycolysis, which produces many waste products in the form of lactate, may then further be exploited by the observation that some tumours also consist of cells that increases lactate consumption for energy production through the citric acid cycle creating a symbiotic mechanism fuelling tumour growth (Hanahan and Weinberg, 2011).

viii. Avoiding destruction from the immune system

The argument that cancerous cells must have an ability to somehow evade the natural surveillance mechanisms of the immune system to avoid either immune detection or destruction has been postulated through an increase in cancer cases in those individuals with a compromised immune system, whether innate or medically induced such as in the case of organ transplant recipients. This mostly holds true for types of cancers that are virally induced where the immune system functions in eradicating virally infected cells but have also been found in other cancer types where the immune function does participate to some degree in preventing tumour progression (Hanahan and Weinberg, 2011).

In addition to the eight core Hallmarks, two enabling characteristics that help with the procurement of the core hallmarks were described (Hanahan and Weinberg, 2011). These were the instability of the genome and tumour-promoting inflammation. Genomic instability involves the occurrence of mutations and chromosomal rearrangement, while tumour-promoting inflammation refers to the involvement of the immune system in creating an inflammatory state in the tumour environment that may promote tumour growth (Hanahan and Weinberg, 2011). In the latest version of these articles another four emerging hallmarks and enabling characteristics are presented. This includes 1) the unlocking of phenotypic plasticity to enable limitless proliferation, a feature that cells lose during differentiation, 2) the attaining of non-mutational epigenetic changes that may facilitate in the acquisition of hallmarks 3) characteristics of the tumour microbiome which can have an effect on the development of cancer, metastasis and response to therapy, and 4) the tumour phenotypic promotion of cell senescence (Hanahan, 2022).

1.2 Breast cancer

1.2.1 Overview

As a serious health challenge for women (and men on occasion) across the whole world, breast cancer (BC) is a growth that starts in the lobules, ducts or the surrounding tissues of the breast (Aznag *et al.*, 2018). Frequently these growths have the potential to spread to the skin, the chest wall, as well as the surrounding lymph nodes. Most BCs are carcinomas (originating from epithelial tissue) while sarcomas (originating from connective tissue) are more rarely found (Feng *et al.*, 2018). BC development is strongly affected by the tumour stroma and the presence of macrophages (Sun *et al.*, 2017).

In 2020, BC was the most diagnosed cancer worldwide, making up about 11.7% (approximately 2.3 million) of all newly diagnosed cancer types. It is also the number one diagnosed cancer type among females (24.5% of total cases) as well as the leading cause of cancer-related deaths amongst females, comprising about 15.5% of total cases. Incidence rates of BC are higher in developed countries; however, the number of deaths due to BC is higher in low- and middle-income countries such as Africa (Sung *et al.*, 2021). In SA, BC was the most diagnosed cancer in 2020 while it was ranked the third most common cause of cancer-related deaths in SA in 2020 (Cairncross *et al.*, 2021). Although BC mostly occurs in females it can also on occasion affect males. Even though male BC represents < 1% of total BC cases, it should not be overlooked as it may be at a more advanced stage when first diagnosed (Lukasiewicz *et al.*, 2021).

As with other types of cancer, early detection of BC is imperative as it can increase the chances of survival and recovery. Screening tools for BC include ultrasound, mammograms and Magnetic Resonance Imaging (MRI) (Bhushan *et al.*, 2021). The vast differences in access to affordable medical care between developed and developing countries contribute to the increase in BC mortality in developing countries. Despite improvements in the costs of genome sequencing as a preventative tool in the fight against BC, this is still not a viable option for poorer countries with technological limitations. It is therefore crucial to educate women worldwide, but especially in middle and low-income countries, on techniques to self-examine their breasts and the importance of early detection (Sun *et al.*, 2017). Currently there is no national screening program for BC in SA (Lipschitz, 2018) or sub-Saharan Africa (Martei *et al.*, 2022). Despite the high incidence of BC in SA, BC screening through mammography is relatively low and highly dependent on sociodemographic factors, lifestyle factors and the presence of chronic diseases (Phaswana-Mafuya and Peltzer, 2018). In SA, recommendations from the Radiological Society of South Africa (RSSA) and the Breast Imaging Society of South Africa (BISSA) are annual mammography screening for women from the age of 40 along with regular self-examination and clinical examination. The Cancer Association of South Africa (CANSA) in turn recommends an annual mammogram for women between the age of 40 and 54, with biennial mammograms for women aged 55 and above (Lipschitz, 2018).

1.2.2 BC subtypes and risk factors

Subdivided based on their mRNA expression profiles, there are four main subtypes of BC: luminal A, luminal B, human epidermal growth factor receptor 2 (HER2)-enriched and basal-

like with a fifth subtype, claudin-low BC, which was added in 2007 (Lukasiewicz *et al.*, 2021). This subdivision is crucial in the clinical setting since different subtypes respond differently to various therapies (Dai *et al.*, 2016). The luminal A subtype consists of tumours that contain the estrogen receptor (ER) and/or the progesterone receptor (PR) without any HER2 (Lukasiewicz *et al.*, 2021). These tumours are often associated with the best prognosis of all the subtypes since they are low-grade tumours with a lower proliferation rate (Lukasiewicz *et al.*, 2021) due to low levels of the cellular proliferation marker Ki67 (Feng *et al.*, 2018) (also used as a biomarker for BC prognosis) (Dai *et al.*, 2016; Lukasiewicz *et al.*, 2021). The luminal B subtype, in contrast, is characterised by the presence of ER and HER2 without any PR and high levels of Ki67 (Feng *et al.*, 2018; Lukasiewicz *et al.*, 2021). Compared to subtype A, subtype B is more aggressive with a worse prognosis (Lukasiewicz *et al.*, 2021). Together luminal A and B subtypes make up around 70% of all BC cases (Lukasiewicz *et al.*, 2021). The third subtype consists of tumours with high levels of HER2 with a lack of ER and PR. These tumours are even more aggressive than the luminal B subtype and make up between 10% and 15% of BC subtypes (Lukasiewicz *et al.*, 2021). The fourth type, basal-like BC, makes up about 20% of BC subtypes and is more commonly referred to as triple-negative BC (TNBC) as it does not contain ER, PR or HER2. These tumours are usually very aggressive and are associated with poorer prognoses (Feng *et al.*, 2018; Lukasiewicz *et al.*, 2021). While also recognized by the lack of ER, PR and HER2, the most recently classified claudin-low BC subtype tumours present with low levels of genes associated with cell-cell adhesion (particularly claudin 3, 4 and 7 as well as E-cadherin and occludin) with very high levels of genes related to epithelial-to-mesenchymal transition (EMT; discussed in detail in section 1.3.3.1). This subtype makes up around 7% to 14% of BC cases (Lukasiewicz *et al.*, 2021).

There are several risk factors related to the development of BC. These include:

a. Gender: Females are 100 times more likely to develop BC compared to men. This may be in part to the fact that female breast tissue is particularly sensitive to variations in estrogen and progesterone levels (Feng *et al.*, 2018; Lukasiewicz *et al.*, 2021).

b. Age: Older women have a higher chance of developing BC. Around 80% of BC sufferers are over the age of 50 while more than 40% of cases are found in females over the age of 65. Interestingly, an association was found between BC subtype and age where TNBC was more common in females younger than 40, while individuals

older than 70 were most frequently diagnosed with luminal A type BC (Lukasiewicz *et al.*, 2021).

c. Family history: Females with first-degree relatives (parent, sibling or child) diagnosed with not only BC but ovarian cancer as well have an increased risk of developing BC themselves. This also holds true for women with a brother or father diagnosed with BC (Feng *et al.*, 2018; Lukasiewicz *et al.*, 2021).

d. Genetics: Apart from the two most well-known genes, breast cancer-associated gene 1 and 2 (*BRCA1* and *BRCA2*), mutations in quite a few other genes are also linked to a higher risk of developing BC to various extents. A summary of these genes is presented in Table 1.1. Mutations in the *BRCA1* and *BRCA2* genes are associated with a lifetime risk of 55-65% and 45%, of developing BC, respectively. In addition, a mutation in either of these two genes increases the chance of developing BC at a younger age, increases the possibility of developing ovarian cancer and developing cancer in both breasts compared to one (Aznag *et al.*, 2018; Feng *et al.*, 2018; Lukasiewicz *et al.*, 2021; Sun *et al.*, 2017).

e. Race and ethnicity: Even though BC is more common among white non-Hispanic women, the number of BC associated deaths are higher among black women of any age. Likewise, the incidence of TNBC is also higher among black females (Feng *et al.*, 2018; Lukasiewicz *et al.*, 2021).

f. Reproductive factors: As mentioned above, circulating levels of hormones can affect the possibility of developing BC in females. Aspects that may lower the risk of developing BC include pregnancy at a younger age (early twenties), an increased number of pregnancies longer than 34 weeks, the occurrence of preeclampsia during pregnancy and breastfeeding for a longer period. Reaching menopause at a younger age may also decrease this risk. In contrast, the occurrence of the first menstrual cycle at an early age (younger than 12), not having any children, not breastfeeding or having the first child after age 30 is correlated to an increased risk of BC development. Receiving hormone replacement therapy (HRT) after the onset of menopause may also increase the probability of developing BC (Feng *et al.*, 2018; Lukasiewicz *et al.*, 2021).

g. Breast tissue density and history of breast disease or radiation therapy: An increase in the density of female breast tissue as well as a history of non-cancerous diseases of the breast (including fibrosis, cysts, hyperplasia, papillomatosis and mastitis) can increase the risk of developing BC. In addition, a history of BC in one breast leads to

a higher chance of developing cancer in the other breast as well as a different type of cancer in the same breast. As with many other types of cancer, previous exposure to radiation treatment (in the chest area specifically) can also increase the possibility of developing BC in future. This is especially dangerous if radiation exposure occurred at a younger age while the breasts were not yet fully developed. Lobular carcinoma *in situ* (LCIS), a benign form of BC, may also transform into an invasive type of cancer if left untreated (Feng *et al.*, 2018; Lukasiewicz *et al.*, 2021).

Table 1.1 Genes commonly linked to a higher risk of BC development along with the % risk of each gene associated with developing BC (adapted from Lukasiewicz *et al.*, 2021).

Gene	Risk associated with BC development
High penetrance	
CDH1	63-83%
PTEN	50-85%
BRCA2	50-85%
BRCA1	45-87%
STK11	32-54%
TP53	20-40% (can be up to 85%)
Moderate penetrance	
PALB2	33-58%
ATM	20-60%
CHEK2	20-25%
BRIP1	unknown
XRCC2	unknown

Besides the abovementioned risk factors, there are also multiple environmental and lifestyle choices related to an increase in the risk of developing BC. These include: 1) taking several drugs including some antidepressants, antibiotics (especially tetracyclines), high blood pressure medication (Lukasiewicz *et al.*, 2021), oral contraceptives (Aznag *et al.*, 2018), statins, nonsteroidal anti-inflammatory drugs (NSAIDs) as well as HRT (Lukasiewicz *et al.*, 2021), 2) high intake of alcohol (Lukasiewicz *et al.*, 2021), 3) smoking (Lukasiewicz *et al.*, 2021), 4) a diet rich in processed foods along with very little physical activity (Lukasiewicz

et al., 2021), 5) inadequate intake of vitamins (an increased level of vitamin D metabolites has been linked to a reduced risk of BC development) (Lukasiewicz *et al.*, 2021) and 6) obesity (Lukasiewicz *et al.*, 2021). Prolonged exposure to some chemicals including diethylstilbestrol (DES), dichlorodiphenyltrichloroethane (DDT), polychlorinated biphenyl (PCB) and polycyclic aromatic hydrocarbons (PAH) could also increase the risk of developing BC by bringing on epigenetic changes (Lukasiewicz *et al.*, 2021). Another interesting and recently discovered risk factor is exposure to artificial light at night. Although this still requires further investigation this effect has been predicted to be caused by epigenetic changes as a result of a disturbance in the melatonin cycle (Lukasiewicz *et al.*, 2021).

1.2.3 BC treatment

There are several treatment options available for BC, the choice of which would depend on an assortment of factors such as the subtype of BC and the presence or extent of infiltration into the surrounding tissue, but also on the overall health and financial capability of the patient.

i. Surgery

Surgical removal of a tumour present in the breast can either be through breast-conserving surgery (BCS) or a single or double mastectomy depending on the tumour classification. During BCS, the tumour as well as surrounding affected areas is removed while keeping the remaining breast tissue intact. Although this is associated with fewer complications after surgery, an overall improved cosmetic outcome and a reduced psychological burden; this does not exclude the possibility of requiring a mastectomy in future. A mastectomy involves the complete removal of one or both breasts which may be followed by breast reconstruction surgery (Lukasiewicz *et al.*, 2021).

ii. Radiation

Radiotherapy can either be administered as adjuvant therapy following chemotherapy or surgery to eradicate any remaining cancerous cells and reduce the risk of recurrence. It can also be used in cases where surgical removal of the tumour is not an option or in cases where metastasis has already occurred. The options available are intraoperative radiation therapy (IORT), three-dimensional conformal radiotherapy (3D-CRT), intensity-modulated radiotherapy (IMRT) and brachytherapy (Lukasiewicz *et al.*, 2021).

iii. Chemotherapy

Chemotherapy can either be administered on its own or in combination with surgery (neoadjuvant or adjuvant). Currently available chemotherapeutic options include a combination of drugs including 5-fluorouracil, carboplatin, cyclophosphamide, docetaxel, doxorubicin, epirubicin and paclitaxel, the choice of which would depend on the molecular subtype of BC (Lukasiewicz *et al.*, 2021). The choice of chemotherapeutic agent also depends on patient preferences and their financial situation. Some patients would prefer a regimen associated with fewer side-effects but a lower chance of success while some might prefer oral over intravenous treatments (Hanna and Mayden, 2021).

iv. Hormone therapy

Dependent on the presence of the ER, hormone therapy is only effective in patients with subtype luminal A or B. These treatments can be divided into two categories: 1) drugs that lower the ability of BC cells to respond to circulating estrogen levels by either blocking the ER or by degradation of the ERs or 2) drugs, that function by decreasing circulating levels of estrogen by inhibition of estrogen synthesis through aromatase (Lukasiewicz *et al.*, 2021; Sun *et al.*, 2017).

v. Biologic therapy and immunotherapy

Biologic therapy or monoclonal antibodies may be useful for the treatment of luminal tumour subtypes and TNBC; however, it is more commonly used for the treatment of HER2-positive tumour subtypes. Another option with abundant potential is immunotherapy, targeting the mechanisms that cancer cells use to evade destruction by the immune system (Lukasiewicz *et al.*, 2021; Sun *et al*., 2017).

Apart from the cosmetic and psychological side-effects of the surgical removal of breast/s, other available treatment options for BC are also associated with significant side-effects (Lukasiewicz *et al.*, 2021). Radiation therapy for instance can lead to skin irritation and darkening of the skin exposed to the radiation as well as lymphoedema (Lukasiewicz *et al.*, 2021). Tamoxifen, a selective estrogen receptor modulator (SERM) that act by blocking ERs (Lukasiewicz *et al.*, 2021), can increase the chance of developing deep-vein thrombosis, pulmonary embolisms, stroke and endometrial cancer (Sun *et al.*, 2017). Aromatase inhibitors can increase the risk of developing osteoporosis, carpal tunnel syndrome, lead to joint pain

and may interfere with the metabolism of lipids (Sun *et al.*, 2017). In turn, monoclonal antibody based treatments (biologic therapy) could result in a reduction of the left ventricular ejection fraction and congestive heart failure as seen with the use of trastuzumab (Herceptin) (Sun *et al.*, 2017). In addition, febrile neutropenia (Sun *et al.*, 2017), a decrease in neutrophil count along with fever (Zimmer and Freifeld, 2019) and diarrhoea were reported side-effects of another example of a biologic therapy, pertuzumab (Perjeta) (Sun *et al.*, 2017).

Other more generally experienced side-effects associated with anti-cancer therapies include nausea and vomiting, diarrhoea, loss of appetite, fatigue, weight loss, depression, anxiety and general malaise (Lukasiewicz *et al.*, 2021). For this reason, the decision between living with the effects of cancer versus the negative effects of the treatments can sometimes be a difficult one to make putting the world in dire need of the development of anti-cancer drugs with less systemic side-effects.

1.3 Cancer metastasis

1.3.1 Overview

Metastatic disease of cancer is defined as the outcome of an intricate series of events where cancerous cells detach from a malignant growth, travel through the circulation to a distant site and succeed in establishing a subsequent growth in a new environment in the body. Metastasis is believed to be accountable for > 90% of cancer-associated deaths in addition to being one of the primary causes of cancer therapy failure (Chitty *et al.*, 2018; Fares, *et al.*, 2020). The term metastasis originates from the Greek words “meta” which pertain to a change or the outcome of a change and “stasis” referring to a state of equilibrium or balance. Importantly, the term thus refers to both the process of the spread of cancer and to the consequence of the process (Welch and Hurst, 2019).

The process of cancer metastasis is by no means a straightforward set of events and many aspects of the process remain unknown. What adds to this complexity is the fact that the process not only depends on the characteristics of the cells themselves but is also affected constantly by the microenvironment that the cell finds itself in at any time. These include interactions with the non-cancerous cells, ECM and the presence of growth factors in the environment (Chitty *et al.*, 2018; Fares, *et al.*, 2020; Hapach *et al.*, 2019). From a cells’ perspective, metastasis is not an easy process as multiple hurdles are encountered along the way, including being able to withstand the pressure of the fluid in the vasculature, avoiding

detection and destruction from the immune system and constantly needing to adapt to a new environment as it travels through the body to where it eventually settles and establishes a new tumour. Facing these challenges along the way, results in less cells in each step that can carry out successful repopulation of a secondary site (Chitty *et al.*, 2018; Fares, *et al.*, 2020; Hapach *et al.*, 2019).

1.3.2 The five stages of the metastatic cascade

Although all the finer details and mechanisms have not yet been fully elucidated, the metastatic process can be divided into five major stages (summarised in Figure 1.1): 1) local migration and invasion, 2) entry into blood or lymph vessels through intravasation, 3) moving through the circulation, 4) arresting at a secondary site and exiting the circulation through extravasation and finally 5) colonising the secondary site (Chitty *et al.*, 2018).

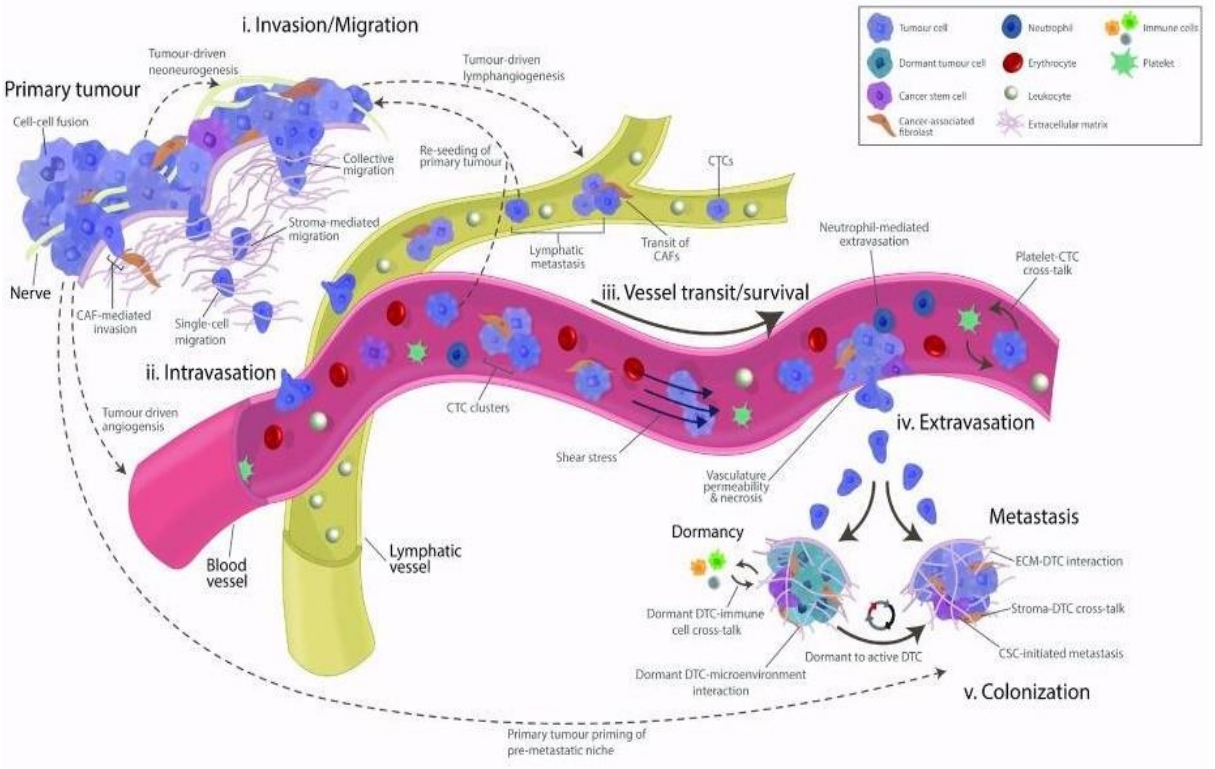

Figure 1.1 An overview of the five stages of the metastatic cascade. Abbreviations: CAF – cancer associated fibroblast, CSC – cancer stem cell, CTC – circulating tumour cell, DTC – disseminated tumour cell. Image taken from Chitty *et al.* (2018) under the terms of the Creative Commons Attribution Licence (http://creativecommons.org/licenses/).

i. Stage I – Local migration and invasion

In order to escape from their current environment, cancer cells must make use of mechanisms that allow for their movement, adhesion and degradation. Cells would

need to detach from their surroundings by severing current cell-cell and cell-ECM connections, acquire the ability to move either as single cells or form new cell-cell contacts to be able to move collectively, and activate the production and secretion of factors capable of degrading the basement membrane and remodelling the ECM (Chitty *et al.*, 2018; Hapach *et al.*, 2019; Riggio *et al.*, 2021).

ii. Stage II – Intravasation

Intravasation refers to the abilities of cancer cells to enter the circulation by traversing the endothelial layer of vessels. This is done by partially degrading the basement membrane of endothelial cells so that tumour cells can wedge themselves in between the endothelial cells. Tumour angiogenesis is also believed to assist in the entry of tumour cells into circulation since tumour vessels are more permeable than regular blood vessels. In addition, the secretion of VEGF by cancer cells can increase the permeability of blood vessels. Cancer cells may also enter lymphatic vessels either through direct intravasation or through the connections between the blood and lymphatic system. Indeed, studies show that tumours are also capable of producing new lymph vessels (lymphangiogenesis) further assisting metastatic spread. Furthermore, cancer cells may also migrate along nerves or the basal side (the side that faces the basal lamina) of endothelial cells without ever reaching the vessel lumen (Chitty *et al.*, 2018; Hapach *et al.*, 2019; Welch and Hurst, 2019).

iii. Stage III – Traveling through circulation

The presence of tumour cells in the bloodstream is not an uncommon occurrence as it is believed that there can be up to 1 million cancer cells for each gram of tumour entering the circulation each day, however, not all of them possess the ability to eventually form metastases. Once inside the blood/lymph vessel, cancer cells encounter sheer forces, immune cells and collisions with red blood cells. In addition, cells must possess the ability to resist a form of cell death known as anoikis which normally occurs in epithelial cells that have lost their cell-cell and cell-ECM connections (Chitty *et al.*, 2018; Hapach *et al.*, 2019; Jin and Mu, 2015; Riggio *et al.*, 2021; Welch and Hurst, 2019). Only those cells that can survive all these encounters and can arrest at a distant site will have the potential to proceed to the next stage. Circulating tumour cells (CTCs) may form clusters with each other or with platelets and leukocytes in order to help protect them from sheer forces and help evade

recognition by natural killer cells while an overexpression of Tropomyosin receptor kinase B (TrkB) or wingless-type MMTV integration site family, member 2 (WNT2) can help with the evasion of anoikis (Chitty *et al.*, 2018; Hapach *et al.*, 2019; Jin and Mu, 2015; Riggio *et al.*, 2021; Welch and Hurst, 2019). Cell arrest can occur through physical occlusion or rolling vascular adhesion. Physical occlusion occurs when CTCs or clusters of tumour cells become too large to pass through the arteries, veins or capillary networks. Rolling adhesion (which can also be used by cells to move through vessels) occurs when CTCs collide with endothelial cells and make use of selective attachment and detachment of cells facilitated through selectins, allowing the cell to roll across the interior surface of the blood vessel. Adhesion molecules including intercellular adhesion molecule-1 (ICAM-1) or vascular cell adhesion molecule-1 (VCAM) then facilitate anchorage which is followed by extravasation (Chitty *et al.*, 2018; Hapach *et al.*, 2019; Jin and Mu, 2015; Riggio *et al.*, 2021; Welch and Hurst, 2019).

iv. Stage IV – Extravasation

After cell arrest, CTCs must exit the circulation through a process that can essentially be described as the reverse of intravasation, however with one major difference. During intravasation cancer cells, in the presence of a familiar stromal environment, are moving towards often leaky vessels created by the tumours (Chitty *et al.*, 2018; Hapach *et al.*, 2019). During extravasation, in addition to being exposed to the sheer forces within blood vessels, cancer cells are moving towards healthier vessels of normal composition into a previously unoccupied environment, further decreasing the number of cells able to proceed to form secondary masses. Extravasation is believed to be facilitated by the secretion of factors including chemokines and ATP which are capable of increasing the permeability of blood vessels and the recruitment of monocytes to the area (Chitty *et al.*, 2018; Hapach *et al.*, 2019).

v. Stage V – Colonization

The final and often most crucial step of metastasis is colonisation of a secondary site. The establishment of macroscopic secondary masses is the outcome of the metastatic process and causes the most clinical concern (Welch and Hurst, 2019). After extravasation from the circulation, cells are now referred to as disseminated tumour cells (DTCs) of which only a small proportion has the ability to successfully form

secondary tumours. It is believed that only 3% of DTCs will be able to form secondary micro-metastases while even less (about 1%) of those will be able to form detectable macro-metastases. These cells are then referred to as metastasis initiating cells (Chitty *et al.*, 2018; Hapach *et al.*, 2019; Jin and Mu, 2015; Riggio *et al.*, 2021). Colonisation is also often seen as the rate limiting step of metastasis. The characteristics of the new environment exert a great influence on the formation of the secondary tumour. These include the characteristic of the stroma and composition of the ECM as well as the presence of cytokines and non-malignant cells (Chitty *et al.*, 2018; Hapach *et al.*, 2019; Jin and Mu, 2015; Riggio *et al.*, 2021).

1.3.3 Features of the metastatic cascade

1.3.3.1 Epithelial-to-mesenchymal transition (EMT)

Under normal conditions, epithelial cells form tight connections with both each other as well as the ECM preventing them from being motile (Fares *et al.*, 2020). The acquisition of mesenchymal characteristics by an epithelial cell with subsequent loss of epithelial characteristics, EMT, gives cells the ability to migrate and to reduce their cell-cell and cell-ECM adhesions along with becoming more stem cell-like. The ECM is degraded and proteins capable of breaking down the basement membrane are activated and secreted. During EMT there is a decrease in the levels of E-cadherin as well as keratins with an increase in the production of vimentin. This process is however reversible with cells colonizing the secondary environment undergoing mesenchymal-to-epithelial transition (MET) (Quintero-Fabián *et al.*, 2019; Welch and Hurst, 2019).

There is some debate on whether EMT is essential for metastasis to occur (Fares *et al.*, 2020; Welch and Hurst, 2019). There is the argument that epithelial cells with characteristics such as immobility and the presence of tight cell-cell and cell-ECM interactions do not have the ability to disseminate, emphasising the need for EMT (Fares *et al.*, 2020). Studies that found the presence of both epithelial and mesenchymal markers during the metastatic process was first interpreted as evidence in support of EMT since it was believed to represent an intermediary stage in the process and not the end stage of the transition (Jolly *et al.*, 2017). Later on, however, the presence of both epithelial and mesenchymal markers as well as the need for cells to maintain cell-to-cell contact for movement in clusters challenged the process of EMT (Welch and Hurst, 2019). Indeed, fluorescent signalling has been used to show that metastases can arise from both cells that have undergone EMT as well as cells that had not

(Welch and Hurst, 2019). In addition, Aiello *et al.* (2018) argued that most of the information on EMT during metastasis has been derived from *in vitro* studies. Through *in vivo* studies of pancreatic cancer in mice, they found that the cancer cells gained mesenchymal characteristics through protein internalization instead of through the repression of transcription factors as previously believed (Aiello *et al.*, 2018). In another study performed by Liu *et al.* (2019) using mouse models of BC, it was found that CTCs with epithelial characteristics had a stronger metastatic potential compared to mesenchymal-type CTCs.

Further investigation into EMT have shown that this process is more of a transitional state with cells having characteristics of both cell types and is not as simple as a cell being either fully epithelial or mesenchymal (Fares *et al.*, 2020; Nieto *et al.*, 2016). This would explain the simultaneous presence of epithelial and mesenchymal markers during metastasis (Welch and Hurst, 2019). Correspondingly, it has been discovered that a combination of epithelial and mesenchymal characteristics gives cells an advantage during their travel through circulation as well as with colonisation (Fares *et al.*, 2020), by allowing CSCs to alternate between epithelial and mesenchymal states (Ribatti *et al.*, 2020). Thus, it seems that even though the acquisition of mesenchymal characteristics does form an important part of the metastatic process, it does not seem to be a necessity for all cancer types (Welch and Hurst, 2019). It has however been found to be a significant contributor to chemotherapeutic resistance in cancer of the lung and pancreas (Fares *et al.*, 2020).

1.3.3.2 Metastatic dissemination, tropism and dormancy

A different topic widely debated is exactly when cancer cells first start to disseminate. Two models have been proposed to answer this question. The linear model states that only tumour cells present in advanced tumours can acquire the necessary genetic aberrations needed to successfully establish secondary metastases, while the parallel model suggests that cells from the primary tumour in its earliest stages may develop mutations enabling them to metastasise simultaneously with the development of the primary tumour (Riggio *et al.*, 2021). Evidence in support of the parallel model includes the detection of secondary tumours that are larger than those that would have been expected to be formed relative to the stage of the primary tumour, as well as the presence of DTCs in the bone marrow of individuals diagnosed with early-stage cancer. This suggests that in most patients, dissemination of cells may already have occurred at the time of diagnosis of the primary tumour, however below levels capable of being detected (Riggio *et al.*, 2021).

When looking at metastatic patterns, most tumours display some sort of organ tropism. This can in part be explained by the direction of blood flow, but it cannot account for all metastatic patterns observed. In 1889, Stephen Paget proposed an explanation for this (Fares *et al.*, 2020; Jin and Mu, 2015). What is now commonly referred to as the "seed and soil" hypothesis and widely accepted by researchers, compares metastatic cancer cells to plant seeds while the secondary tumour site is described as the soil. This hypothesis states that the organs which would eventually be colonised by DTCs do not only depend on the cancer cell but on the secondary environment as well. Thus a "seed" would not be able to grow just anywhere but only in a place where the "soil" is of such a nature as to support its survival and growth (Chitty *et al.*, 2018; Jin and Mu, 2015). Metastatic organ tropisms of various cancer types are depicted in Figure 1.2.

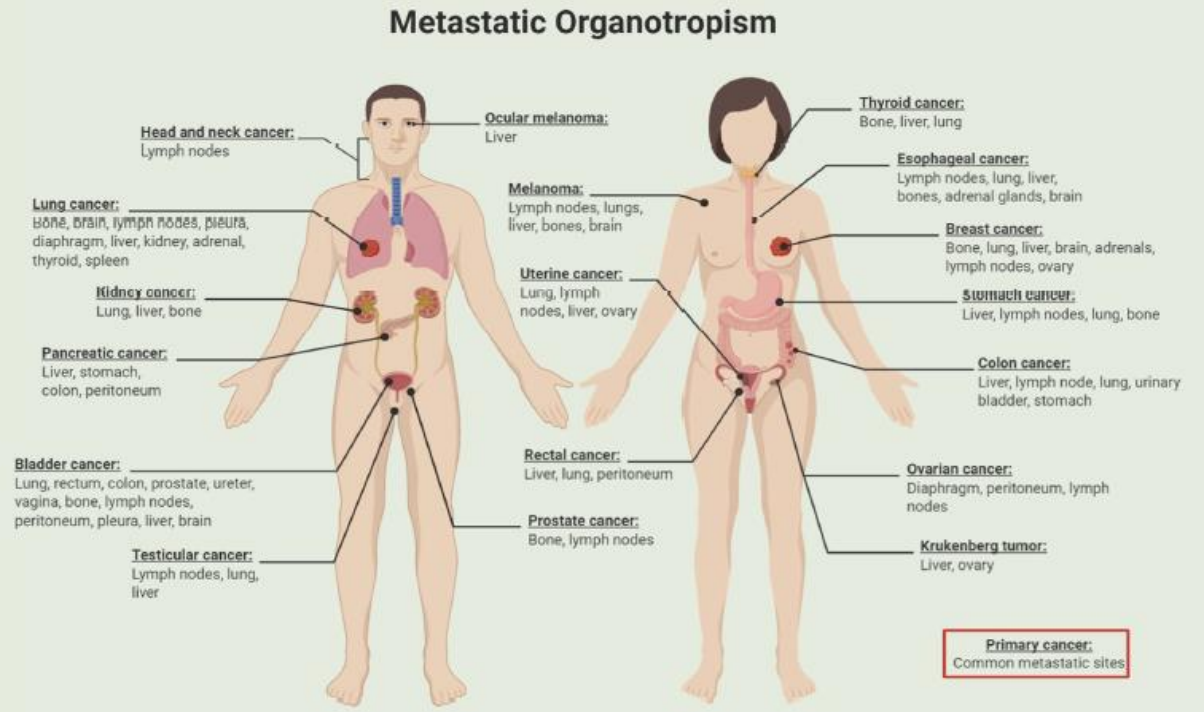

Figure 1.2 Organ tropism of various cancer types. This can be partially explained by the patterns of blood flow as well as the "seed and soil" hypothesis proposed by Stephen Paget. Image taken from Fares *et al.* (2020) under the terms of the Creative Commons Attribution 4.0 International License (http://creativecommons.org/licenses/by/4.0/).

Another factor contributing to the lethality of metastasis is the ability of DTCs to undergo a period of dormancy. This may occur after spreading to the secondary tumour environment but before proliferation into detectable secondary lesions. Furthermore, dormancy not only exists among single DTCs but tumour dormancy within small tumours can also occur where there is an equilibrium between cell death and cell proliferation with no net increase in tumour size.

The lack of symptoms and clinically detectable masses during this stage might be misinterpreted as a state of remission. Most of the metabolic reactions occurring in cells during dormancy as well as exactly what would enable the dormant state to end and proliferation to resume remain a mystery (Riggio *et al.*, 2021; Welch and Hurst, 2019).

1.3.3.3 The influence of the environment on metastasis

In agreement with Paget's hypothesis made 134 years ago, suggesting the soil (tumour microenvironment) is just as important as the seed (DTCs), the metastatic spread is not at all solely dependent on the characteristics and activities of the cancer cells themselves. A factor's importance that cannot be emphasised enough is the influence of the tumour microenvironment and other associated cells that CTCs come across during the metastatic cascade (Riggio *et al.*, 2021). These factors are summarized in Figure 1.3. Indeed, it has been found that even before cells escape from the primary tumour, communication between the primary tumour and cells within other regions of the body occurs through various soluble factors to establish a "premetastatic niche". The result of this communication is the deployment of stem cells to secondary sites where they will restructure the ECM, preparing the environment for the arrival of DTCs and metastatic growth (Welch and Hurst, 2019). In addition, exosomes are released that activate epidermal growth factor receptor (EGFR), induce EMT, increase the permeability of blood vessels and suppress the immune system at the secondary site collectively facilitating metastasis (Fares *et al.*, 2020).

The interaction of cancer cells with cells in their environment also contributes to metastatic progression. Microscopic studies have revealed that cancer cells may share biological material with other cells. Vesicles containing mRNA that are released by cancer cells can be engulfed by neighbouring cancer cells providing them with metastatic characteristics (Fares *et al.*, 2020). In addition, inflammatory cells residing in the primary tumour may assist cancer cells with migration and invasion (Welch and Hurst, 2019). Another interesting environmental factor aiding tumour growth is the tumour microbiome. Anaerobic bacteria can take advantage of the hypoxic conditions inside the tumour, where their metabolic reactions may contribute to suppressing the immune system and even altering their response to chemotherapeutic drugs (Fares *et al.*, 2020).

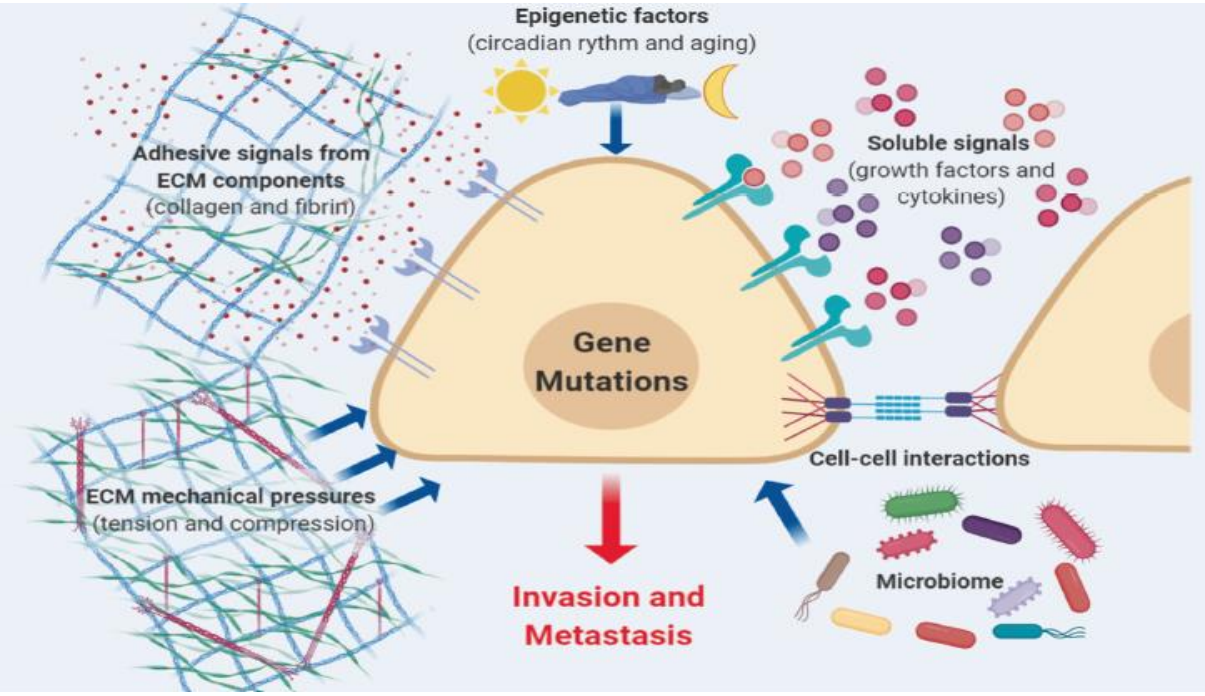

Figure 1.3 Graphical depiction of the influences of the tumour microenvironment on the acquisition of characteristics that may eventually lead to metastasis of a cancer cell. Image taken from Fares *et al.* (2020) under the terms of the Creative Commons Attribution 4.0 International License (http://creativecommons.org/licenses/by/4.0/).

1.3.4 The importance of MMPs

1.3.4.1 MMP structure, function and regulation

Matrix metalloproteinases (MMPs) or matrixins are members of a group of zinc-dependent metallopeptidases that participate in the remodelling of the ECM in the presence of calcium. They form part of the metzincs protease superfamily (Klein and Bischoff, 2011; Laronha and Caldeira, 2020). To date, 28 different MMPs have been discovered in vertebrates of which 23 are expressed in humans (Laronha and Caldeira, 2020). Based on substrate specificity, MMPs can be arranged into: collagenases, gelatinases, stromelysins, stromelysin-like, matrilysins, MMP-19 like, membrane type MMPs (MT-MMPs) and other MPPs (Klein and Bischoff, 2011; Laronha and Caldeira, 2020). Details on the characteristics of MMPs in the different subgroups are summarised in Table 1.2. All MMPs are structurally related with a typical structure consisting of an N-terminal, a catalytic site, a hinge region as well as a C-terminal. The N-terminal is the pro-peptide domain and consists of around 80 amino acids, while the catalytic site contains around 170 amino acids separated into two modules connected by a zinc ion containing cleft, held in place by three histidine residues. The catalytic site binding motif containing zinc is a highly conserved structure amongst all MMP types. The hinge

region linking the catalytic and C-terminal domains is rich in proline residues and is made up of between 15 and 65 amino acids while the highly conserved hemopexin-like C-terminal domain consists of around 200 amino acids with a disulphide bridge essential for substrate binding. These proteins are vital for growth and development as they participate in angiogenesis, embryogenesis, the repair, growth and morphogenesis of tissues, the uterine cycle, uterine involution, gestation, formation of foetal organs and giving birth (Cabral-Pacheco *et al.*, 2020; Reunanen and Kähäri, 2013; Quintero-Fabián *et al.*, 2019).

In vivo, MMP activity is tightly regulated by numerous mechanisms. MMP levels and activity can be controlled at a transcriptional level by growth factors and cytokines, through the regulation of mRNA half-life as well as the regulation of their extracellular absorption or removal (Reunanen and Kähäri, 2013). In addition, MMPs are produced as zymogens requiring the removal of the N-terminal for functionality. Pro-MMPs are maintained in the zymogen form by a bond between a cysteine residue located on the N-terminal domain and the zinc of the catalytic site forming a cysteine switch. This arrangement blocks the zinc ion, preventing the substrate from binding and being catalysed (Cabral-Pacheco *et al.*, 2020; Quintero-Fabián *et al.*, 2019; Reunanen and Kähäri, 2013). Proteolytic cleavage by plasmin, trypsin and other serine proteinases including other MMPs can then activate the pro-MMP to its functional state by removing the N-terminal pro-domain (Klein and Biscoff, 2011; Reunanen and Kähäri, 2013). In addition, certain chemical agents including reactive oxygen species (ROS), compounds containing mercury, and detergents may also lead to a disruption in the cysteine switch (Klein and Biscoff, 2011). Localization of the proteolytic activity of MMPs to the pericellular space as well as the fact that they are bound to the surface of the cells also assists with their regulation (Reunanen and Kähäri, 2013). Lastly, MMP activity can be repressed by serine protease inhibitors, serum proteinase inhibitors, as well as tissue inhibitors of metalloproteinases (TIMPs) (Reunanen and Kähäri, 2013). TIMPs consist of four proteins that are made up of between 184 and 194 amino acids and range from 21 to 30 kDa in size and consist of an inhibitory N-terminal and a C-terminal (Cabral-Pacheco *et al.*, 2020; Klein and Biscoff, 2011). They inhibit MMP activity through reversible binding of the N-terminal to the active site of MMPs and participate in their removal from the ECM (Cabral-Pacheco *et al.*, 2020; Reunanen and Kähäri, 2013). TIMP-1,-2 and -4 are secreted in the ECM, while TIMP-3 remains attached to the ECM (Reunanen and Kähäri, 2013). The TIMPs are themselves regulated by cytokines, chemokines and growth factors (Cabral-Pacheco *et al.*, 2020).

Table 1.2 The subclasses of MMPs divided based on their substrate specificity along with diseases associated with a deregulation in their activity and expression levels. Compiled from Cabral-Pacheco *et al.* (2020), Galea *et al.* (2014), Jabłońska-Trypuć *et al.* (2016), Klein and Bischoff (2011), Laronha and Caldeira (2020), Maldonado *et al.* (2018) and Reunanen and Kähäri, (2013).

Subclass	Name	Substrate	Physiological processes normally involved in	Diseases associated with their deregulation
Collagenases	MMP-1 or collagenase-1	Collagen type I, II, III, VII, VIII and X, aggrecan, versican, perlecan	Embryonic development and tissue repair	Arthritis, cancer, cutaneous ulcers, fibrotic diseases and wound healing disorders
	MMP-8 or collagenase-2, neutrophil collagenase	Collagen type I, II, III, aggrecan	Embryogenesis, inflammation, postpartum uterine involution and wound healing	Atherosclerosis, bronchiolitis and pulmonary emphysema
	MMP-13 or collagenase-3	Collagen I, II, III, IV, IX, X, XIV, gelatin, aggrecan, perlecan, biglycan, fibrillin, fibrinogen, laminin	Activation of other pro-MMPs, foetal bone development, foetal cutaneous wound repair, gingival wound repair and postnatal bone remodelling	Arthritis, cancer, cutaneous ulcers, diabetes and periodontitis
Gelatinases	MMP-2 or gelatinase A	Collagen type I, IV, V, VII, X, gelatin, elastin, vitronectin, fibronectin, fibrillin, osteonectin	Angiogenesis, inflammation, infiltration of neutrophils and lymphocytes, neurogenesis and wound healing	Amyotrophic lateral sclerosis (ALS), aortic aneurysm, cancer, cardiovascular disease, chronic kidney disease, diabetes and pulmonary disease
	MMP-9 or gelatinase B	Collagen type IV, V, VII, XI, XIV, XVII, gelatin, elastin, fibrillin, fibronectin, osteonectin	Angiogenesis, female reproductive cycle, immune cell migration, neurogenesis and wound healing	ALS, aortic aneurysm, asthma, chronic obstructive pulmonary disease (COPD), cancer, diabetes, hypertension, multiple sclerosis, polycystic ovarian syndrome and spontaneous abortion
Stromelysins	MMP-3 or stromelysin-1	Collagen type IV, V, VII, IX, X, XIV, fibronectin, gelatin, laminin, elastin, proteoglycans, globular portion of collagen type IV	Activation of pro-MMP-2, -9 and -13, development of mammary gland, ECM turnover and mammary involution	ALS, Alzheimer's disease, aneurism, arthritis, asthma, cancer, impaired wound healing and Parkinson's disease
	MMP-10 or stromelysin-2	Collagen type IV, V, IX, X, XIV, fibronectin, gelatin, laminin, elastin	Cutaneous wound healing	Arthritis, cancer, fibrosis, idiopathic pulmonary fibrosis, peripheral arterial disease, and wound healing

Table 1.2 (continued)

Subclass	Name	Substrate	Physiological processes normally involved in	Diseases associated with their deregulation
Stromelysin-like MMPs	MMP-11 or stromelysin-3	Casein, protease inhibitors, insulin-like growth factor-binding protein-1 (IGF-BP-1)	Embryonic development, female reproductive cycle, inhibition of adipogenesis and wound healing	Cancer and diabetes
	MMP-12 or macrophage metalloelastase, human macrophage elastase	Elastin , vitronectin, fibrillin, plasminogen	Penetration of macrophages through the basement membrane	Asthma, COPD and emphysema
Membrane-type MMPs	MMP-14 or membrane-type-1 MMP	Collagen I, II, III, fibronectin, gelatin, vitronectin, tenascin, aggrecan, fibrin, fibrillin, fibrinogen, laminin-5	Activation of pro-MMP-2 and -13, angiogenesis	Cancer
	MMP-15 or membrane-type-2 MMP	Collagen I, II, III, fibronectin, vitronectin, tenascin, aggrecan, fibrin, fibrinogen, laminin-5	Activation of pro-MMP-2 and -13, angiogenesis and ovulation	Cancer
	MMP-16 or membrane-type-3 MMP	Collagen type III, casein, gelatin, fibronectin, vitronectin, laminin, aggrecan	Activation of pro-MMP-2 and-9, adhesion	Cancer
	MMP-17 or membrane-type-4 MMP	Fibrin, fibrinogen, gelatin	Activates a disintegrin and metalloproteinase with thrombospondinmotifs-4 (ADAMTS-4)	Cancer
	MMP-25 or membrane-type-6 MMP	Collagen IV, fibronectin, fibrin, gelatin, proteoglycans	Activate pro-MMP-2	Cancer
Matrilysins	MMP-7 or matrilysin	Collagen type IV, elastin, fibronectin, gelatin, laminin	Immunity, inflammation, postpartum involution of endometrium and wound repair	Cancer
	MMP-26 or matrilysin 2, endometase	Collagen type IV, fibrin, fibronectin, fibrinogen, gelatin	Implantation and the menstrual cycle	Tissue remodelling in cancer
MMP-19 like MMPs	MMP-19	Collagen type IV, gelatin, aggrecan, fibronectin, laminin	Angiogenesis	Arthritis and wound healing
	MMP-28 or epilysin	Casein	Homeostasis	Arthritis, homeostasis and repair of tissue
Other MMPs	MMP-20 or enamelysin	Aggrecan, amelogenin	Development of teeth	Development of teeth
	MMP-23 or cysteine array-MMP	Gelatin	Reproduction	Cancer, inflammatory diseases

1.3.4.2 MMPs in cancer progression and metastasis

A disruption in the tight regulation of the activities of MMPs, as well as TIMPs resulting in a disproportionate ECM degradation, can result in the development of numerous diseases such as arthritis, aneurysms, periodontitis, autoimmune skin disorders, destruction of tissues and fibrosis (Cabral-Pacheco *et al.*, 2020; Reunanen and Kähäri, 2013). MMPs have also been found to participate prominently not only in the invasion and metastasis of cancer but in various other steps of cancer progression (Cabral-Pacheco *et al.*, 2020). MMPs, mostly secreted by the stromal cells, play a large role in the migration, invasion and angiogenesis of tumour cells. In various cancer types including cancer of the breast, lungs, colon, ovaries, thyroid, head and neck as well as the prostate there is a strong correlation between the level of MMPs and the tumour metastatic potential (Reunanen and Kähäri, 2013). In addition, the expression of cytokines and chemokines by tumour cells can lead to the expression and activation of MMPs resulting in the activation of inflammatory pathways. Inflammation in turn assists in generating tumour immune tolerance and further assists tumours with angiogenesis and metastasis. Furthermore, tumour-associated macrophages (TAMs) can secrete MMPs, promoting ECM degradation and modulation of signalling proteins, facilitating cancer progression and the introduction of tumour blood vessels (Quintero-Fabián *et al.*, 2019). MMPs themselves, through degradation of the ECM, can also result in the release of stimulators of angiogenesis and growth, interfere with cell adhesion and induce apoptosis of anchorage-dependent cells thereby favouring the growth of anchorage-independent cells (Reunanen and Kähäri, 2013).

In contrast to their tumour promoting activities, MMPs may also have anti-cancer functions depending on the tumour type and the MMP involved. Examples include, MMP-8 and -12 (Cabral-Pacheco *et al.*, 2020). MMP-8 was found to inhibit growth and metastasis in breast and tongue cancer and an increase in the incidence of skin tumours was found in mice that did not express MMP-8 (Dufour and Overall, 2013). The anti-cancer effects of MMP-12 include inhibiting angiogenesis and metastasis. In lung cancer, MMP-12 was found to suppress the growth and metastasis of tumours through the production of the anti-angiogenic factor angiostatin (Dufour and Overall, 2013). Mice studies have also shown MMP-3, -7, -9 and -12 can also lead to a decrease in vessel formation. This is done through MMP-mediated production of angiostatin (Reunanen and Kähäri, 2013). On the other hand, overexpression of TIMPs has been shown in several cancer types to lead to a reduction in the invasion, metastasis and tumour angiogenesis but have also been found to enhance tumour growth and

inhibit apoptosis in other tumour types (Reunanen and Kähäri, 2013). It was thus proposed that the levels of either MMPs or TIMPs alone are not an accurate enough predictor of tumour growth and metastatic ability but that the ratio of MMPs to TIMPs should rather be taken into consideration (Reunanen and Kähäri, 2013).

1.3.5 Treating metastatic disease

1.3.5.1 Targets for anti-metastatic drug development

Regardless of the type of mechanism targeted, the development of drugs with specific anti-metastatic activities is an important field of research as it has been shown that therapeutic approaches used for the treatment of the primary tumour alone, are not sufficient to treat metastatic disease (Anderson, *et al.*, 2019; Gandalovičová *et al.*, 2017). The metastatic process itself presents many opportunities that can be exploited as therapeutic targets. Due to the rapid rate that drug resistant mutations occur in rapidly dividing cancer cells, the tumour microenvironment is a promising therapeutic target. Targeting cells in the tumour stroma seems like a valid approach since these cells do not contain the characteristic genomic instability and variability of the cancer cells. An example of this includes preventing the recruitment of osteoclasts in an attempt to inhibit metastasis to the bone. This approach has shown some degree of success however failed to significantly increase overall patient survival (Weber, 2013).

A different approach is through targeting angiogenesis with the reasoning that macroscopic secondary tumours would not be able to form without a steady blood supply. These types of therapies are often aimed at inhibiting the proliferation of endothelial cells; however, because only the final stage of metastasis is targeted while the initial stages are left untreated, it is seen as merely a delay to metastatic progression instead of an eradicating treatment (Weber, 2013). In addition, through a process referred to as co-option, cancer cells can form tumours in the vicinity of already established blood vessels in the lungs and brain, circumventing the need for angiogenesis and rendering these therapies impractical (Fidler and Kripke, 2015). One way to overcome the problems associated with targeting angiogenesis is through “the normalization of blood vessels” where the abnormal blood vessels in secondary tumours are targeted as a way to eradicate them. This was previously done by using antibodies against VEGF-A or by targeting the pericytes. This approach however, produced contradicting results and the resulting decrease in vascular permeability, had the adverse effect of decreasing the concentration of co-administered chemotherapeutic drugs reaching the tumour

(Fidler and Kripke, 2015). In another line of attack, the growth factor receptors of the endothelial cells in tumour vasculature can be targeted resulting in apoptosis of the endothelial cells, decreasing the growth of secondary masses (Fidler and Kripke, 2015).

A third approach involves targeting molecules that suppress metastasis of which several have been identified. However, the approach of activating a suppressed gene that may or may not be present is considerably more complex than targeting a gene that is overexpressed (Weber, 2013). Targeting molecules that facilitate metastasis can also be useful. The reasoning behind the multitude of MMP inhibitors that have been developed is based on inhibiting intravasation, invasion and extravasation mechanisms in which MMPs are highly involved. The ability of CTCs to increase their survival in circulation by forming aggregates with platelets has also been targeted in mice through the administration of aspirin (Fidler and Kripke, 2015).

Lastly, an approach that focuses on brain metastasis in particular, involves decreasing endothelin-1 to reduce chemo resistance. When bound to its receptor in cancer cells, this protein may induce the expression of anti-apoptotic proteins making these cells more resistant to chemotherapeutic drugs (Fidler and Kripke, 2015).

1.3.5.2 Troubles associated with the development of anti-metastatic drugs

By the time macroscopic metastases have developed, metastasis is considered a systemic disease considerably changing the approach to treatment compared to localised tumours (Ganesh and Massagué, 2021). Anti-metastatic therapies have two main subtypes: 1) therapies aiming to prevent the spread of cancer cells or the manifestation of secondary tumours and 2) therapies that are targeted against the already established secondary growths. What poses a significant problem with the first approach (preventing metastasis formation) is the fact that experimental drugs are often only given to patients with advanced stage disease that have already received standard treatments that have either failed or patients that experienced recurrence (Weber, 2013). However, when considering the parallel model of tumour dissemination where cancer cells from tumours in the early stages can start to spread (Riggio *et al.*, 2021), by the time a patient reaches the point of advanced stage cancer when they would be considered for clinical trials, the metastatic spread may already have occurred to a significant degree which means that preventing metastasis would not be an achievable option anymore. These treatments will be more beneficial when administered at the time of diagnosis of the primary tumour. This might contribute to the reason why many approaches

to anti-metastatic therapies including inhibitors of MMPs have not been as successful. The first hurdle to overcome is thus reconsideration in the structuring of experimental drug administration (Weber, 2013).

Secondly, there is the financial burden related to drug development. The low success rates associated with the development of anti-metastatic drugs discourage investors from taking the risk (Weber, 2013). Due to the radical speed at which metastasis progresses, an advantage of testing new treatments on patients with advanced stage cancer is that it allows for faster feedback on treatment effectiveness. Only those drugs that have shown enough promise at treating advanced macroscopic tumours will then be tested on patients with early-stage disease to try and prevent the formation of secondary growths. Several of these treatments that were successful for advanced stage disease were however found to be ineffective as neo-adjuvant or adjuvant treatments to prevent metastasis, contributing to the low success rate and financial losses associated with anti-metastatic drug trials. Furthermore, drugs that prevent metastatic spread that would have to be administered at an early stage and possibly for a longer time interval would require clinical trials with follow-up times of several years to assess the long-term treatment effects. Studies of this length are considerably more costly than short-term trials such as those involving patients with advanced stage cancer (Ganesh and Massagué, 2021).

Another complication arises from the inherent complexity of the metastatic process and our lack of complete understanding thereof, as well as the heterogeneity of malignant cells. Cells require a multitude of abilities to successfully establish metastases. The acquisition of one trait on its own (e.g., invasion) is necessary but not sufficient for the completion of the metastatic cascade. Similarly, the inhibition of only one trait therapeutically, would not be adequate to inhibit the entire metastatic process as cells may quickly compensate by using another method as a result of their characteristic plasticity (Fidler and Kripke, 2015; Wang and Huang, 2017). In addition, metastatic traits are not always acquired in a set order (Welch and Hurst, 2019) thus the pathways of acquisition of these traits differ between individuals, adding another level of variation among patients (Wang and Huang, 2017).

The genomic instability of metastatic cells may also contribute to the low success rate associated with anti-metastatic drugs. The immense speeds at which new variants can arise give those variants that are resistant to a particular treatment strategy an advantage, which

they are able to exploit by multiplying and eventually replacing the non-resistant variants (Fidler and Kripke, 2015).

1.3.5.3 Treatments for metastatic cancer

Treatments for metastatic disease (stage IV cancer) involve mostly systemic approaches including immunotherapy, targeted therapy and mainly chemotherapy either to eradicate metastases or for palliative care (Ganesh and Massagué, 2021; Hanna and Mayden, 2021). An important aspect of anti-metastatic treatment involves combining several different treatments in an attempt to overcome the rapid rates at which resistance occurs. Strategies in improving the delivery of treatments directly to the tumour using nanoparticles and drugs conjugated to antibodies are also highly investigated to reduce systemic side-effects (Ganesh and Massagué, 2021). Immune checkpoint inhibitors have shown some success in treating metastatic cancer. Down-regulators of T cell activities including cytotoxic T-lymphocyte associated protein-4 (CTLA-4) that can help cancer cells to avoid immune destruction are targeted through this treatment strategy. By inhibiting the interaction between these receptors and their ligands, B7 proteins, T cell activity is not suppressed and thus able to target cancer cells (Ganesh and Massagué, 2021; Oyewole-Said *et al.*, 2020). Since the tumour microbiome was found to contribute to metastatic development, recent attempts to target the tumour microbiome including strains of *Fusobacterium* have also shown some success in mouse xenograft models (Ganesh and Massagué, 2021). On the other hand, another strategy for increasing the targeted delivery of drugs may be accomplished using microorganisms as delivery vehicles, taking advantage of the tissue specificity of some microorganisms (Forbes *et al.*, 2018).

Systemic treatment strategies for metastatic BC (mBC) depend on the molecular subtype of BC. Recent advances have made great strides toward managing this disease but are still associated with a multitude of side-effects depending on the type of treatment. Some of these include anaemia, hyperglycaemia, leukopenia, neutropenia and thrombocytopenia (Jazieh *et al.*, 2020). Table 1.3 provide a summary of the current treatment strategies for mBC. The main chemotherapeutic agents administered for mBC are the taxanes docetaxel, paclitaxel and nab-paclitaxel, whereas anthracyclins are only given to chemo-naïve individuals (Hanna and Mayden, 2021). In addition, the drug denosumab is used in cases where BC has metastasised to the bone tissue (Lukasiewicz *et al.*, 2021). Patients with a high tumour load and severe organ dysfunction due to mBC, are preferably treated with a combination of

chemotherapeutic drugs, irrespective of subtype or related side-effects (Hanna and Mayden, 2021).

In addition, there are several new approaches currently being investigated including inhibitors of the androgen receptor (AR) which were found to be present in almost 25% of TNBC patients (Jazieh *et al.*, 2020). Margetuximab, another antibody against HER2 has shown great promise for HER2 subtype tumours when used in conjunction with chemotherapy. Furthermore, additional inhibitors of FGF and protein kinase B (AKT) as well as histone decetylase are currently under investigation (Jazieh *et al.*, 2020).

Table 1.3 Summary of treatment strategies for the various molecular subtypes of mBC. Constructed from Hanna and Mayden (2021), Jazieh *et al.* (2020) and Yu *et al.* (2022).

Treatment target	Description	Examples
luminal A and B subtypes		
Cyclin-dependent kinase (CDK) 4 and 6	Inhibition of key proteins involved in the proliferation of tumour cells. Usually used together with hormone therapy. The excellent outcomes of clinical trials have made this combination the standard treatment for ER-positive subtypes.	abemaciclib, palbociclib, ribociclib
Phosphatidylinositol-3-kinase (PI3K) / AKT pathway	Inhibits PI3K/AKT pathway activation involved in tumour cell proliferation and expression of ER.	alpelisib, buparlisib, ipatasertib
Mammalian target of rapamycin (mTOR)	Targets the pathway involved in growth and differentiation of cells. This pathway has been linked to resistance to hormone therapy.	everolimus, temsirolimus
HER2 positive subtype		
HER2	Monoclonal antibodies against HER2. Most used together with taxanes for this subtype of BC. Alternatively, it can be used as the drug conjugates trastuzumab emtansine (inhibits microtubules) or trastuzumab deruxtecan (inhibits topoisomerase I).	pertuzumab, trastuzumab
HER2 tyrosine kinase	Reversibly or irreversibly inhibits autophosphorylation of HER2, thereby inhibiting the PI3K and mitogen-activated protein kinase (MAPK) pathways.	lapatinib, neratinib
TNBC		
Programmed cell death protein 1 (PD-1)	Immune checkpoint inhibitors of PD-1 or its ligand PD-L1.	atezolizumab, nivolumab, pembrolizumab
Polyadenosine diphosphate-ribose polymerase (PARP)	Inhibits PARP 1 and 2, responsible for repairing single stranded DNA breaks leading to double-stranded DNA breaks and eventually cell death.	olaparib, talazoparib

1.4 Metals used in cancer treatment

1.4.1 Overview

Metals often play a contradictory role in nature. Metals such as copper, cobalt, manganese and zinc form part of the normal functioning of living organisms, participating in redox reactions and forming an important part of enzyme structure and function (Ndagi *et al.*, 2017). In contrast, metals such as arsenic, cadmium, chromium, lead, mercury and nickel can in turn be toxic to living organisms, many of them being carcinogenic (Ndagi *et al.*, 2017). The knowledge of the potential medicinal properties of metals has been around for a long time. Among these were the use of mercury sulphide for venereal diseases, a mercury-based ointment for skin conditions, the use of gold and copper for the treatment of syphilis and one of the first proposed treatments for leukaemia, arsenic trioxide. However, due to the lack of pharmacological knowledge at the time, there were numerous challenges associated with these treatment strategies (Ndagi *et al.*, 2017). Nowadays quite a few metal-based drugs are used in the clinical setting to treat a large variety of cancer types (e.g. cervical, colorectal, lung, oesophageal and ovarian cancer) or are being studied in various stages of clinical trials to be used as anti-cancer treatments (Lucaciu *et al.*, 2022). Metals are of particular interest in the drug industry due to their unique behaviours such as the ability to participate in redox reactions, multiple coordination modes and the ability to react with organic substances. Consequently, the demand for more metal-based drugs is ever increasing (Ndagi *et al.*, 2017).

Arguably the most well-known metal-based compound is cisplatin (CDDP) discovered by Barnett Rosenberg in the 1960s (Ndagi *et al.*, 2017). Praised for its DNA interacting abilities leading to apoptosis, it is widely used as a treatment for a large variety of cancer types (Yu *et al.*, 2008). CDDP treatment is however associated with numerous systemic side-effects and often drug-resistance, which prompted research into other less toxic and more selective compounds including carboplatin and oxaliplatin (Lucaciu *et al.*, 2022). These findings have opened a whole new branch of research on metal-based drugs. A lot of the research is based on the development of new drugs containing metals such as iron, gold, titanium, copper and zinc but also on the modification of existing complexes and combining metal complexes with peptides, sugars, steroids or bile acid to aid in drug delivery to cancer cells (Ndagi *et al.*, 2017). A downside that has hindered the use of metal-based drugs is their low aqueous solubility and short half lives *in vivo*, leading to an increased investigation into the use of nanoparticles as delivery vehicles of metal-based drugs (Ndagi *et al.*, 2017).

Of particular interest are ruthenium compounds that have the potential of binding to more ligands and are also associated with fewer side-effects (Ndagi *et al.*, 2017; Riccardi *et al.*, 2019). In addition, the mechanism of transport of ruthenium complexes into cells has been described as a strategy akin to the "Trojan horse" phenomenon. Cells with a higher proliferation rate, such as cancerous cells, require more Fe, resulting in increased levels of transferrin receptors. Due to their structural similarity to Fe(III) ions, Ru(III) ions can bind to serum transferrin and albumin proteins, replacing iron, allowing them to be transported throughout the circulation system. Thus, through essentially hijacking the body's iron transport mechanisms, ruthenium complexes are able to accumulate to a higher degree in cancerous cells, thereby reducing their systemic toxicity (Lucaciu *et al.*, 2022).

1.4.2 Silver and its use in medicine

The use of the transition metal silver, in the medicinal industry, has a history equally as rich as that of the use of metals in general. It is believed to have its origin in ancient civilisations where water and wine were kept in silver containers (Medici *et al.*, 2019). This was later continued when settlers and pioneers would add silver coins or tableware to their water and milk to avoid spoilage (Medici *et al.*, 2019). From there, its applications in medicine only increased with its use to suture surgical wounds, help with wound healing and prevent infections in soldiers injured in war (Medici *et al.*, 2019). In addition, silver was employed in the treatment of burn wounds while silver acetate was used as a pesticide and as a treatment for cigarette addiction (Medici *et al.*, 2019). Nowadays, silver is used in the dental industry and in the medical field for its anti-microbial properties (Medici *et al.*, 2019), as well as in consumer, agricultural and industrial industries (Sim *et al.*, 2018). Over the past few years, several silver-containing products have been patented including the coating of needles and surgical instruments with an antibacterial layer of silver nanoparticles, the incorporation of silver in deodorants and lotions, the distribution of silver ions in fridges to delay spoilage of food and anti-microbial food packaging containing silver nanoparticles (Sim *et al.*, 2018).

1.4.3 Silver anti-cancer complexes

The cytotoxic and genotoxic effects of silver-based compounds are believed to be caused by the interaction of silver ions and thiol containing proteins in cell and organelle membranes, DNA and the cytoplasm (Korman *et al.*, 2022). These interactions lead to the inactivation of enzymes, the formation of disulphide bonds with DNA and peroxidation of membrane lipids resulting in increased membrane permeability and the release of lysosomal and cytoplasmic contents. Damage to the mitochondria interferes with the electron transport chain and

synthesis of ATP while leading to an increase in ROS production. Collectively, these effects may induce apoptosis (Korman *et al.*, 2022; Raju *et al.*, 2022).

A number of different silver-based complexes were synthesized and evaluated for their anti-cancer potential with varying degrees of success which were highly dependent on the ligands (Raju *et al.*, 2022). These include silver complexes of 5-fluorouracil, carboxylates, dehydronorcantharidin, N-heterocycles, N-heterocyclic carbenes, NSAIDs, phosphines and Schiff bases (Medici *et al.*, 2019; Raju *et al.*, 2022). Some of these silver-based complexes were found to be more effective as an anti-cancer agent compared to CDDP in breast, colorectal, lung and ovarian cancer (Raju *et al.*, 2022). The complexes that showed the most potential were those containing ligands of N-heterocycles and N-heterocyclic carbenes as well as phosphines (Medici *et al.*, 2019).

A silver(I) nitrate complex was found to induce apoptosis in A549 lung cancer cells after 24 hr at an IC_{50} value of 24.75 µM (Kaplan *et al.*, 2017). Silver(I) coupled to N-heterocyclic carbenes showed toxicity towards BC (MCF-7 and MDA-MB-231), colorectal cancer (HCT116) (Asif *et al.*, 2016) and prostate cancer (DU145) cells (Şahin-Bölükbaşi *et al.*, 2019). A sodium thiosulfate based silver(I) complex was found to be toxic to MCF-7 BC cells with an IC_{50} value of 21.3 µM while showing no toxicity towards non-malignant human mammary epithelial cells (HMEC) or human bone marrow derived mesenchymal stem cells (HMSC) (Ota *et al.*, 2021).

Phosphine as a ligand coupled to silver is of particular interest due to phosphine being lipophilic, which enables them to target cell mitochondria (Raju *et al.*, 2022). Silver(I) phosphine complexes that have shown promising anti-cancer activity include a binuclear silver(I) triphenylphosphine complex. This complex showed promising cytotoxic effects against HCT116 colorectal cancer cells as well as MDA-MB-231 BC cells with IC_{50} values of 4.93 µM and 4.15 µM, respectively (Zheng *et al.*, 2020) Another class of complexes, the silver(I)-5,5-diethylbarbiturate-bis(diphenylphospino)alkanes, showed promising cytotoxicity towards A549 lung cancer and MCF-7 BC cells while showing minimal toxicity towards a MCF 10A normal breast epithelial cell line. These complexes were shown to lead to cell cycle arrest, production of ROS, oxidative damage to DNA and apoptosis (Yilmaz *et al.*, 2017). In addition to these, silver complexes with a mixture of phosphine and thiazolidine ligands have also been investigated and have shown *in vitro* cytotoxic activity against MCF-7 and MDA-MB-231 BC and HT-29 colon cancer cells (Sofyan *et al.*, 2018).

A class of silver(I) phosphine complexes were synthesized by the Department of Chemical Sciences at the University of Johannesburg (UJ) under the supervision of Prof Reinout Meijboom. Initially designed for another purpose (predicting the structure of complexation), their cytotoxicity towards cancer cells *in vitro* was discovered by chance, through collaboration with the Department of Biochemistry at UJ, and several articles that illustrate these findings have been published since (Engelbrecht *et al*., 2018; Ferreira *et al*., 2015; Human *et al*., 2015; Human-Engelbrecht *et al*., 2017; Potgieter *et al*., 2017). Several silver(I) phosphine complexes, with different ligands and different ratios of silver ions to ligands, have been shown to be cytotoxic against SNO oesophageal cancer and MCF-7 BC cell lines at a significantly lower concentration compared to CDDP. In addition, these complexes have shown minimal toxicity to non-cancerous cells including human dermal fibroblast adult (HDF-a) and human embryonic kidney (HEK-293) cells (Engelbrecht *et al*., 2018; Ferreira *et al*., 2015; Human *et al*., 2015; Human-Engelbrecht *et al*., 2017; Potgieter *et al*., 2017). Four silver(I) thiocyanaye complexes were found to selectively induce apoptosis in MCF-7 cells with IC_{50} values ranging between 3 and 3.6 µM. Minimal toxicity towards non-malignant HDF-a cells were also found at these IC_{50} concentrations (Ferreira *et al*., 2015). Silver(I) thiocyanate 4-methoxyphenyl phosphine induced apoptosis in SNO cells along with depolarization of the mitochondrial membrane, release of cytochrome *c* and cleavage of caspase-9 (Engelbrecht *et al*., 2018). Similarly, a silver(I) cyanide-phosphine complex induced apoptosis in SNO cells with a IC_{50} concentration of 4.02 µM. This complex, however, was also toxic to HDF-a and HEK-293 cells limiting its use as an anti-cancer complex (Human-Engelbrecht *et al*., 2017). Three silver(I) cyclohexyldiphenylphosphine complexes also resulted in apoptotic cell death in SNO cells with IC_{50} values of less than 5 µM (Potgieter *et al*., 2017).

Forming part of these studies, while investigating the effects of silver(I) phosphine treatment on the expression of various genes, it was found that there was a down-regulation in genes participating in the metastatic pathway. These genetic studies were carried out on A375 melanoma cells (Jenkins, 2015), SNO cells (Engelbrecht, 2017) and MCF-7 cells (Ferreira, 2015). A summary of the genes involved in tumour metastasis that were found to be down-regulated in the abovementioned studies can be found in Table A1 (Appendix A). These findings have led to question whether these complexes might have anti-metastatic properties *in vitro* in addition to their cytotoxic effects, forming the basis of this research which is now being continued at the University of the Witwatersrand.

Hypothesis

Previous studies have shown that three silver(I) phosphine complexes (UJ1, UJ2 and UJ3) caused a down-regulation of genes participating in the metastatic cascade of several human cancer cell lines (A375 melanoma, SNO oesophageal and MCF-7 BC cell lines).

Here, it is thus hypothesised that these complexes (UJ1, UJ2 and UJ3) along with six related silver(I) phosphine complexes (UJ50, UJ92, UJ102, UJ115, UJ116 and UJ118) will have the ability to reduce the *in vitro* metastatic potential of two malignant human BC cell lines, MCF-7 and MDA-MB-231.

Aims and Objectives

Aim

The overall aim of this study was to investigate whether a selected collection of silver(I) phosphine complexes, that have shown cytotoxic activity against other cancer cell lines, have the ability to reduce the metastatic potential of two malignant human BC cell lines *in vitro*. In addition to UJ1, UJ2 and UJ3, six related silver(I) phosphine complexes (UJ50, UJ92, UJ102, UJ115, UJ116 and UJ18) that have shown cytotoxicity towards MCF-7 and MDA-MB-231 cell lines, were also assessed for their anti-metastatic properties. To achieve this, several characteristics of metastatic cells were evaluated *in vitro* in response to each silver(I) phosphine complex. If any of the complexes showed a promising reduction in BC metastatic potential *in vitro*, key proteins involved in metastasis were assessed for determination of the anti-metastatic mechanism of action of the silver(I) phosphine complexes.

Objectives

1) Sub-lethal concentrations of silver(I) phosphine complexes were determined for commencement of metastasis studies.
2) The abilities of the silver(I) phosphine complexes to inhibit *in vitro* cancer cell migration using the wound healing/scratch assay were assessed.
3) The abilities of the silver(I) phosphine complexes to reduce or inhibit *in vitro* invasion through collagen type I were evaluated with the use of the Transwell® invasion assay.
4) Whether the silver(I) phosphine complexes led to a change in the *in vitro* cell adhesion to collagen type I was investigated.
5) The *in vitro* (a) anchorage-dependent and (b) -independent colony-forming abilities of cancer cells after treatment with silver(I) phosphine complexes were assessed.
6) Possible changes in the expression levels of MMP-2 and -9 were quantified through the use of western blot analyses.
7) Possible changes in MMP activity were detected using substrate zymography.

Chapter 2: Methodology

A complete list of manufacturers is presented in Appendix B. Except where otherwise stated, prior to use reagents were warmed to 37°C.

2.1 Cell culture

Two human BC cell lines were used for this study, the poorly invasive MCF-7 (Cellonex™, SA) and the highly invasive MDA-MB-231 cell line (gifted by Dr Eloise van der Merwe at WITS University). Cells were cultured from frozen stocks (-80°C; denoted as p0), and maintained in 13.53 g/L Dulbecco's Minimal Essential Medium (DMEM) containing 3.7 g/L $NaHCO_3$ (pH 7.45). Growth media was supplemented with 5% (v/v) heat-inactivated foetal calf serum (FCS; 56°C for 30 min) and 1% penicillin / streptomycin / fungizone antibiotics and maintained at 37°C under humidified and sterile conditions supplied with 5% CO_2.

Subculturing of cells was performed every two to four days. Cells were rinsed using Hanks Balanced Salt Solution (HBSS) with $NaHCO_3$ (0.35 g/L, pH 7.45) and detached from culture flasks via a Trypsin (1%) / Versene (0.1%) mixture and incubation for 1 – 2 min (37°C). Cells were then centrifuged at 400 *xg* (4 min) and re-suspended in fresh growth media.

Frozen cell stocks were prepared by collecting cells from a confluent cell-culture flask (through trypsinization and centrifugation, as described above). Cell pellets were re-suspended in FCS containing 10% dimethyl sulphoxide (DMSO), transferred to cryovials and kept frozen (-80°C). Two cell stocks (1 mL each) were made from one confluent flask; consequently the concentration of cells present in cryovials varied as it was dependent on the confluency of the flask.

Sterile conditions were maintained with the use of a tissue culture hood decontaminated with UV, ethanol (70%) and sodium hypochlorite (10%) solutions. Before use, all liquid reagents were filtered (0.2 micron) and glassware was autoclaved.

2.2 Cell seeding

Once pelleted, a Trypan Blue (0.4%) and NaCl (0.81%) solution was used to count cells (cell sample: Trypan blue solution 1:1) and determine their viability using a Countess™ automated cell counter. Cell solutions with a viability of > 80% were seeded into 96-well culture plates (100 µl of cell solution per well i.e. 3 x 10^4 MCF-7 cells or 2 x 10^4 MDA-MB-231 cells per

well) or 3 cm Petri dishes (3 mL/dish i.e. 9 x 10^5 MCF-7 cells or 6 x 10^5 MDA-MB-231 cells per dish). Plates were incubated overnight (37°C) to allow for cell attachment, after which growth media was replaced and the respective treatments added. Following another 24 hr incubation to allow for the uptake of treatments, cells were collected for evaluation. Unless stated otherwise this was done using Trypsin / Versene solution to detach cells, followed by centrifugation for 4 min at 400 *xg*. Cell pellets were re-suspended in DMEM supplemented with FCS (5%M) or in serum-free DMEM (SFM), depending on the requirements of the assay. Three independent biological repeats of each treatment were carried out for each assay along with 1, 2 or 3 technical repeats each.

2.3 Preparation of treatments

Silver(I) phosphine complexes were provided by Prof Reinout Meijboom (Department of Chemical Sciences, UJ) as part of a collaboration with UJ. Stock solutions of 1 mM were made in cell culture grade DMSO followed by incubation at 70°C in a heating block for 60 – 90 min. Stock solutions of 3.33 mM CDDP were prepared in filtered saline solution (freshly prepared every two weeks). Solutions were stored at 4°C protected from light and warmed to 70°C in a heating block for 30 min prior to use. Reference cell solutions comprised of an untreated control (no treatments, UC) as well as a vehicle control (0.125% or 0.25% DMSO in DMEM for MCF-7 and MDA-MB-231 cells, respectively; VC). Details on the synthesis and chemical characterisation of complexes as well as complex structures can be found in Appendix C.

2.4 Confirmation of sub-lethal silver(I) phosphine treatment concentrations

Cells seeded in 96-well culture plates (3 x 10^4 MCF-7 cells or 2 x 10^4 MDA-MB-231 cells per well) were treated with 1.25 µM (MCF-7) or 2.5 µM (MDA-MB-231) of each respective silver(I) phosphine complex or 12.5 µM (MCF-7) or 25 µM (MDA-MB-231) CDDP prepared in 5%M and incubated for 24 or 48 hr at 37°C. These sub-lethal treatment concentrations were obtained from Dr. Kim Roberts (Roberts, 2023) and Dr. Zelinda Engelbrecht (Z Engelbrecht, personal communication, May 30, 2021). AlamarBlue™ dye (10 µl) was added to cell solutions and plates were incubated at 37°C for a further 2 hr protected from light. The fluorescence of the cell solutions was then determined (530/30 nm excitation; 580/20 nm emission) using a VICTOR® Nivo™ multimode plate reader.

Cell viability at these treatment conditions were further evaluated after 24 hr treatment in 5%M and SFM using a Trypan Blue (0.4%) and NaCl (0.81%) solution and a Countess™ automated cell counter

2.5 Metastasis studies

2.5.1 Scratch / wound healing assay

Cells were added to 3 cm Petri dishes and incubated overnight to form a confluent monolayer. A wound was made in the monolayer using a sterilized 100 µl plastic pipette tip. Cell layers were gently washed with SFM to remove loose cells and cellular debris followed by treatment with the respective complexes in SFM. Light microscopy images (40X magnification) were then captured at 0 and 24 hr. A reference line was drawn on the bottom of each plate to ensure that subsequent images were taken at the same position. Images were analysed using ImageJ® software (freely available at https://imagej.nih.gov) and a *Wound_healing_size_tool* plugin feature. This plugin may be found at https://github.com/AlejandraArnedo/Wound-healing-size-tool/wiki, obtained from Suarez-Arnedo *et al.*, 2020. The total area of the wound at each time point was calculated as a percentage value of the total area of the image. The total wound closure over the selected time-period was then calculated (area at 0 hr – area at 24 hr). Finally, this value was converted to a percentage of the VC (set at 100%).

2.5.2 Transwell® invasion through collagen type I

Confluent cell culture flasks were serum-starved by incubation in SFM (24 hr, 37°C) while Transwell® inserts (polyester (PET) membrane, 8 µm pore size) were inserted into 24-well plates and incubated overnight (4°C) with 100 µL collagen type I (200 µg/mL dissolved in dH_2O containing 2 µL acetic acid). The next day, the cells were collected and a concentration of 3 x 10^5 cells/mL for MCF-7 or 2 x 10^5 cells/mL for MDA-MB-231 (100 µL per insert) in SFM was added to each Transwell® insert. Cells were incubated for 2 hours at 37°C to allow them to settle before the respective treatments were added. Treatment of samples involved preparing 2X concentration treatments in SFM after which 100 µl of each treatment was mixed with the cells in the insert, resulting in a 1X final treatment concentration (i.e. 1.25 µM silver(I) phosphine complexes or 12.5 µM CDDP for MCF-7 cells and 2.5 µM silver(I) phosphine complexes or 25 µM CDDP for MDA-MB-231 cells). Into the lower compartment, 750 µL of DMEM supplemented with 10% FCS (10%M) was added and

inserts were incubated for 48 hr (37°C). The layer of collagen in the upper compartment mimics part of the ECM through which cells must invade before being able to transverse through the pores towards the chemoattractant (10% FCS). After incubation, conditioned media in each Transwell® was discarded and cells were fixed onto the membrane with 4% formaldehyde in HBSS (20 min, 37°C) followed by staining with 0.05% crystal violet (CV) in dH_2O (30 min, room temperature (Rt)). Cells that were present on top of the membrane representing cells that have not invaded through the collagen layer were removed by gentle scraping with a cotton tip (until the tip was no longer stained purple, to ensure removal of all non-invaded cells). Transwell® inserts were then incubated in a 24-well plate containing 750 µL of 10% acetic acid to extract the CV dye after which absorbance of the solutions were read at 595 nm using a VICTOR® Nivo™ multimode plate reader. An UC cell sample, added to a Transwell® without prior addition of collagen, was included and served as a migration control to ensure collagen coating of porous membranes.

2.5.3 ECM adhesion

The cells, untreated (UC) or treated (1.25 µM silver(I) phosphine complexes or 12.5 µM CDDP for MCF-7 cells and 2.5 µM silver(I) phosphine complexes or 25 µM CDDP for MDA-MB-231 cells) for 24 hr in SFM were plated in 3 cm Petri dishes (3 mL/dish i.e. 9 x 10^5 MCF-7 cells or 6 x 10^5 MDA-MB-231 cells per dish). Cells were removed from dishes, pelleted and re-suspended in fresh SFM before the cells were counted using a Trypan Blue dye / NaCl solution and an automated cell counter. In order to avoid degradation of key cell surface proteins needed for adhesion, cells were removed with a cell scraper instead of trypsinization. Collagen coated 96-well culture plates were prepared by overnight incubation at 4°C with 20 µg/mL collagen type I (prepared in dH_2O containing 2 µl acetic acid) to allow the binding of collagen to culture plates. The next day, excess collagen solution was removed and a blocking solution (1% BSA in dH_2O; 200 µl per well) was added. This was once more incubated at 37°C for 1 hr before the addition of cells. Respective cell solutions containing a total number of 3 x 10^5 cells/mL for MCF-7 and 2 x 10^5 cells/mL for MDA-MB-231 cells prepared in SFM were added to the collagen-coated plate (100 µl per well). Cells were then incubated for 30 min in a 37°C humidified incubator to allow for cell attachment. Following this, cells were rinsed three times (100 µl) with HBSS to remove all non-adhered and loosely adhered cells, before the remaining adhered cells were fixed using formaldehyde (4%) in HBSS (20 min, 37°C) and stained with 0.1% CV (prepared in dH_2O) for 30 min at Rt. Excess

dye was removed by washing with dH_2O after which CV was extracted through the addition of DMSO. Adhesion was quantified via absorbance measurement (595 nm). Included in each biological repeat were three experimental control samples: 1) UC cell solution added to uncoated wells (no collagen) in order to confirm the presence of collagen in coated wells, 2) UC cells added to wells containing 1% BSA blocking solution only that served as a negative adhesion control and 3) wells stained with 0.1% CV without cells to compensate for the background staining of plastic wells.

2.5.4 Anchorage-dependant colony formation

After detaching seeded cells from 3 cm Petri dishes (3 mL/dish i.e. 9 x 10^5 MCF-7 cells or 6 x 10^5 MDA-MB-231 cells per dish), the cells, untreated (UC) or treated (1.25 µM silver(I) phosphine complexes or 12.5 µM CDDP for MCF-7 cells and 2.5 µM silver(I) phosphine complexes or 25 µM CDDP for MDA-MB-231 cells) for 24 hr, were counted using a Trypan Blue / NaCl solution and an automated cell counter. A solution of 1 x 10^4 cells of each treatment condition was prepared in 5 mL of 5%M. Cell suspension solutions were gently mixed with a pipette ensuring even distribution of cells before addition to a 6-well plate. Plates were then incubated until visible colonies started to form (MCF-7: 10-14 days; MDA-MB-231: 7 days). Following incubation, the spent media was discarded, and the cells were lightly washed with 1X PBS (1 mL, pH 7). Cells were fixed (4% formaldehyde in 1X PBS, 20 min at 37°C) and stained with 0.1% CV in dH_2O for 30 min at Rt. After staining, excess dye was removed by rinsing with dH_2O. Plates were left to dry before imaging. Images were taken with a Bio-Rad ChemiDoc™ image analyzer equipped with Image Lab™ software, v 5.2.1. Images were analyzed using ImageJ® software along with a *ColonyArea* plugin tool (http://www.btk.fi/research/research-groups/abankwa/downloads/; Guzmán *et al.*, 2014) to determine the surface area covered with stained cells for each treatment condition.

2.5.5 Anchorage-independent colony formation

To assess cells' ability to grow without being attached to a substratum, cells were seeded in a low concentration of agarose and DMEM. Agarose solutions were prepared in dH_2O and autoclaved, followed by storage at 4°C. Solidified solutions were heated to 85°C on a heating block and left to cool before use. A 0.5% bottom layer was prepared by mixing 1% agarose solution with equal volumes of 2X DMEM supplemented with 20% FCS. Then 1.5 mL per well of this solution (final concentration: 0.5% agarose in DMEM with 10% FCS) was added

to a 6-well plate. Plates were left at Rt for 30 min to allow agarose-DMEM solutions to set. The cells (treated/untreated for 24 hr) that were detached from Petri dishes were counted (Trypan Blue / NaCl solution) and solutions of 1 x 10^4 cells of each respective treatment condition in 750 µL of 2X DMEM supplemented with 20% FCS were prepared. This was mixed with an equal volume of 0.6% agar and added to a 6-well plate (1.5 mL per well) on top of the bottom layer (final concentration 0.3% agarose in DMEM with 10% FCS and 1 x 10^4 cells). Plates were incubated at Rt for 30 – 40 min to allow for solidification of the top layer after which 250 µl of supplemented DMEM (10% FCS) was added on top to prevent the drying of agarose. Cell-agarose solutions were incubated at 37°C until sizeable colonies were noticeable with the naked eye (MCF-7: 10 – 14 days; MDA-MB-231: 7 – 10 days). Four representative light microscopy images of each treatment condition were taken and the numbers of colonies present in each image were counted manually. The area of each colony was also determined using ImageJ® software using the built-in area determination function. A hand-drawn grid was used when taking images to ensure that images were taken at the same position for each treatment condition.

2.6 Anti-metastatic mechanism of action of selected complexes

2.6.1 Isolation and quantification of cell proteins

Cells seeded and treated in SFM for 24 hr (1.25 µM silver(I) phosphine complexes or 12.5 µM CDDP for MCF-7 cells and 2.5 µM silver(I) phosphine complexes or 25 µM CDDP for MDA-MB-231 cells) were removed from 3 cm Petri dishes (3 mL/dish i.e. 9 x 10^5 MCF-7 cells or 6 x 10^5 MDA-MB-231 cells per dish) with a plastic cell scraper. The cells were pelleted through centrifugation (400 *xg*, 4 min) followed by re-suspending the cell pellets in radioimmunoprecipitation assay (RIPA) buffer (100 µL) and incubating them at 4°C for 15 min before being stored (-20°C).

Total protein was quantified using Amido black dye. Protein dots of 1.5 µl were spotted (in duplicate) on a nitrocellulose membrane. Membranes were then washed in 50% methanol (5 min, Rt) and stained with Amido black solution for 5 min (Rt) followed by additional washing in 50% methanol (three times) to remove excess dye. Cut out protein dots were incubated in 0.1M NaOH (800 µL) for 2 hr with gentle agitation before absorbance was read at 600 nm. BSA prepared in PBS (0.625 - 5 mg/mL) was used for the construction of a standard curve from which the protein concentration was determined.

2.6.2 Western blot analyses to evaluate MMP-2 and -9 expression levels

Protein samples were combined with 2X Laemmli buffer (1:1) containing 2.5% β-mercaptoethanol and protease inhibitors (one tablet for each 30 mL Laemmli buffer). The protein samples were heated to 95°C for 15 min. A total amount of 15 to 75 µg protein from each treatment condition was separated on a polyacrylamide gel (10%) at 15 mA per gel together with a standard protein marker (10 - 250 kDa) for identification of molecular mass. Electrophoresis buffer was made up of tris (25 mM), glycine (192 mM) and SDS (1%). After electrophoresis, the gels were rinsed with Towbin buffer, made from tris (25 mM), glycine (192 mM) and methanol (20%), for 15 min and transferred to a polyvinylidene difluoride (PVDF) (Immun-Blot®) membrane at 70 V for 1 hr (4°C). Prior to transfer, the PVDF membrane was activated in 100% methanol, rinsed three times with dH_2O and left in Towbin buffer for 20 min with gentle agitation. Following transfer, membranes were rinsed two times in 1X TBS buffer made with tris (5mM) and NaCl (15 mM), pH 7.5, before being incubated in blocking solution (2.5% or 5% skimmed milk in TBS (SM-TBS)) for 1 hr at Rt. Primary (1°) antibody (Ab) prepared in blocking solution was added to membranes and these were incubated at 4°C overnight with gentle agitation. Following 1°Ab binding, membranes were rinsed three times (10 min each) with TBS-T buffer (1X TBS with 0.1% Tween-20) and incubated with blocking solution for 10 min (this was repeated twice using fresh blocking solution each time). Secondary (2°) Ab prepared in blocking solution was added to membranes and these were incubated for 1 hr with gentle agitation at Rt. Membranes were washed four times for 15 min each time with TBS-T after which they were developed for 5 min using the Clarity™ western ECL Substrate (peroxide:luminol/enhancer solution, 1:1). Images were captured with a Bio-Rad ChemiDoc™ image analyzer with Image Lab software (v 5.2.1). Conditions and blocking solutions for individual Abs are summarised in Table 2.1; β-actin was used for normalisation of expression.

2.6.3 Detection of MMP activity through substrate zymography

Conditioned media from cells (untreated (UC) or treated with 1.25 µM silver(I) phosphine complexes for MCF-7 cells and 2.5 µM silver(I) phosphine complexes for MDA-MB-231 cells for 24 hr in SFM) were obtained and total protein was quantified with the use of Amido black dye (section 2.6.1, paragraph 2). One part conditioned media was combined with one part freshly prepared MMP zymography sample buffer (2X stock) containing tris (125 mM), glycerol (20%), SDS (4%) and bromophenol blue (0.005%) (pH 6.8). Equal amounts of protein were separated through SDS-PAGE (8%, 15 mA per gel containing either 0.1%

gelatin (heated at 60°C for 20 min to dissolve), 0.3 µg/mL collagen type I or 1% casein). After separation, gels were rinsed in renaturing buffer (2.5% Triton X-100 in dH_2O) for 30 min with gentle agitation. Gels were then rinsed in developing buffer (tris (50 mM), NaCl (0.2M), $CaCl_2$ (5mM), $ZnCl_2$ (1 µM) and Triton X-100 (1%)) for 30 min. Developing buffer was discarded and gels were incubated in fresh developing buffer (37°C) for 24-72 hr before staining (Coomassie blue R-250 (0.5%), isopropanol (25%) and acetic acid (10%)) for 1 h at Rt. Gels were destained with methanol (50%) and acetic acid (10%) in dH_2O four times (15 min each), until clear bands were observed on a blue background. Images of gels were obtained with a Bio-Rad ChemiDoc™ image analyzer with Image Lab software, v 5.2.1.

Table 2.1 1° and 2°Ab conditions for analysis of MMP-2 and -9 levels in MCF-7 and MDA-MB-231 cells by western blot analysis.

	1° Ab conditions			2° Ab conditions		
	Blocking solution	**1° Ab**	**Dilution (Ab in SM-TBS)**	**Blocking solution**	**2° Ab**	**Dilution (Ab in SM-TBS)**
β-actin	5% SM-TBS	anti-human monoclonal anti-β-actin produced in mouse	1:1000	2.5% SM-TBS	anti-mouse IgG-HRP conjugate produced in goat	1:2500
MMP-2	2.5% SM-TBS	anti-human MMP-2 produced in rabbit	1:500	1.25% SM-TBS	anti-rabbit IgG-peroxidase produced in goat	1:2500
MMP-9	5% SM-TBS	anti-human MMP-9 produced in rabbit	1:500	2.5% SM-TBS	anti-rabbit IgG-peroxidase produced in goat	1:2000

* SM-TBS - skimmed milk in 1X TBS buffer

2.7 Statistical analyses

Values showed were calculated as the average of three independent biological repeats. Error bars on graphs signify the standard error of the mean (SEM). The statistical significance of findings was determined with the student's t-test (two-tailed, type two) with a P value of < 0.05 being regarded as statistically significant or $P < 0.01$ as highly significant. All statistical analyses and construction of graphs were done with Microsoft Excel software.

Chapter 3: Results

Two BC cell lines were chosen to evaluate whether silver(I) phosphine complexes had the potential to aid in preventing the formation of metastases. The potential anti-metastatic effects of these complexes were thus compared between an ER positive cell line with a lower metastatic ability (MCF-7) and a triple negative MDA-MB-231 cell line, representative of an extremely aggressive and highly metastatic type of cancer. MCF-7 cells are a slow proliferating cell line appearing as cuboidal aggregates in culture (observed under light microscopy), while the rapidly proliferating MDA-MB-231 cells appear more elongated, and spindle shaped under light microscopy. The findings of the original MSc and PhD studies (Engelbrecht, 2017; Ferreira, 2015; Jenkins, 2015) that led to the formulation of the hypothesis of this study, were done using three silver(I) phosphine complexes, termed UJ1, UJ2 and UJ3. In addition to these three, six related silver(I) phosphine complexes were also included to assess their potential anti-metastatic effects. As a starting point these complexes, known as UJ50, UJ92, UJ102, UJ115, UJ116 and UJ118, were selected out of a myriad of different silver(I) phosphine complexes, since they were found to be cytotoxic to the MCF-7 and MDA-MB-231 cell lines specifically (studies performed by Dr. Zelinda Engelbrecht and Dr. Kim Roberts). Percentage viability values for the treatment of all nine silver(I) phosphine complexes at 10 µM for 24 hr on MCF-7 and MDA-MB-231 BC cells as well as non-malignant HDF-a, MRHF-1 (human fibroblast) and HEK-293 cells can be found in Table D1 (Appendix D). These studies were performed by Dr. Eloise van der Merwe, Ms Alisha Badal, Dr. Zelinda Engelbrecht and Dr. Kim Roberts). All nine silver complexes were prepared in DMSO, consequently, in addition to UC cell samples, cells treated with DMSO at a concentration equivalent to the final concentration of DMSO in silver(I) phosphine treated cell samples, served as the VC. In addition, CDDP the golden standard of metal containing cytotoxic chemotherapeutic drugs (Ma *et al.*, 2016) was also included for comparison.

3.1 Silver(I) phosphine treatment conditions

To ensure that any subsequent anti-metastatic effects were not a consequence of the cytotoxicity of the complexes towards the cells, non-toxic treatment conditions were used for metastatic studies. To confirm the absence of toxicity the alamarBlue™ dye reduction assay was used for assessment of cellular toxicity through mitochondrial activity. With this assay an indicator dye, alamarBlue™, is enzymatically reduced by mitochondria to produce a

fluorescent signal (De Fries and Mitsuhashi, 1995). The silver(I) phosphine complexes have in the past shown a tendency to target the mitochondria (Engelbrecht *et al.*, 2018), hence the use of mitochondrial activity as an indicator of toxicity. Importantly, in order to fairly compare the effects between the different complexes and keep the treatment conditions with respect to final DMSO concentration the same, one non-toxic concentration across all nine complexes was used for each of the two cell lines. These were 1.25 µM for the treatment of MCF-7 cells and 2.5 µM of each complex for MDA-MB-231 cells. Similarly, non-toxic CDDP treatment concentrations of 12.5 µM and 25 µM for MCF-7 and MDA-MB-231 cells, respectively, were used. Figure 3.1A and B depicts MCF-7 and MDA-MB-231 mitochondrial activity following treatment with the various silver(I) phosphine complexes, DMSO or CDDP at the pre-selected concentrations, demonstrating the lack of statistically significant mitochondrial toxicity at 24 and 48 hr.

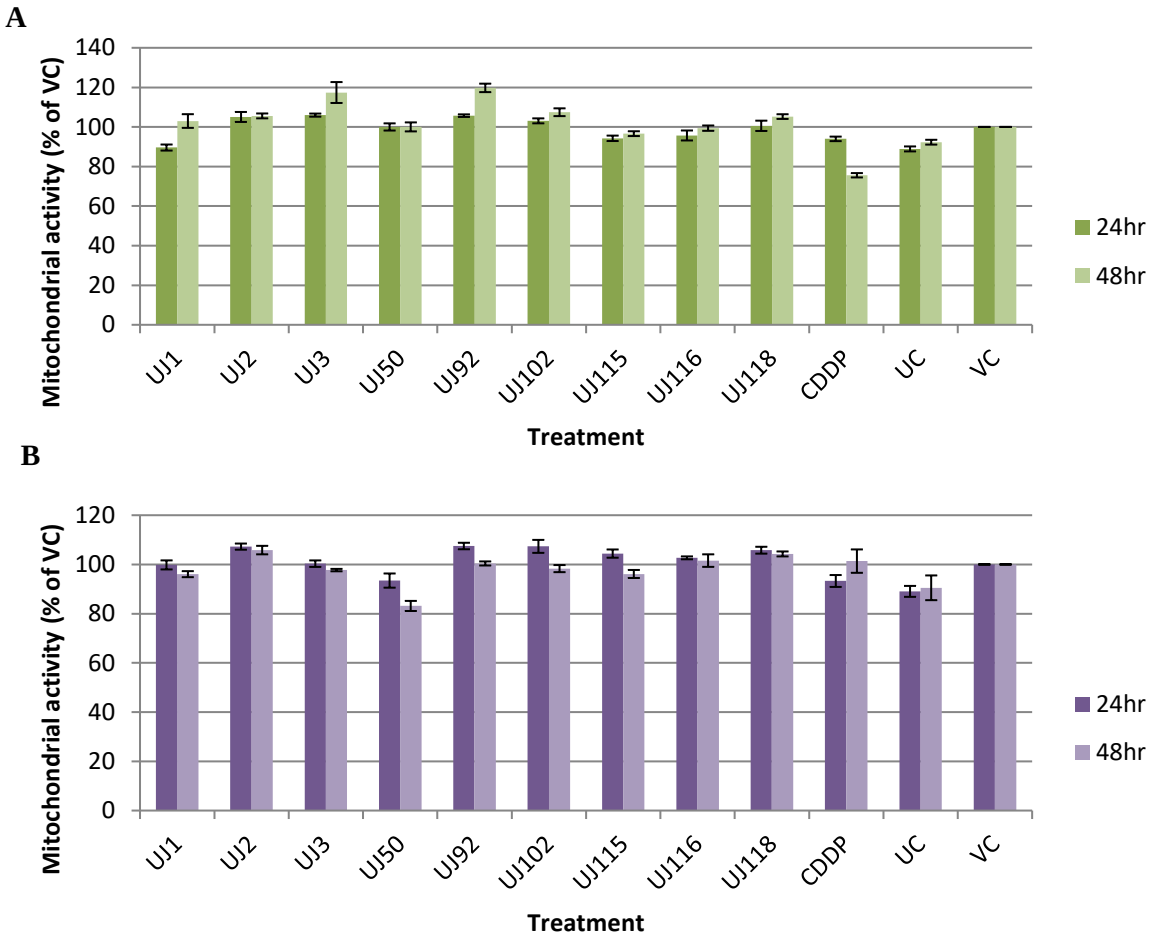

Figure 3.1 Mitochondrial activity of **MCF-7** (A) and **MDA-MB-231** (B) cells treated with 1.25 µM (MCF-7) and 2.5 µM (MDA-MB-231) of silver(I) phosphine complexes for 24 and 48 hr assessed by means of the alamarBlue™ dye reduction assay. Values are displayed as a percentage of the VC (set as 100%). Error bars were constructed based on ±SEM relative to the VC (n=3). No statistical significant effects were observed.

In addition, Trypan blue dye was used to confirm that treatment at the pre-selected concentrations did not result in any damage to the plasma membrane as well as significantly decrease the overall cell viability. Since many of the assays require treatment in SFM, the viability of cells was determined under both serum and serum-free conditions (Figure 3.2A and B).

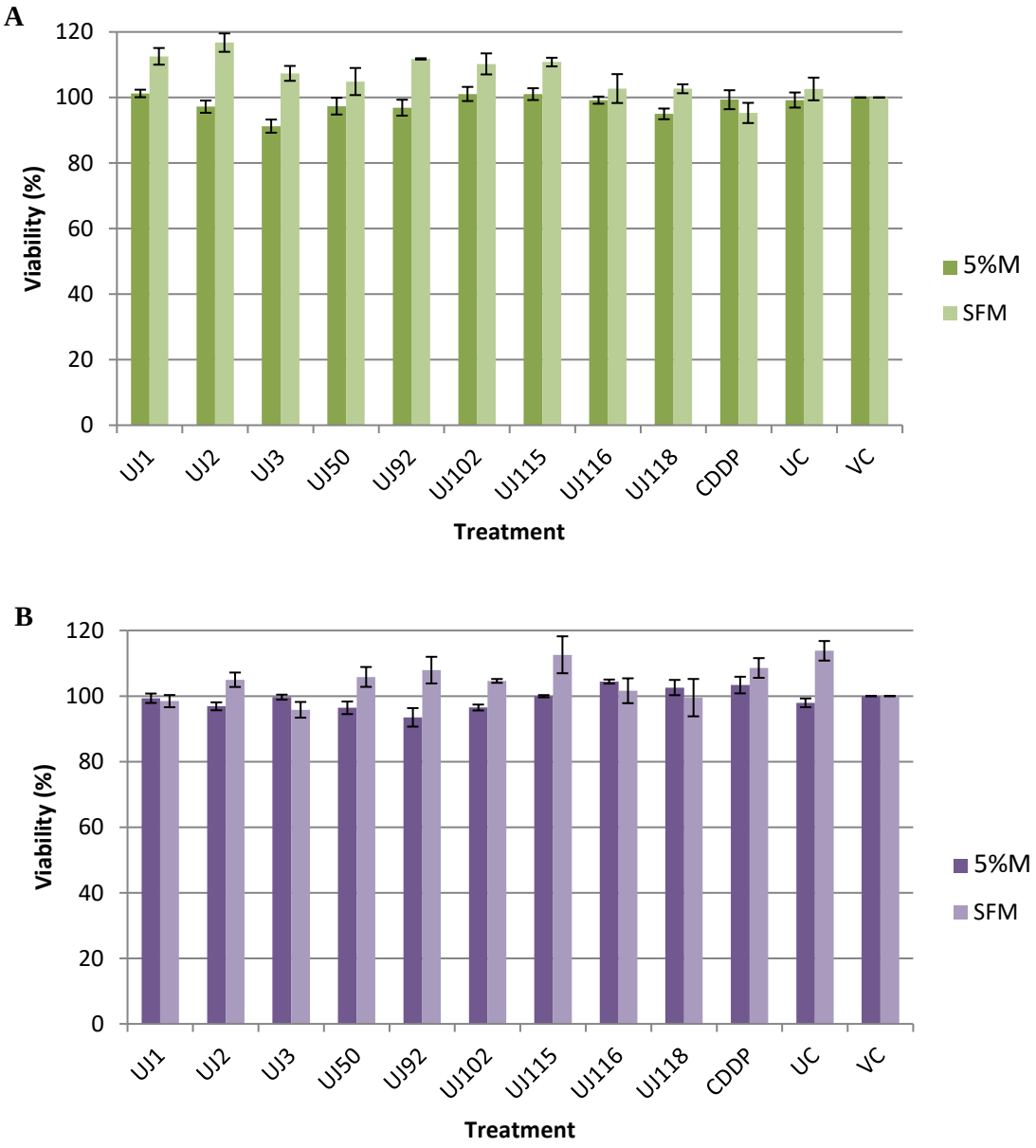

Figure 3.2 Viability of **MCF-7** (A) and **MDA-MB-231** (B) cell populations following silver(I) phosphine treatment at 1.25 µM (MCF-7) and 2.5 µM (MDA-MB-231) for 24 hr. Treatments were prepared in DMEM containing 5% FCS (5%M) or no FCS (SFM). Values are displayed as a percentage of the VC (set as 100%). Error bars were constructed based on ±SEM relative to the VC (n=3). No statistical significant effects were observed.

3.2 Effect of silver(I) phosphine treatment on cell migration

As an important part of the metastatic process, cell migration in response to treatments was assessed with the help of the scratch/wound healing assay during which cells migrated horizontally to attempt to close the wound (Justus *et al.*, 2014). From images taken, the area of the wound at 24 hr was compared to the initial wound area (0 hr). The scratch assay is a simple, inexpensive and widely used method of assessing cell migration which makes it an ideal assay to begin with. Any treatment conditions that might lead to a decrease in the ability of cells to migrate or result in a lower rate of migration, compared to the VC would be beneficial as a potential anti-metastatic treatment.

An important aspect of this assay is the presence of a confluent monolayer of cells. Migration would be affected if the confluency of the cells was too low. To ensure confluency 24 hr after seeding, MCF-7 cells were plated at a higher initial concentration (3×10^5 cells/mL in 3 cm Petri dishes) compared to MDA-MB-231 cells (2×10^5 cells/mL in 3 cm Petri dishes). These concentrations were also used for toxicity studies (Figures 3.1 and 3.2), when optimising treatment concentrations and were kept constant for the remainder of the experiments. Directly following the creation of the wound, the cell monolayer is washed with SFM to remove detached cells and cellular debris. This prevents detached cells from simply re-attaching in the wounded area. Lastly, since scratches are made manually, using a pipette tip, the width of the wounds can vary. Therefore, marks were made at the bottom of the plates to ensure that subsequent photos were taken at the exact same spot each time.

ImageJ software was used to quantify migration after 24 hr and average % wound closure values are displayed in Figure 3.5A and B. The amount of wound closure of the VC was set to 100%, consequently a value of less than 100% would indicate that less of the wound had been closed over the same time period i.e., less migration took place, therefore migration was slowed down by the relevant treatment.

Overall, the degree of migration observed was more for MDA-MB-231 cells compared to the less invasive MCF-7 cells (Figures 3.3 and 3.4). In fact, very little difference in migration in response to most complex treatment was seen after 24 hr in MCF-7 cells (Figure 3.5A).

Only three complexes, UJ92, UJ116 and UJ118, lead to a statistically significant decrease in % wound closure compared to the VC for MCF-7 cells. The decrease seen however is only by 6% for UJ116 and 11% for UJ92 and UJ118. UJ50 showed an average % wound closure similar to the VC while UJ1, UJ2, UJ3, UJ102 and UJ115 tended to lead to a decrease in %

migration although these effects were not statistically significant (Figure 3.5A). Similarly, CDDP treatment did not result in any statistically significant effects on MCF-7 cells (P = 0.186).

A more substantial reduction in % wound closure was seen with MDA-MB-231 cells. UJ2, UJ3, UJ50 and UJ115 resulted in a statistically significant reduction in cell migration (Figure 3.5B). The largest reduction in % migration was seen for UJ3 leading to a 75% reduction (P < 0.001) followed closely by UJ50 resulting in a decrease of 62% (P < 0.001). In addition, CDDP treatment also displayed a significant decrease in migration of MDA-MB-231 cells (53% reduction, P < 0.05). UJ1, UJ92, UJ102 and UJ116 showed a non-significant reduction in migration, while UJ118 showed a similar migration pattern to DMSO-treated cells (VC). Interestingly, for MDA-MB-231 cells, UC cells migrated significantly less compared to cells of the VC with less than half the amount of migration displayed by UC cells. This effect was not seen for MCF-7 cells where UC and VC cell populations showed similar patterns of migration.

3.3 Invasion of cells through collagen type I

Invasion involves the breakdown of the ECM components and plays an important role in the metastatic process, not only during the escape from the primary tumour but also during intravasation and extravasation where cells gain entry to and exit from circulation (Chitty *et al.*, 2018). A modified Boyden chamber assay using Transwell® inserts containing a porous membrane that separates cells from a solution containing a chemoattractant is a commonly used method of mimicking cell migration *in vitro*. When combined with ECM proteins, which must first be broken down by cells before they are able to traverse the membrane, invasion can be mimicked *in vitro* (Justus *et al.*, 2014). Collagen was used to coat porous membranes for this purpose.

Optimisation of experimental conditions consisted of varying the incubation times allowed for invasion to occur as well as varying the number of cells added to the upper chamber. Initially, both MCF-7 and MDA-MB-231 cells were incubated for 24 hr, however very little to no cells was detected below the membrane, so the incubation period was extended to 48 hr. In addition, a range of different cell concentrations applied to the upper chamber was tested and an optimum concentration was established as 3 x 10^5 cells/mL for MCF-7 cells and 2 x 10^5 cells/mL for MDA-MB-231 cells (the same concentration used for toxicity studies). The addition of fewer cells resulted in insufficient cells invading through the collagen layer over

the 48 hr incubation period, with little to no differences between treated and control groups, while more cells (> 3 x 10^5 cells/mL for MCF-7 cells and > 2 x 10^5 cells/mL for MDA-MB-231 cells) made the manual counting of the amount of invaded cells more difficult due to trouble distinguishing individual cells from each other. To serve as validation that Transwells® were successfully coated with collagen solution, a migration control was included. The presence of collagen which the cells would have to degrade before being able to migrate will theoretically result in less traversed cells over the same incubation period compared to the absence of collagen. The amounts of untreated cells present below the membrane after 48 hr for the migration control were considerably higher than the invasion UC sample, confirming the presence of collagen.

Following the quantification of extracted CV dye, a similar trend was seen for both MCF-7 and MDA-MB-231 cells (Figure 3.6). UJ1, UJ2, UJ3, UJ50 and UJ92 all resulted in a decrease in the number of cells able to invade through collagen while the effect of UJ102 was negligible. Interestingly, UJ115, UJ116 and UJ118 as well as CDDP treatment resulted in an increase in invasive ability. For MCF-7 cells, only UJ1 ($P < 0.01$), UJ2 ($P < 0.001$) and UJ92 ($P < 0.05$) however showed a statistically significant reduction of invasive ability, while only UJ118 ($P < 0.01$) resulted in a statistically significant increase in invasion compared to the VC (Figure 3.6 green bars). For MDA-MB-231 cells, all complexes apart from UJ102 resulted in statistically significant effects with UJ50 leading to the greatest decrease (40%, $P < 0.001$) and UJ118 leading to the greatest increase in invasion (60%, $P < 0.001$; Figure 3.6 purple bars). In addition, when comparing cells between the UC and the VC, treatment with DMSO only, seemed to significantly reduce the invasive abilities of both MCF-7 and MDA-MB-231 cells. Interestingly, for both cell lines CDDP treatment seemed to slightly increase average invasive ability; however, this effect was only significant in MDA-MB-231 cells ($P < 0.05$).

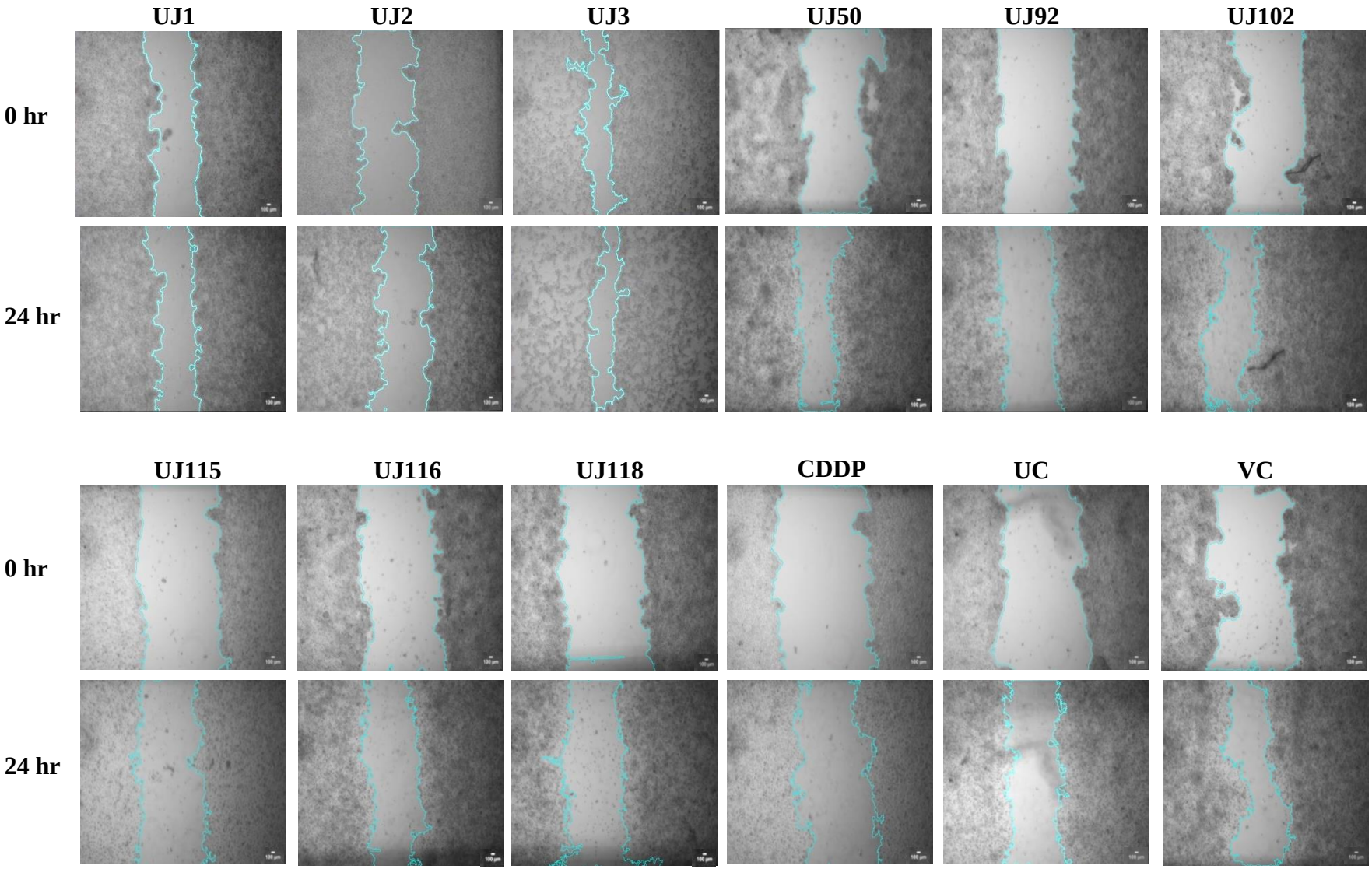

Figure 3.3 Light microscopy images (40X magnification) of **MCF-7** cell migration following silver(I) phosphine treatment in SFM. A vertical wound was created in a confluent monolayer of cells and cell migration was monitored for 24 hr. Scale bars represent 100 µm. Images are representative of one biological experiment.

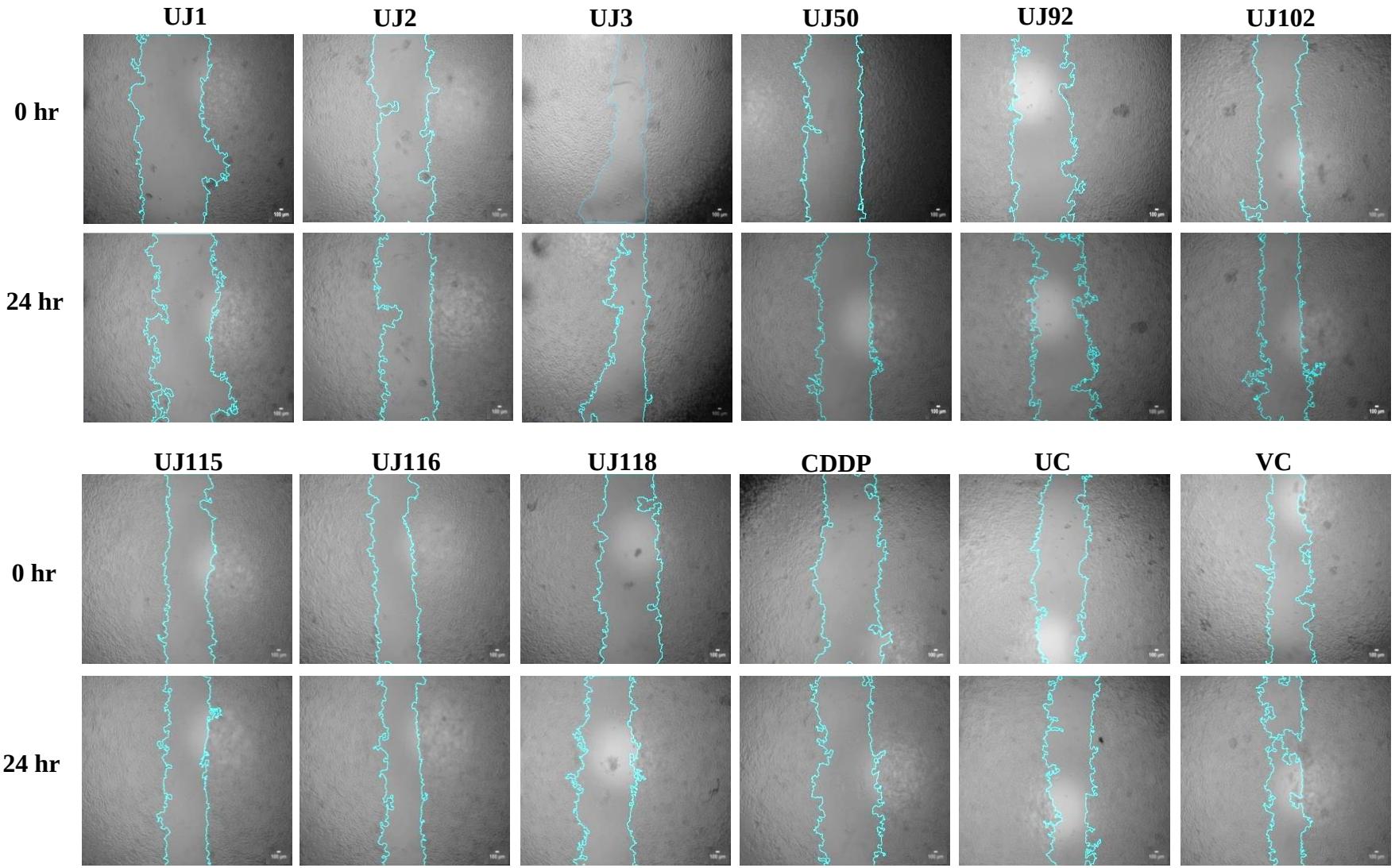

Figure 3.4 Light microscopy images (40X magnification) of **MDA-MB-231** cell migration following silver(I) phosphine treatment in SFM. A vertical wound was created in a confluent monolayer of cells and cell migration was monitored for 24 hr. Scale bars represent 100 µm. Images are representative of one biological experiment.

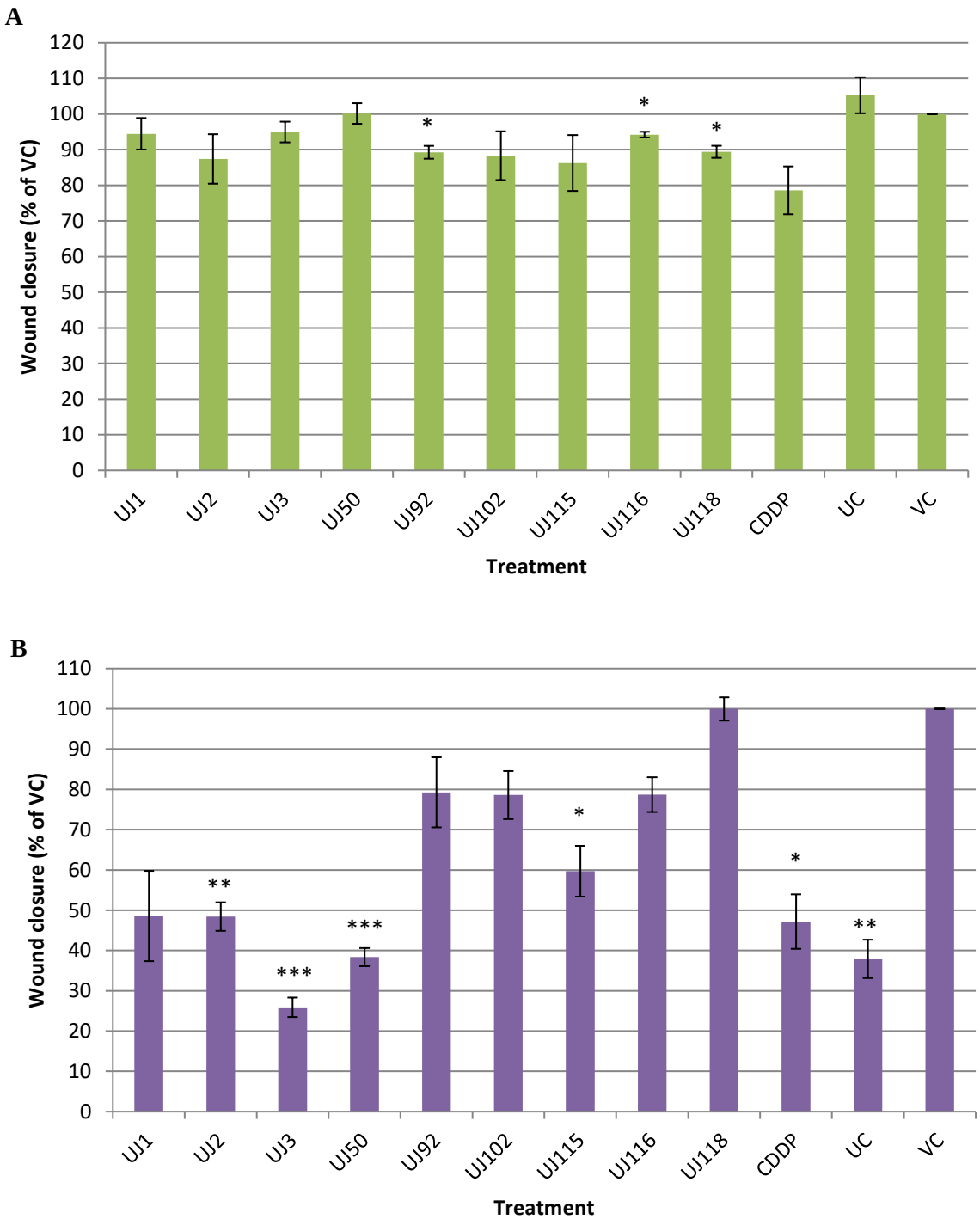

Figure 3.5 The total wound closure over time as quantified using ImageJ® software and the *Wound_healing_size_tool* plugin. Average percentage wound closure of three biological repeats relative to the VC (set as 100%) is displayed for **MCF-7** (A) and **MDA-MB-231** cells (B). Error bars were constructed based on ±SEM relative to the VC (n=3) (* $P < 0.05$, ** $P < 0.01$, *** $P < 0.001$).

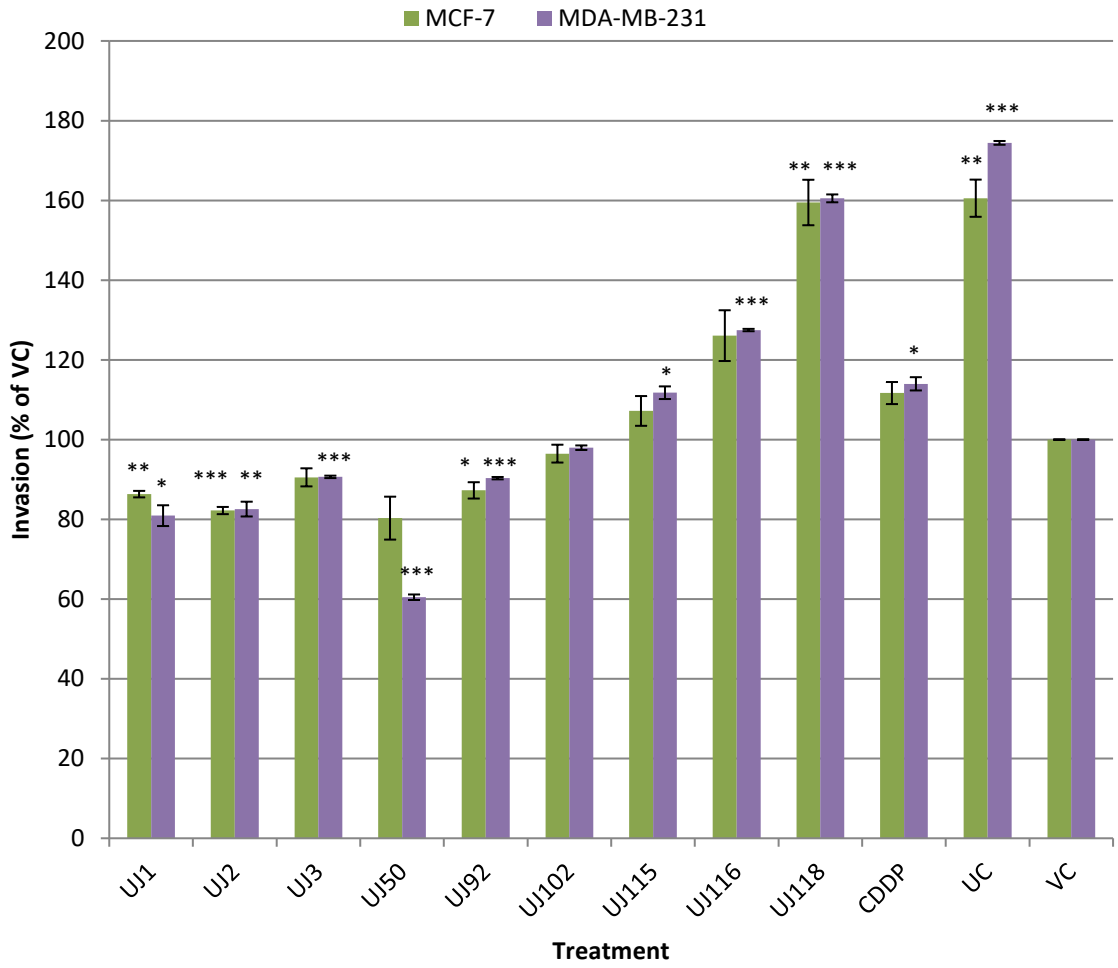

Figure 3.6 CV extracted from cells with 10% acetic acid and quantified through absorbance measurement (595 nm). Values represent the % invasion relative to the VC (set as 100%) for **MCF-7** and **MDA-MB-231** cells. Error bars were constructed based on ±SEM relative to the VC (n=3) (* $P < 0.05$, ** $P < 0.01$, *** $P < 0.001$).

3.4 Cell adhesion to collagen

Collagen was also used to assess the adhesive abilities of cells following treatments. Adhesion of cells to ECM is important in various steps of metastasis including invasion and extravasation where cells interact with endothelial cells, as well as during the formation of secondary colonies (Chitty *et al.*, 2018). Cell culture plates (96-well) were coated overnight at 4°C with various concentrations (10 – 40 µg/mL) of collagen. The optimum adhesion of a UC cell sample was established at 20 µg/mL using the protocol described by Humphries (2001). Included with each experimental repeat were UC cells that were added to wells blocked with BSA only (no collagen). This was included to assess the effectiveness of the blocking solution. Absorbance values of ≤ 1% of those values obtained for positive control samples (UC cells + collagen coated + blocked with BSA) were considered acceptable. In

addition, the UC cells adhered to uncoated wells without blocking solution was also included. Absorbance values of these samples, where the cells had adhered to the culture plate, were consistently lower than those of cells that adhered to the collagen coated wells. Cells more readily adhere to surfaces coated with ECM extract (Somaiah *et al.*, 2015), hence confirming the presence of collagen. Lastly, before quantification, all wells were washed with HBSS to remove non-adhered or loosely adhered cells, ensuring only those cells with a tight interaction to collagen were quantified.

Quantification of the adhered cells following treatment was done by staining cells with CV. Absorbance values were then converted to a percentage value of the VC and represented in Figure 3.7A and B. Thus, an average absorbance value of 57% for example (UJ1, MCF-7 cells; Figure 3.7A) would mean that there is a 43% reduction in the number of cells that adhered to collagen, for the silver(I) phosphine treated sample compared to the VC when equal amounts of cells were added.

For both cell lines, all the silver(I)-complexes resulted in a decrease in cell adhesion, however, a more pronounced effect was seen with MCF-7 cells. For MCF-7 cells, treatment with all the silver(I) phosphine complexes except for UJ2 and UJ115 led to a statistically significant reduction in cell adhesion (Figure 3.7A) with UJ92 and UJ102 producing the greatest effect (78% and 74% reduction, respectively; $P < 0.001$). Only UJ50, UJ92, UJ102 and UJ115 showed a similar significant decrease in MDA-MB-231 cells (Figure 3.7B) with UJ50 and UJ92 producing the greatest reduction (50% reduction for UJ50; $P < 0.01$ and 58% reduction for UJ92; $P < 0.001$). The effects of CDDP on the adhesion of MCF-7 cells were negligible (Figure 3.7A) while CDDP treatment caused a decrease in MDA-MB-231 cell adhesion, however, the effects were not significant (Figure 3.7B).

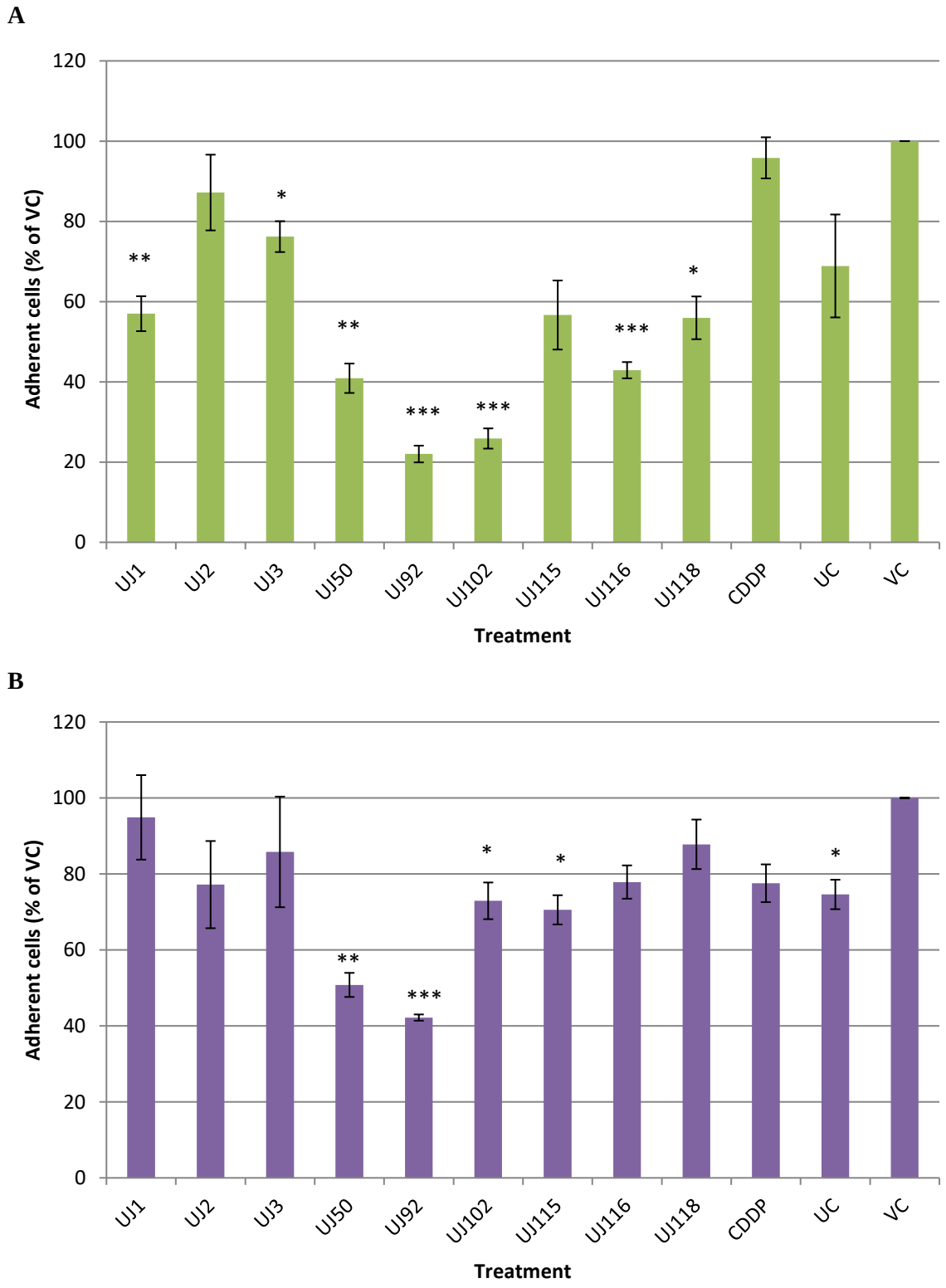

Figure 3.7 Adhesion of **MCF-7** (A) and **MDA-MB-231** (B) silver(I) phosphine treated cells to collagen type I following incubation for 30 min at 37°C and stained with CV. CV was extracted with DMSO and absorbance values (595 nm) of solutions were determined. Values are represented as the average absorbance relative to the VC (set as 100%). Error bars were constructed based on ±SEM relative to the VC (n=3) (* $P < 0.05$, ** $P < 0.01$, *** $P < 0.001$).

3.5 Colony forming abilities under anchorage-dependent and independent conditions

Once metastatic cells have succeeded in travelling through the circulatory or lymphatic system and exited blood or lymph vessels through extravasation, they need to be able to colonise the secondary site to form additional tumour masses. Colonisation is often described as the rate-limiting step of metastasis (Hapach *et al.*, 2019).

To assess a possible reduction in the ability of individual cells to proliferate and form sizeable colonies, a colony formation assay was carried out. Following 24 hr treatment with silver(I) phosphine complexes, a small subset (1×10^4) of cells was seeded in single cell suspension. Gentle dispersion of the cell sample using a pipette was done to disperse any cell aggregates that may have formed. Prolonged incubation (1 – 2 weeks) in supplemented media (5%M) allowed cells to proliferate and form colonies both when attached to a cell culture dish (colony formation assay) and in the absence of attachment, embedded in a semi-solid matrix consisting of agarose and supplemented culture medium (soft agar assay).

For both the above-mentioned assays, cells were pre-treated with the respective treatments for 24 hr before being detached, counted and added to culture plates or mixed with agarose. Often in literature this is done differently, where a low concentration of cells is added to culture plates or embedded in agarose and only then the treatments are added (Franken *et al.*, 2006). This was not done in this study for two reasons. Firstly, sub-lethal treatment concentrations were established at a higher cell concentration (3×10^5 and 2×10^5 cells/mL for MCF-7 and MDA-MB-231 cells, respectively). The effect of those concentrations on the reduced number of cells (1×10^4 cells/mL) used for the colony forming assays are unknown. In addition, cytotoxicity studies of the effects of the sub-lethal concentrations were only done up to 48 hr. Thus, it remains unknown whether any of the treatments may only show cytotoxicity over longer incubation periods such as those necessary for colony formation from a single cell (1 – 2 weeks). These factors could negatively affect the interpretation of the results and thus the choice was made to use pre-treated cells.

For both colony formation and soft agar assays the ideal number of cells was optimised by seeding a range of 1×10^3 – 2×10^4 cells with varying incubation times. With the addition of 1×10^3 cells to each well of a 6-well plate, no visible colonies were seen for either cell line after 21 days of incubation. In contrast, an amount of 2×10^4 cells per well resulted in noticeable colonies after 7 days of incubation but a large amount and overlapping of the

colonies, especially with MDA-MB-231 cells, made analysis difficult. A total number of 1 x 10^4 cells were thus seeded for both assays per treatment condition.

Findings for the colony formation assay were quantified with the use of ImageJ software and the *ColonyArea* plugin. This application determines the area of a standard cell culture well (6-, 12- or 24-well plate) that is covered with cells and gives a colony area percentage value for each treatment condition. Representative images of anchorage-dependent colony forming abilities of MCF-7 and MDA-MB-231 cells are shown in Figure 3.8A and B, while average colony area values shown as a percentage of the VC were displayed in Figure 3.9A and B. Overall, the rate of colony formation as well as the total percentage colony area was considerably lower for MCF-7 cells even after an incubation period of twice as long compared to MDA-MB-231 cells.

For MCF-7 cells UJ1, UJ3, UJ102 and UJ115 all showed a significant reduction in colony area percentage. Surprisingly, complex UJ2, UJ92, UJ116 and UJ118 all increased the colony area percentage values compared to the VC; however, the effects were only statistically significant for UJ116. CDDP treatment resulted in a negligible change in MCF-7 cell colony forming abilities compared to the VC. The UC cells resulted in a larger colony area percentage value compared to the VC, but these were not statistically significant (Figure 3.9A).

For MDA-MB-231 cells, UJ3, UJ50, UJ102, UJ115 and UJ116 significantly reduced cells' colony forming abilities compared to the VC (Figure 3.9B). UJ2, UJ92 and UJ118 showed an average increase in colony area percentage value; however, these values did not reach statistical significance. CDDP treatment significantly decreased the colony forming abilities of MDA-MB-231 cells to a greater extent than any of the silver(I) phosphine complexes, with an 83% reduction ($P < 0.001$). The greatest significant reduction in colony area values for the silver(I) phosphine complexes in MDA-MB-231 cells were seen for UJ3 ($P < 0.001$) and UJ115 ($P < 0.05$) which both resulted in an average of 38% surface area of the well covered by cell growth compared to the VC, however, this value is still more than double the colony area percentage value of CDDP treated cells (17%). For MDA-MB-231 cells no significant difference was seen between UC cells and VC cells.

Cells embedded in a layer of agarose and DMEM supplemented with 10% FCS was used to look at the potential of silver(I) phosphine treatments to reduce the ability of cancer cells to not only survive but proliferate in the absence of attachment to the ECM or to neighbouring

cells. This ability is an important feature of cancer cells that enables them to survive after detachment from the primary tumour and subsequent spread through the circulatory or lymphatic systems to establish secondary metastatic lesions (Chitty *et al.*, 2018). Once again, a low concentration of cells in single cell suspension (1 x 10^4 cells per treatment condition) was used; however, here they were mixed with an agarose-DMEM solution which was added onto a bottom layer of 10%M and agarose. This bottom layer prevents the attachment of cells to the bottom of the culture dish..

Once again there was a marked difference between the two cell lines of varying metastatic potential (Figures 3.10 and 3.11). MCF-7 cells produced fewer, as well as smaller colonies (Figure 3.10) despite an incubation time of twice as long as that of the highly invasive MDA-MB-231 cells (Figure 3.11). For each treatment condition, a grid drawn on a transparent sheet was used to count the number of colonies present in four areas in the centre of each well. The average number of colonies for each experimental repeat was calculated and is expressed as a percentage of the VC (Figures 3.12 and 3.13).

For MCF-7 cells there was a slight difference in the appearance of colonies when observed under light microscopy. For each treatment condition, there was a small variation in the overall sizes of the colonies, however, those treated with UJ115, UJ116 and UJ118 were overall larger than those treated with the other complexes. They were however not larger than those of the VC (Figure 3.10). Most of the silver complexes resulted in a reduction of the average number of colonies formed with two complexes: UJ2 and UJ116 showing a statistically significant effect (Figure 3.12). The greatest reduction in colony formation was observed in the cells treated with CDDP (61% reduction, $P < 0.01$). In contrast to the anchorage-dependent colony formation assay, none of the treatments resulted in the formation of more colonies than the VC population with little difference between the VC and UC.

In contrast to MCF-7 cells where there was no visible difference in the colour of the growth media after 2 of weeks of incubation, obvious differences were seen for MDA-MB-231 treated cells in terms of the colour of the growth media following incubation for 7 days. UC samples as well as cells treated with UJ92 and UJ118 appeared yellow. Media from those colonies formed from cells treated with the VC as well as UJ102 had orange coloured media, while cells treated with UJ50, UJ115, UJ116 as well as CDDP were a light pink colour.

When the colonies were visualised under the light microscope, the UC and VC ones appeared considerably larger with colonies often overlapping and growing over each other making it difficult to distinguish individual colonies. In contrast, the cell samples treated with UJ1, UJ3, UJ50, UJ115 and UJ116 as well as CDDP were much smaller than those of the VC, corresponding to the light pink colour of the media. In addition, a visible reduction in the number of colonies formed was seen for CDDP treated samples compared to the VC (Figure 3.11).

Treatment of MDA-MB-231 cells with UJ1, UJ2, UJ3 and UJ50 did not show any significant effect on average % colony formation in soft agar. In contrast to the observation of the drastic change in colour of the culture media, UJ92 treated cell solutions had significantly less ($P < 0.001$) colonies compared to the VC (Figure 3.13). Furthermore, UJ102, UJ115, UJ116 as well as CDDP treatment also significantly reduced the average number of colonies formed with UJ115 showing the greatest effect (55% reduction, $P < 0.01$). MDA-MB-231 cells treated with UJ118 showed an increase in the number of colonies formed however these values did not reach statistical significance.

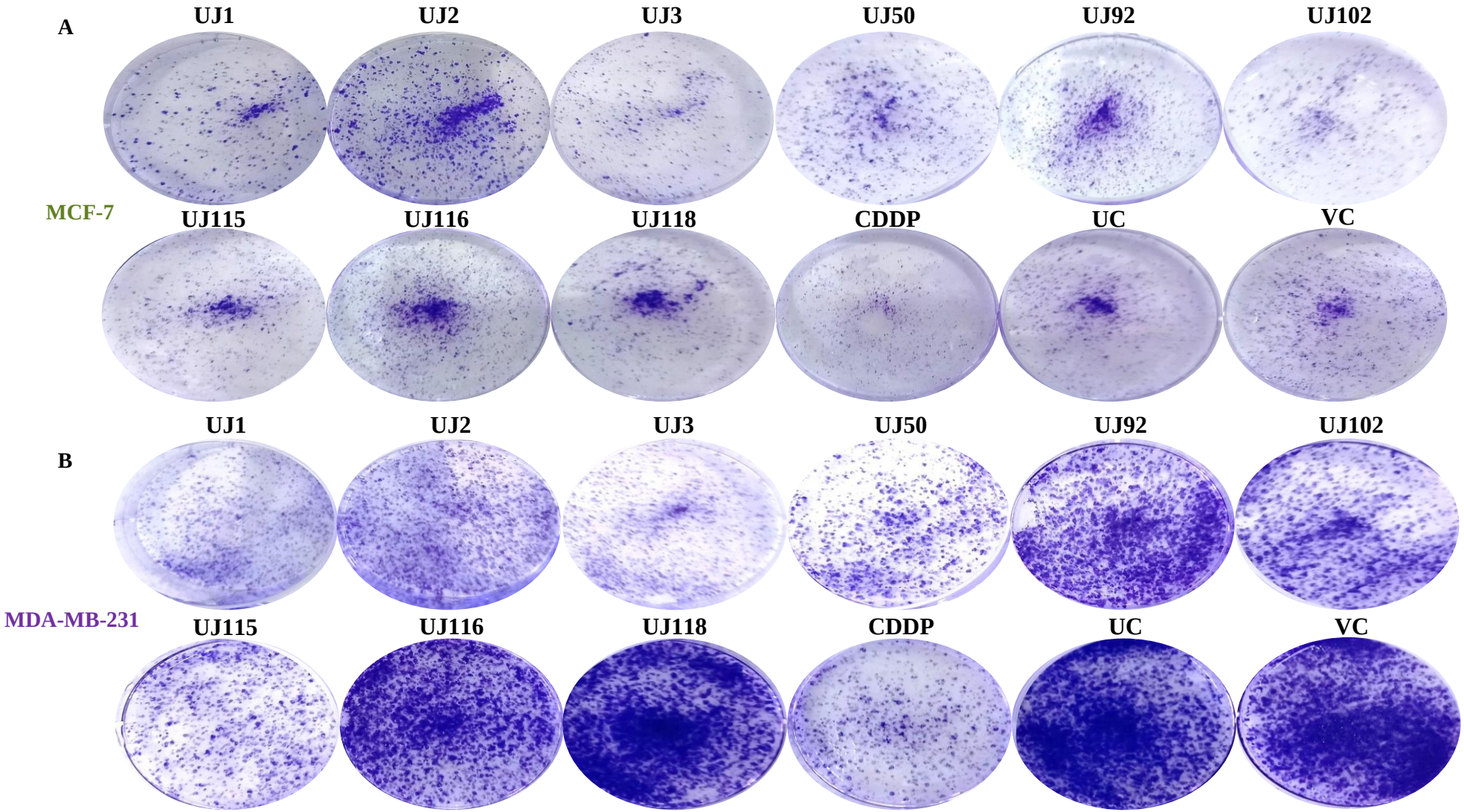

Figure 3.8 Colony forming abilities of **MCF-7** (A) and **MDA-MB-231** (B) cells treated with silver(I) phosphine complexes following incubation for 14 (MCF-7) or 7 (MDA-MB-231) days. Images are representative of one biological experiment.

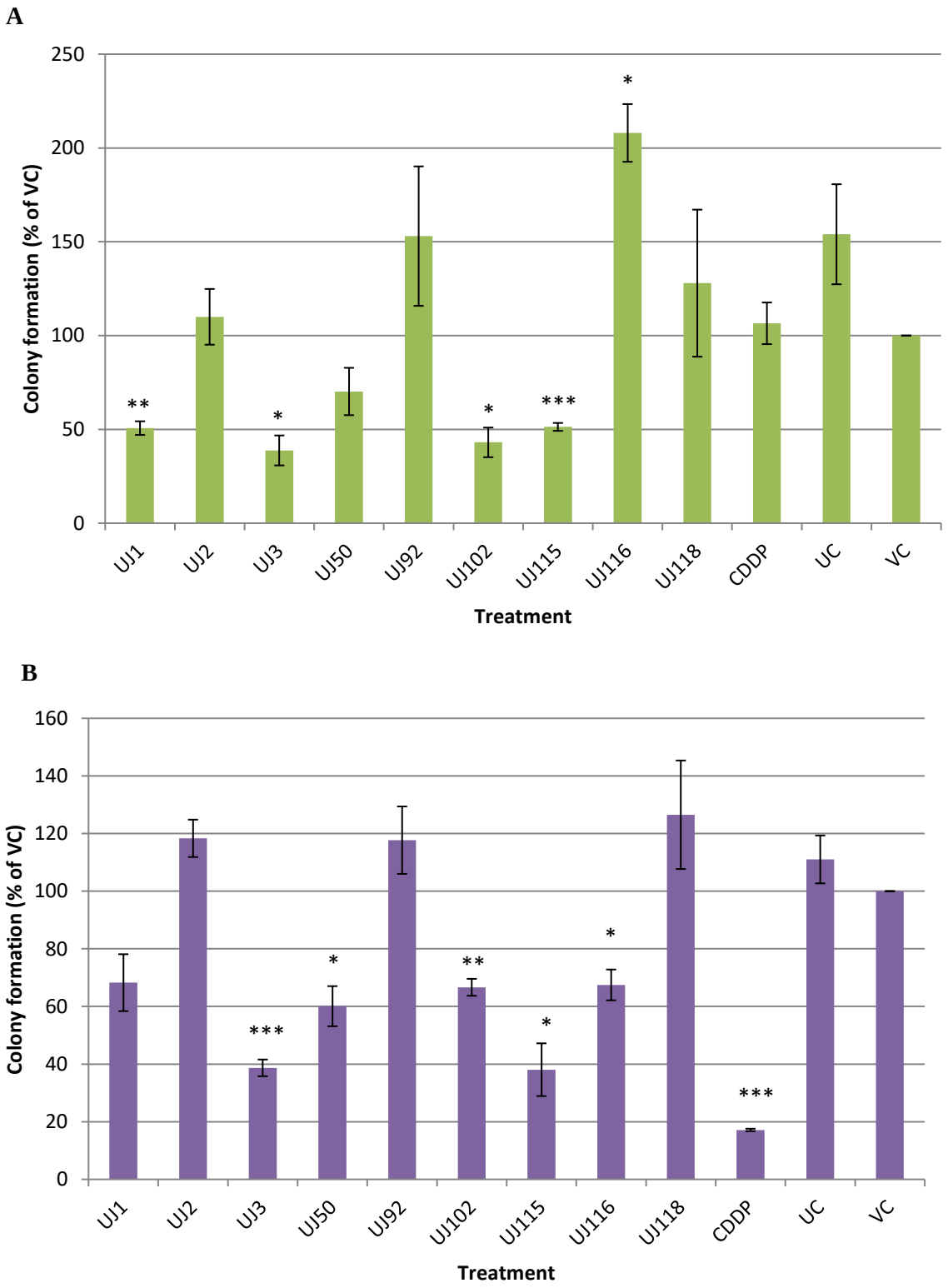

Figure 3.9 Quantification of the anchorage-dependent colony forming abilities of **MCF-7** (**A**) and **MDA-MB-231** (**B**) cells treated with silver(I) phosphine complexes following incubation for 14 (MCF-7) or 7 (MDA-MB-231) days. ImageJ® software was used to quantify colony formation. Bar graphs represent the average colony area percentage values relative to the VC (set as 100%) for three independent biological repeats. Error bars were constructed based on ±SEM relative to the VC (n=3) (* $P < 0.05$, ** $P < 0.01$, *** $P < 0.001$).

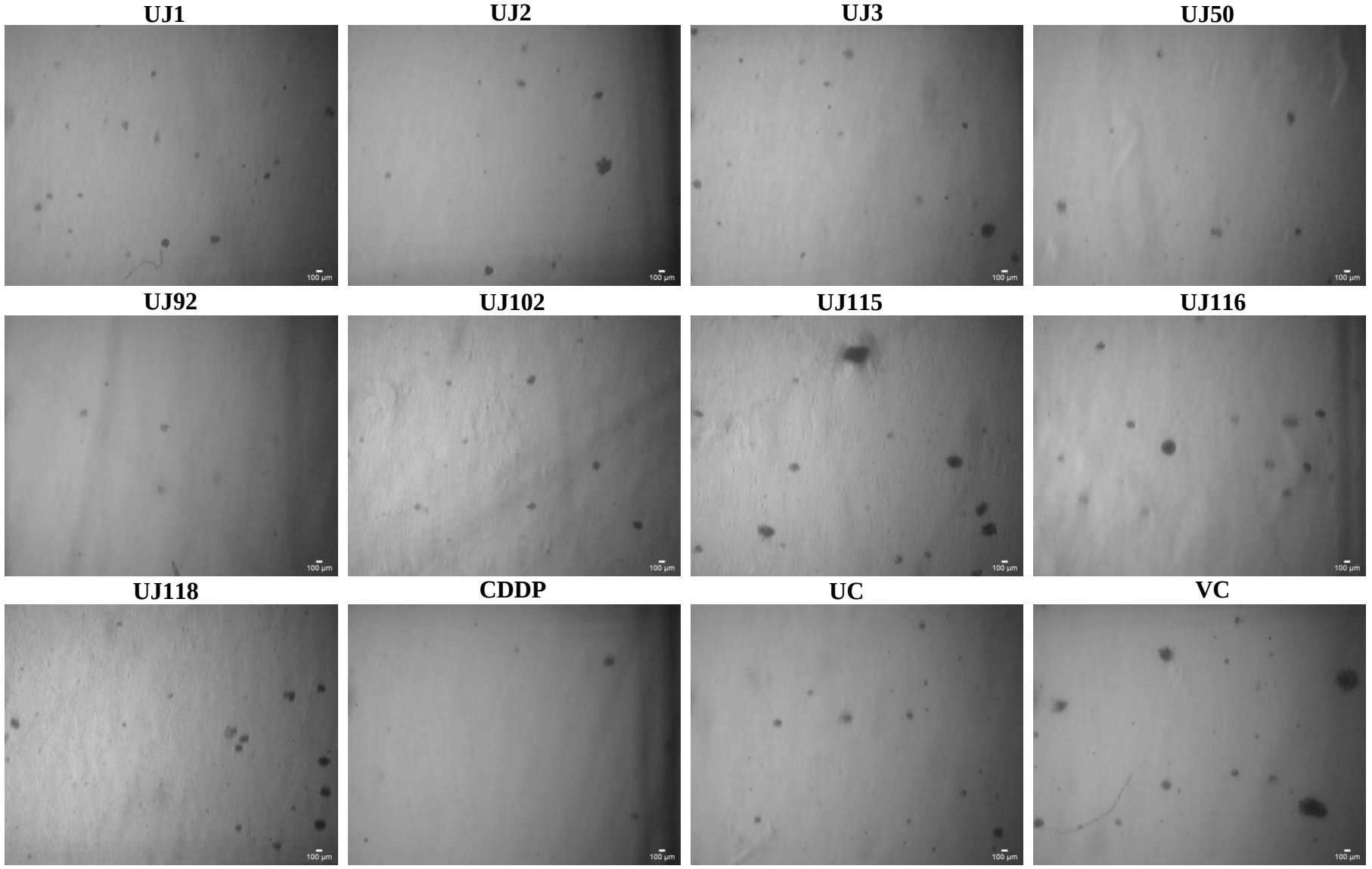

Figure 3.10 **MCF-7** colony formation in soft agar (40X magnification) after incubation for 14 days. Four images were taken for each treatment condition and the average number of colonies per image was counted manually. Scale bars represent 100 µm. Images are representative of one biological experiment.

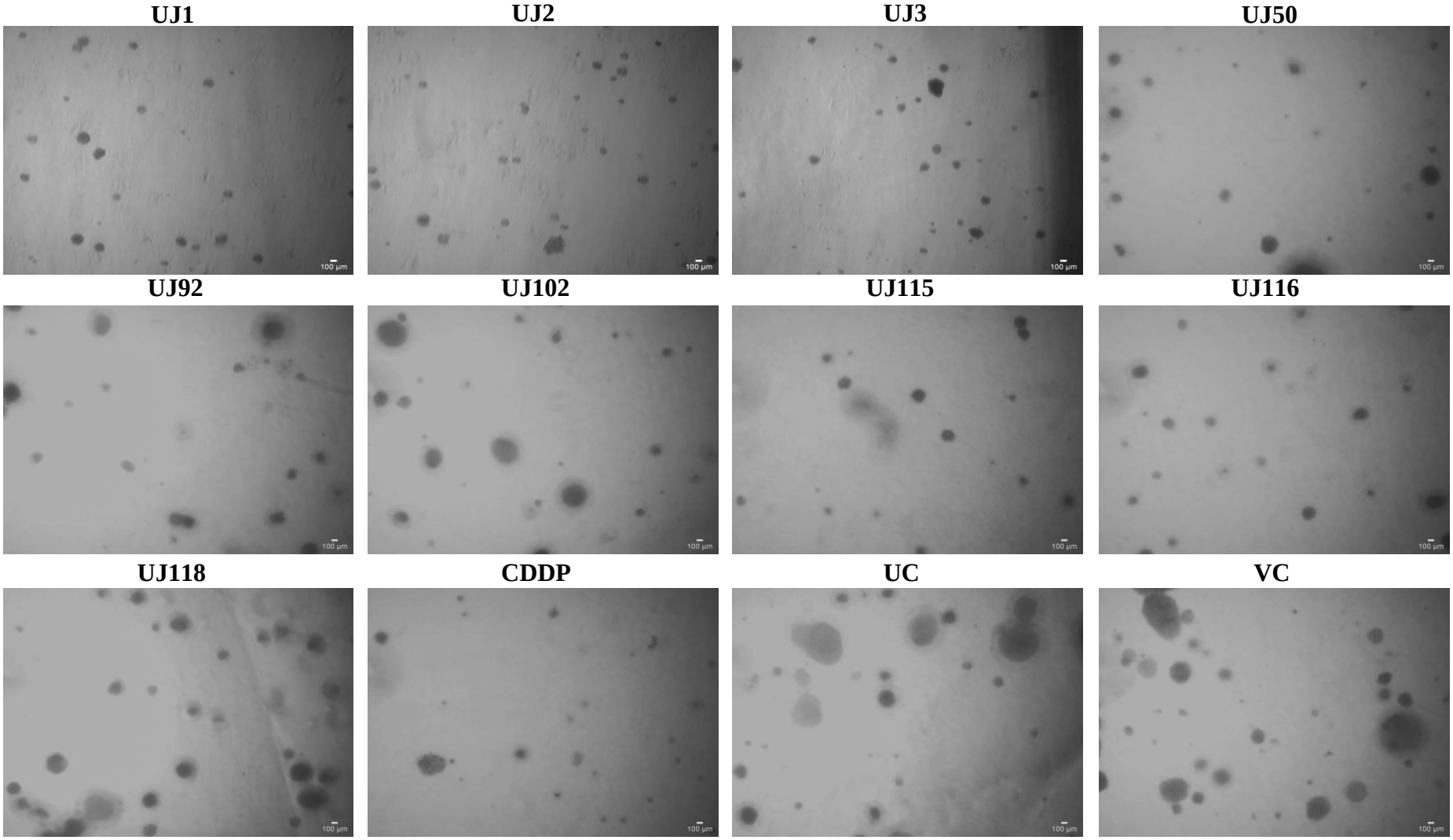

Figure 3.11 MDA-MB-231 colony formation in soft agar (40X magnification) after incubation for 7 days. Four images were taken for each treatment condition and the average number of colonies per image was counted manually. Scale bars represent 100 µm. Images are representative of one biological experiment.

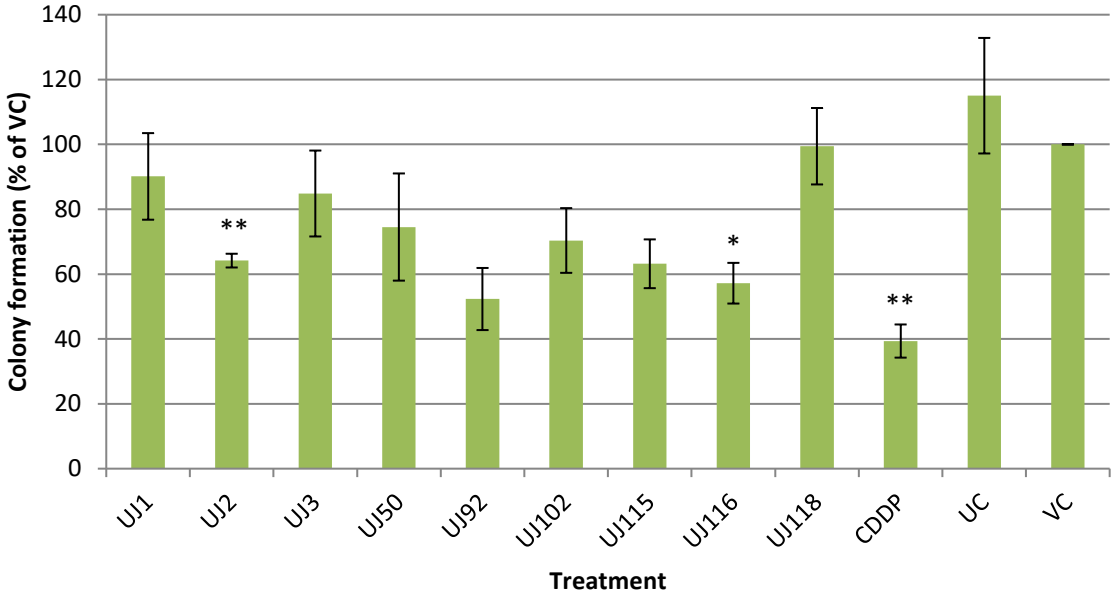

Figure 3.12 **MCF-7** anchorage-independent colony formation after 14 days incubation in soft agar. Values represent the average for three independent biological repeats relative to the VC (set as 100%). Error bars were constructed based on ±SEM relative to the VC (n=3) (* $P < 0.05$, ** $P < 0.01$).

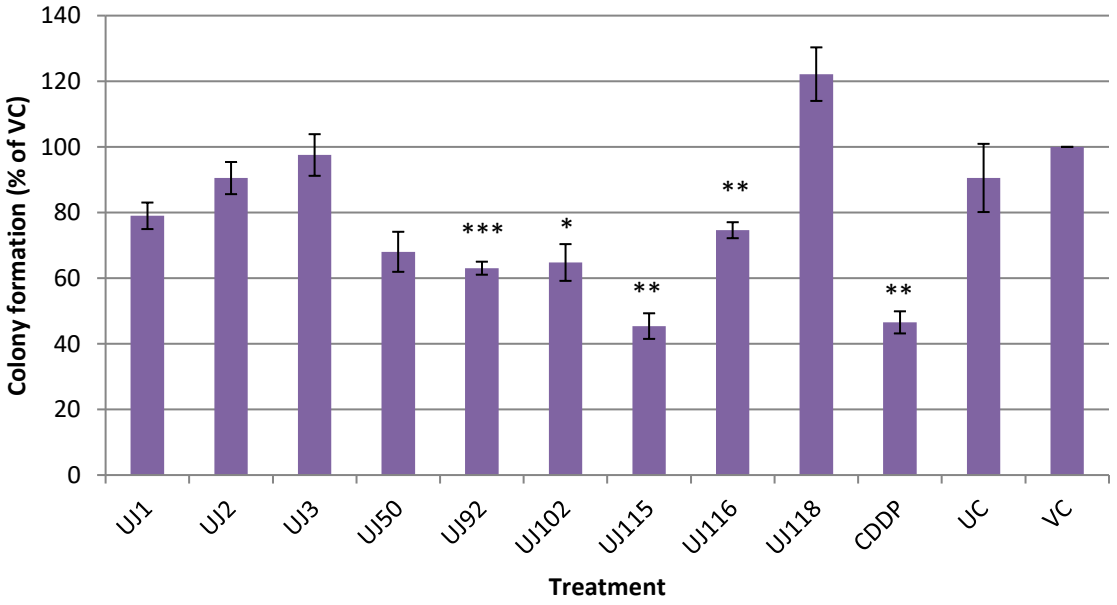

Figure 3.13 **MDA-MB-231** anchorage-independent colony formation after 7 days incubation in soft agar. Values represent the average for three independent biological repeats relative to the VC (set as 100%). Error bars were constructed based on ±SEM relative to the VC (n=3) (* $P < 0.05$, ** $P < 0.01$, *** $P < 0.001$).

The observations made regarding the large differences in the sizes of colonies of each treatment condition prompted the analysis of the colony areas. On images taken under 4X objective, colonies appeared dark grey on a light grey background. The colonies were mostly round with well-defined borders. A macro tool for ImageJ, SA_NJ, was developed in order to automate the analysis of colony area in soft agar, however, with the images obtained here; this macro could not properly isolate all the colonies visible on each image even after several calibration attempts. ImageJ also has a built-in manual thresholding function that makes use of the difference in intensity between the darker pixels of the colonies and the lighter grey pixels of the background. Through this, colonies can be isolated from the background manually, and the area of all the selected colonies can be determined. This feature however also did not work optimally for this application. Not all the colonies could be effectively isolated from the background. Consequently, at a threshold where all the colonies were successfully highlighted, there was a large amount of background areas highlighted as well. In contrast, by removing most or all the background highlighting, not all the desired colonies were highlighted. This occurred even after using other built-in functions such as background subtraction and the use of several filters. None of these attempts solved the abovementioned problems with isolating colonies vs. low background so the decision was made to determine the area of each colony manually. This was done by using the built-in circular tool in ImageJ to manually draw a border around each colony and determine the area using the built-in area function. In those cases where colonies were not adequately round, the freehand drawing tool was used to delineate the borders of the colony instead of the circular tool. After analysis, each colony was marked to ensure it was only analysed once. The time taken for the manual analysis was considerably longer than any of the automated features or macros would have taken and there is the disadvantage of bias in selecting colonies with manual analysis, however, each colony could be isolated from the background more distinctly than any of the automated methods.

Since there were very little visible differences in colony size observed between treatment groups of MCF-7 cells, area analysis was only carried out for MDA-MB-231 cells. UJ3, UJ50, UJ115 and CDDP treated samples all had significantly smaller colonies than those of the VC (Figure 3.14). When comparing these results with those of Figure 3.13, it was only UJ115 along with CDDP that lead to a significant decrease in both the number and size of colonies. Treatment with UJ1, UJ2 and UJ116 lead to a decrease in the average colony area, however, these findings were not statistically significant. Treatment with UJ102 resulted in a

negligible change in average colony area relative to the VC. In addition, although not statistically significant, UJ92 and UJ118 treated samples showed on average an increase in colony size compared to the VC, corresponding to the drastic change in media colour seen for these two treatments.

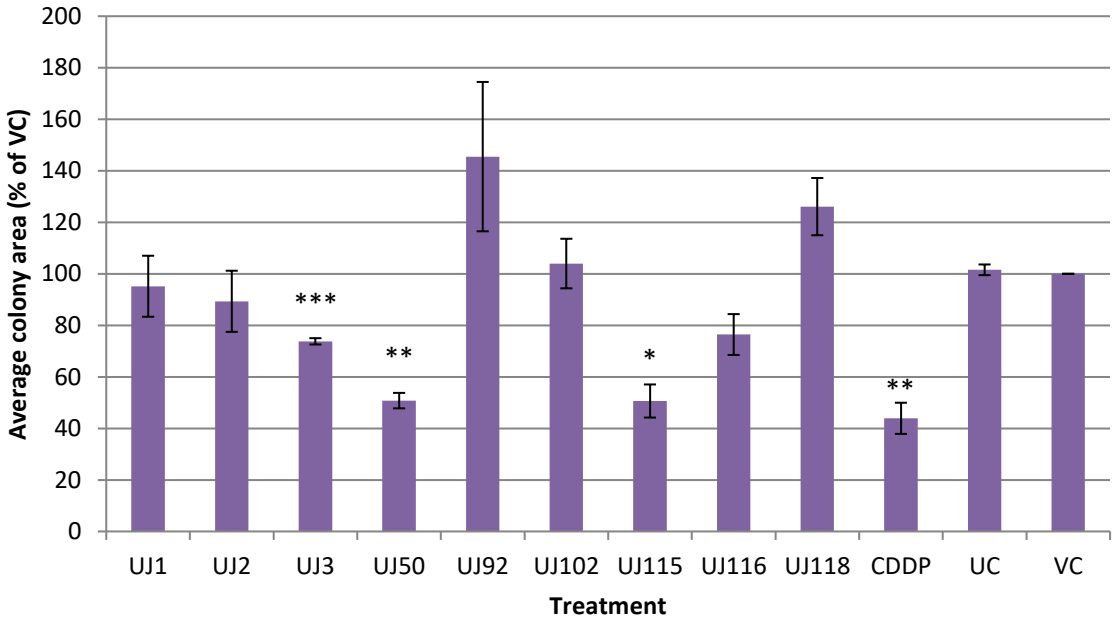

Figure 3.14 Average colony area formed from **MDA-MB-231** cells embedded in soft agar incubated for 7 days. Four images were taken for each treatment condition and the area of each colony in an image was determined using ImageJ® software. Bars represent the average areas of colonies for three independent biological repeats relative to the VC (set as 100%). Error bars were constructed based on ±SEM relative to the VC (n=3) (* $P < 0.05$, ** $P < 0.01$, *** $P < 0.001$).

3.6 Comparison of phenotypic anti-metastatic changes of the nine silver(I) phosphine complexes

To summarize and effectively compare all the effects of the nine silver(I) phosphine complexes, a table was constructed (Table 3.1) showing all the statistically significant effects. In instances where treatment with the relevant complex led to a decrease in a particular metastatic aspect, these were indicated with a green tick. Similarly, a red cross was used to indicate where treatment led to a significant increase in metastatic ability. From this table, the complexes with the most potential could be selected for further analysis. When comparing the effects of all nine complexes between the two cell lines UJ1, UJ92 and UJ116 treatments were the most successful for MCF-7 cells, each resulting in a decrease in three out of the five metastatic aspects assessed. For MDA-MB-231 cells, UJ50 showed the most potential

causing a decrease in all five metastatic parameters assessed, followed closely by UJ3 and UJ115 each leading to a decrease in four of the features. Regrettably there seems not to be a single complex identified as a potential lead complex for the treatment of both BC cell lines. Apart from UJ92 which successfully led to a decrease in three metastatic aspects in both cell lines, effects seem to be contradictory between MCF-7 and MDA-MB-231 cells. For example, UJ50 and UJ115 the frontrunners for MDA-MB-231 cells did not show much success in MCF-7 cells.

When selecting complexes for further analysis a few things were taken into consideration. Firstly, if a red cross was present for any of the complexes, those complexes were not considered for further analysis. Consequently UJ115, UJ116 and UJ118 were eliminated from being considered due to their increased effect on cell invasion and colony formation (Table 3.1). Furthermore, if at any stage a complex showed an average increase in any of the metastatic parameters assessed, even if it was not found to be statistically significant, that complex was also eliminated. None of the complexes led to an increase in cell migration (Figure 3.5A and B) or adhesion (Figure 3.7A and B), however, UJ115, UJ116 and UJ118 led to an average increase in cell invasive ability for both MCF-7 and MDA-MB-231 cells (Figure 3.6). In addition, UJ2, UJ92, UJ116 and UJ118 (Figure 3.9A) showed an increase in the average colony area percentage compared to the VC for MCF-7 cells, while the same effect was seen for UJ2, UJ92 and UJ118 in MDA-MB-231 cells (Figure 3.9B). None of the complexes led to an increase in anchorage-independent colony formation for MCF-7 cells (Figure 3.12), however, UJ118 showed an increase in both the amounts of colonies formed (Figure 3.13) as well as the average sizes of the colonies (Figure 3.14) compared to the VC for MDA-MB-231 cells. In addition, UJ92 also showed an increase in the average colony size despite a reduction in the number of colonies formed compared to the VC (Figures 3.13 and 3.14). Lastly, as explained in Chapter 1, section 1.3.5.2 (paragraph 3), the heterogeneity of metastatic cells would require a treatment that preferentially targets more than one aspect of the metastatic process simultaneously, thus only those complexes that led to a reduction in two or more of the metastatic parameters assessed, were chosen for further analysis. Taking all of this into consideration, UJ1, UJ3 and UJ102 were selected for further analysis in MCF-7 cells, while UJ3, UJ50 and UJ102 were selected for MDA-MB-231 cells.

Table 3.1 A summary of the effects of silver(I) phosphine complexes on MCF-7 and MDA-MB-231 cell migration, invasion, adhesion and colony formation. Tick marks and crosses represent cases where treatments led to a statistically significant reduction or increase in metastatic parameters, respectively. Complexes with the most potential as inhibitors of metastasis *in vitro* without leading to an increase in any metastatic parameter evaluated were selected for further analysis. These complexes are indicated in blue.

Treatment	Cell migration	Invasion	Adhesion	Colony formation (anchorage-dependent)	Soft agar (anchorage-independent)
MCF-7					
UJ1		✓	✓	✓	
UJ2		✓			✓
UJ3			✓	✓	
UJ50			✓		
UJ92	✓	✓	✓		
UJ102			✓	✓	
UJ115				✓	
UJ116	✓		✓	✗	✓
UJ118	✓	✗	✓		
MDA-MB-231					
UJ1		✓			
UJ2	✓	✓			
UJ3	✓	✓		✓	✓ *(colony area)*
UJ50	✓	✓	✓	✓	✓ *(colony area)*
UJ92		✓	✓		✓ *(no of colonies)*
UJ102			✓	✓	✓ *(no of colonies)*
UJ115	✓	✗	✓	✓	✓ *(no of colonies and colony area)*
UJ116		✗		✓	✓ *(no of colonies)*
UJ118		✗			

3.7 Effect of silver(I) phosphine treatment on levels and activity of MMPs

Complexes with the most potential as anti-metastatic treatments based on the metastasis-related phenotypes evaluated in this study were identified from Table 3.1. The studies conducted here were however limited to only five metastasis-related parameters and only under *in vitro* conditions. Additional *in vivo* studies are needed to confirm the anti-metastatic effects of these complexes. Nevertheless, the selected silver(I) phosphine complexes were studied further to attempt to elucidate the *in vitro* anti-metastatic mechanism of action in MCF-7 and MDA-MB-231 cells.

Due to their extensive participation in the metastatic process and being common anti-metastatic therapeutic targets, the MMPs were considered a logical starting point to evaluate upstream events leading to inhibition of metastasis. Several correlations between the prognosis of various cancer types and MMP-2 and -9, in particular, have been detected (Toth and Fridman, 2001). Western blot analyses were used to quantify intracellular levels of MMP-2 and -9 expressions (Figure 3.15).

Anti-metastatic treatments were anticipated to decrease MMP levels. Contrary to these expectations, silver(I) phosphine treatments seemed to increase the intracellular levels of MMP-2 in both MCF-7 (UJ1 and UJ3, Figure 3.15B) and MDA-MB-231 cells (UJ3 and UJ50, Figure 3.15D). UJ3 resulted in an average of double the MMP-2 levels in MCF-7 cells compared to the VC, however, none of the values reached statistical significance (Figure 3.15B). The antibody used was specific for both the 72 kDa pro-enzyme as well as the 64 kDa active enzyme of MMP-2. Only the active form however was detected in MCF-7 cells. In contrast, both forms were detected in MDA-MB-231 cells, where UJ3 and UJ50 treatments led to an increase in both the pro- and active forms of MMP-2. The only statistically significant effect however was the increase in pro-MMP-2 as a result of UJ50 treatment. Interestingly, pro-MMP-2 levels for the VC were significantly more compared to the UC (Figure 3.15D), suggesting an effect of DMSO on intracellular MMP-2 levels in MDA-MB-231 cells. Despite several attempts neither the pro- nor active forms of MMP-9 could be detected by western blot analysis in either MCF-7 or MDA-MB-231 cells.

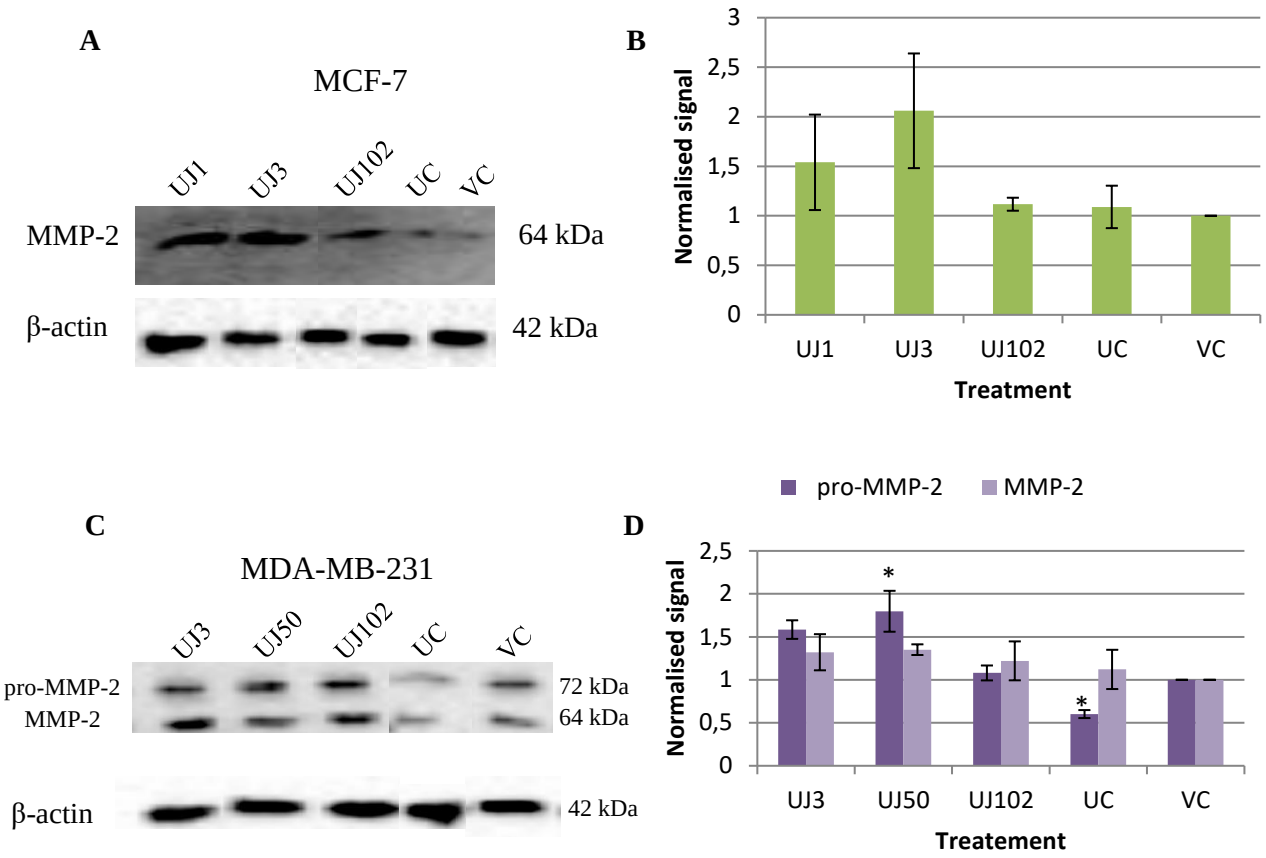

Figure 3.15 Normalised band density values for MMP-2 proteins extracted from **MCF-7** cells (**B**) or **MDA-MB-231** cells (**D**) following 24 hr treatment with silver(I) phosphine complexes. Values were normalised against β-actin and represent the average of three independent biological repeats relative to the VC (set as 1). Error bars were constructed based on ±SEM relative to the VC (n=3) (* $P < 0.05$). Representative images of one biological experiment are shown in A and C.

In the absence of quantification of accumulated intracellular levels of MMP-2 and -9 to infer anti-metastatic effects, it was decided to attempt to detect levels of extracellular active MMP activity present in the conditioned media of MCF-7 and MDA-MB-231 cells. Both MMP-2 and -9 form part of the subclass gelatinases where gelatin is one of their major substrates (Chapter 1, Table 1.2). For this reason, gelatin zymography was used, to evaluate gelatinase activity. MMPs are secreted enzymes (Nagase *et al.*, 2006) hence for this reason gelatinase activity was assessed using the conditioned media from MCF-7 and MDA-MB-231 cells. Proteins present in conditioned media were separated on an 8% SDS-PAGE gel containing 0.1% gelatin. After separation, gels were washed in a renaturation buffer containing 2.5% Triton X-100 leading to the removal of SDS from the gel and allowing the enzymes to renature back to their active conformation. Overnight incubation in a developing buffer then allows the gelatin in the gels to be degraded by MMP-2 and -9. After staining gels with Coomassie blue and washing away excess stain with the destaining solution, white bands

were visible on a blue background corresponding to where the gelatinases have degraded the gelatin.

Neither MMP-2 nor -9 activity could be detected for MCF-7 treated or control conditioned media despite increasing the amount of protein loaded (up to 75 µg) to the gel as well as extending the incubation period in developing buffer to 72 hr. Only MMP-2 activity could be detected for MDA-MB-231 conditioned media.

Extracellular MMP-2 activity in MDA-MB-231 conditioned media was significantly reduced as a result of UJ3 treatment (Figure 3.16B). Treatment with UJ50 and UJ102, however, showed a negligible effect on MMP-2 activity compared to the VC.

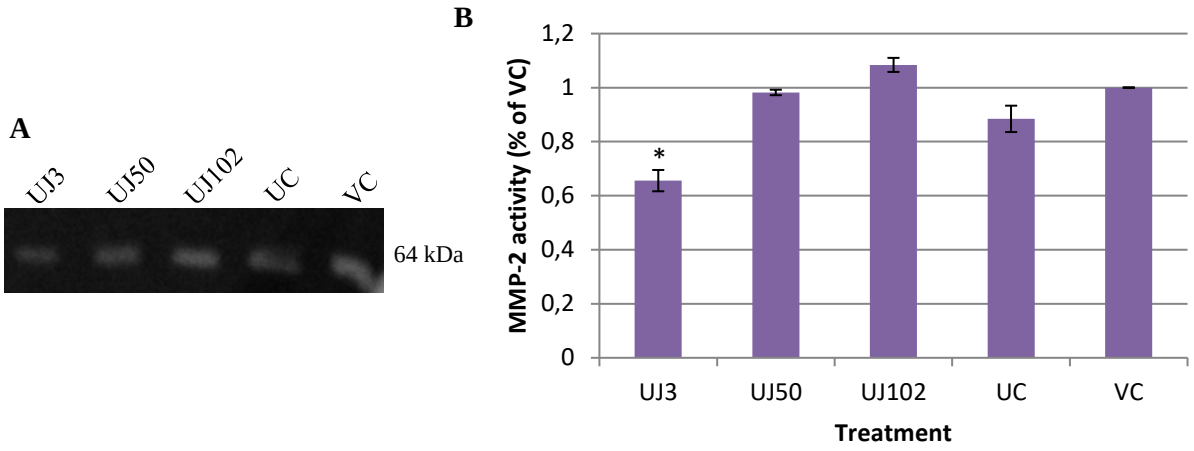

Figure 3.16 Activity of MMP-2 in conditioned media of **MDA-MB-231** cells treated with silver(I) phosphine complexes for 24 hr and detected through gelatin zymography. Values represent the average of three independent biological repeats relative to the VC (set as 1) (B). Error bars were constructed based on ±SEM relative to the VC (n=3) (* $P < 0.05$). Image in A is representative of one biological experiment.

It thus seems that despite the increase in intracellular levels of MMP-2 (albeit non-significant; Figure 3.15D), treatment with UJ3 possibly exerts its effects partly through decreasing the activity of secreted MMP-2 ($P < 0.05$; Figure 3.16B). The mechanism of action of UJ50 and UJ102 however remains elusive. MMP activity was also studied with alternatives to gelatin, i.e. collagen and casein, both known to be highly active in metastasis. Again, no MMP activity could be detected on either casein or collagen containing gels for MCF-7 conditioned media. Similarly, no casein degrading activity could be detected for MDA-MB-231 conditioned media on casein gels.

Out of all the possible MMPs that can cleave collagen type I, only one band of around 70 kDa was visible for the conditioned media of MDA-MB-231 cells on collagen gels (Figure 3.17A). Once more, only UJ3 treatment showed a significant reduction in collagenase activity ($P < 0.01$), while UJ50 and UJ102 showed a slight decrease, however, these values did not reach statistical significance (Figure 3.17B).

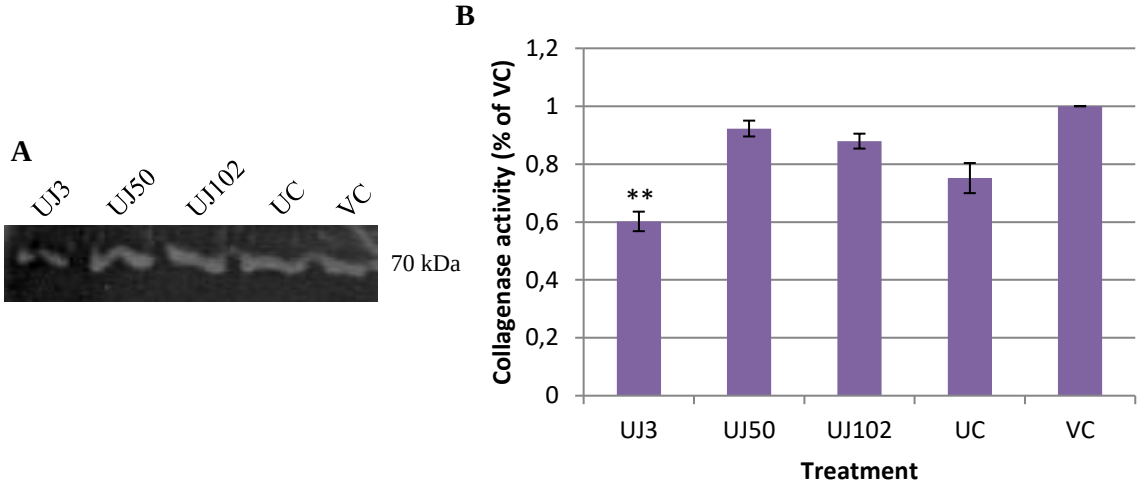

Figure 3.17 Activity of collagenase in the conditioned media of **MDA-MB-231** cells treated with silver(I) phosphine complexes for 24 hr and detected through collagen zymography. Values represent the average of three independent biological repeats relative to the VC (set as 1) (B). Error bars were constructed based on ±SEM relative to the VC (n=3) (** $P < 0.01$). Image in A is representative of one biological experiment.

Taken together, UJ3 seems to exert its anti-metastatic effects through decreasing MMP extracellular activity in MDA-MB-231 cells in metastasis-related phenotypes. This occurred despite an increase in intracellular levels of MMP-2. In contrast, the mechanism of action of UJ50 and UJ102 seems to occur through MMP-independent mechanisms. In addition, UJ1 and UJ3 appear to result in increased intracellular levels of MMP-2 in MCF-7 cells, however, their effect on MMP activity could not be assessed through substrate zymography.

Chapter 4: Discussion

4.1 The importance of anti-metastatic drug discovery

Decades of research have shown that metastases are physiologically and biochemically distinct from the primary tumour and simply administering the same treatments will not help in alleviating the burden of stage IV cancer (Anderson, *et al.*, 2019; Gandalovičová *et al.*, 2017). Despite an increase in research into metastasis and advances in the development of anti-metastatic treatments, metastasis remains responsible for the majority of cancer-related deaths (Anderson *et al.*, 2019). This effect was adequately described in an article written by Sleeman and Steeg (2010) which stated that patients started fearing the "M word" more than the "C word" since a diagnosis of stage IV cancer is often synonymous with incurable. The search for anti-metastatic treatments is thus a branch of cancer research that should not be underappreciated.

The seriousness of metastatic disease is not always reflected in the distribution of funds allocated to anti-metastatic drug discovery (Sleeman and Steeg, 2010). In addition to the reasoning regarding the difficulties contributing to the lack of anti-metastatic drugs (Chapter 1, section 1.3.5.2); another major caveat contributing to this effect is the criteria used to assess the effectiveness of anti-cancer drugs. The main condition that a potential cancer drug is assessed on remains its ability to induce tumour shrinkage. This characteristic alone is not sufficient to prevent the metastatic spread of the tumour and the need for the development of drugs targeting metastatic aspects specifically is great (Anderson *et al.*2019).

Because early dissemination of the primary tumour is possible (Riggio *et al.*, 2021), it is proposed that treatment of the primary tumour should be accompanied by an anti-metastatic treatment helping to prevent the formation of metastases as early as possible. It is also predicted that these anti-metastatic treatments would have to be administered continuously rather than intermittently as is the case for chemotherapeutic drugs. For this reason, the systemic toxicity of these drugs is of great concern (Gandalovičová *et al.*, 2017). Sub-lethal concentrations are mostly used for the evaluation of the anti-metastatic properties of drugs to ensure that any effect seen is not a consequence of its cytotoxicity (Muscella *et al.*, 2010). However, the use of the lowest possible dose of a drug in a clinical setting would also be highly beneficial towards achieving the smallest possible systemic toxic effect.

The research presented here aimed to establish whether carefully selected members of a novel class of silver(I) phosphine complexes, that have already shown great potential as anti-cancer agents in terms of their superior cytotoxicity and selectivity, can also inhibit key steps of metastasis. Three of these complexes were chosen based on previous research findings conducted on an A375 melanoma (UJ1), SNO oesophageal (UJ2) and MCF-7 breast (UJ3) cancer cell lines (Chapter 1, section 1.4.3). In addition, in line with the abovementioned main criteria of cytotoxicity, an additional six complexes found to be toxic to MCF-7 and MDA-MB-231 cells, were evaluated as well.

Another concerning discovery in addition to the fact that standard chemotherapeutic drugs are not adequate to prevent metastasis is that ironically some treatments may exacerbate the problem. Sub-lethal doses of CDDP in a lung cancer cell line were shown to increase migration (Maiuthed and Chanvorachote, 2014), while doxorubicin was found to increase migration and invasion of two BC cell lines, BT549 and MDA-MB-231 (Sun *et al.*, 2022). This is not only seen in chemotherapeutic drugs but also in cases where radiation therapy was administered which led to an increase in metastatic recurrence in the areas where radiation was applied. Moreover, some anti-angiogenesis treatments have also been associated with increased metastasis (Sleeman and Steeg, 2010).

4.2 *In vitro* BC cell culture models

BC is a worldwide burden responsible for countless numbers of deaths, but TNBC is of greater concern (Riggio *et al.*, 2021). TNBC is not only a more aggressive BC that has a higher chance of re-occurrence but also lacks effective treatment options (Sun *et al.*, 2017). Therapies that target hormone receptors (ER and PR) or HER2 have shown tremendous promise in the treatment of BC and greatly improved patient survival rates (Caulfield *et al.*, 2019). Since TNBC patients however, do not express ER, PR or HER2, therapies targeting these receptors, or their ligands are futile (Sun *et al.*, 2017). For this reason, several biomarkers for TNBC have been investigated as potential therapeutic targets. This includes the EGFR, AR, PARP, mTOR and several microRNAs. Cetuximab and bicalutamide are examples of such drugs, inhibiting EGFR and AR, respectively, while everolimus inhibits mTOR (Sun *et al.*, 2017). Another example is, olaparib, a PARP inhibitor that was approved in 2018 for patients with HER2 negative mBC carrying the *BRAC1/2* mutation (Caulfield *et al.*, 2019).

TNBC has the highest rate of formation of mutations of all the BC subtypes and contains many associating lymphocytes. It would therefore be the subtype most likely to benefit from immunotherapy (Jazieh *et al.*, 2020). An interesting phase II clinical trial found that pre-treatment of TNBC with CDDP or doxorubicin increased the immunogenicity of tumours. Consequently, there was an increase in the tumour response to nivolumab, an immune checkpoint inhibitor (Voorwerk *et al.*, 2019).

Compared to other types of cancer, BC overall has an extremely large window period associated with recurrence, spanning from months to even decades after surgical removal of the primary tumour. In addition, the different molecular subtypes of BC have different recurrence patterns with HER2-enriched and triple-negative subtypes usually associated with early metastatic relapse (within 5 years) while the luminal subtypes are associated with late metastatic relapse periods (10 years or longer). Consequently, the longer disease-free intervals of the luminal A and B subtypes often lead to the metastatic relapse of these tumours being underestimated (Riggio *et al.*, 2021).

In line with the observations of organ tropism of different cancer types, BC mainly spreads to the bone, brain, liver and lung as well as the lymph nodes. Often metastatic spread to the bone is most seen while spread to the brain is the least common (Riggio *et al.*, 2021). In addition to the different molecular subtypes of BC having different rates of recurrence, the different subtypes also display differences in organ tropism. Luminal subtypes tend to preferentially spread to the bone while the other subtypes tend to spread mostly to the visceral organs (Riggio *et al.*, 2021).

The MCF-7 BC cell line was established 50 years ago with cells that were isolated from the pleural effusion of a female with mBC (Comşa *et al.*, 2015). This cell line represents the luminal A subtype of BC with the presence of the ER and PR and the absence of HER2. This cell line is poorly aggressive with a low metastatic potential (Comşa *et al.*, 2015; Dai *et al.*, 2017). The MDA-MB-231 cell line on the other hand is an example of the TNBC subtype, characterised by a high aggressiveness and high potential for metastasis (Dai *et al.*, 2017). These two BC cell lines are two of the most frequently used cell lines for *in vitro* BC studies and together with the T47D cell line, make up more than 60% of studies involving BC cell lines (Dai *et al.*, 2017).

The mitochondrial function of MCF-7 and MDA-MB-231 cells were assessed using the alamarBlue™ dye reduction assay. Using population mitochondrial activity as the

determinant factor, one concentration where all nine silver(I) phosphine complexes did not show any significant toxic effect on each of the two cell lines was chosen. Using the same concentration for all the complexes made the comparison of the effect of each complex much simpler. Furthermore, considerable differences between the UC and VC values can be observed (Figures 3.5B, 3.6A and B and 3.7B). Therefore, by using the same concentration of DMSO for all complexes, any influence of variation in the VC is eliminated.

When comparing the selected concentrations between the two cell lines, those used for MCF-7 cells (1.25 µM silver(I) phosphine complexes and 12.5 µM CDDP) were half that of those used for MDA-MB-231 cells (2.5 µM silver(I) phosphine complexes and 25 µM CDDP). This corresponds to the difference in aggressiveness and observed proliferation rate between the two cell lines, with the more aggressive MDA-MB-231 cell line being more tolerant to higher concentrations of the same treatment compared to MCF-7 cells. For all subsequent assays, except the Transwell® invasion assay, the treatment period was 24 hr for both MCF-7 and MDA-MB-231 cells. The only treatment condition resulting in a decrease of mitochondrial activity below 80% was CDDP treatment for 48 hr on MCF-7 cells (Figure 3.1A). Even though this was not statistically significant, these effects were kept in mind when interpreting the findings of the Transwell® invasion assay (requiring 48 hr of exposure to treatments).

When the migration, invasion and adhesion treatments were administered and assessed, SFM was used since the presence of FCS would alter key mechanisms involved in these processes, potentially leading to the incorrect interpretation of the results. Therefore, an additional assessment of overall cell viability using Trypan blue dye was carried out, both to confirm the findings of the alamarBlue™ assay as well as confirm the effects of treatments in serum-free conditions (Figure 3.2A and B). None of the treatment conditions showed any significant effect on overall cell viability in the presence or absence of serum for both MCF-7 and MDA-MB-231 cells.

4.3 Silver(I) phosphine complexes show some effects against migration, invasion and adhesion of BC cells *in vitro*

Analogous to the “Hallmarks of cancer” proposed by Hanahan and Weinberg (2000) a set of characteristics termed the “Hallmarks of metastasis” have been compiled by Welch and Hurst (2019). They proposed that cancer cells would, in addition to the eight original hallmarks,

need to acquire the ability to: 1) migrate and invade, 2) induce changes to their environment, 3) adapt to environmental changes and 4) colonise a distant secondary niche.

Cell migration by definition is the directional movement of a cell across a substrate which can either be the ECM, basal membrane or plastic culture plates without the need for the degradation of a fibrous network (Kramer *et al.*, 2013). Migration is necessary for embryogenesis, immune response, tissue regeneration and wound healing. Consequently, uncontrolled or inadequate migration is associated with several diseases, and it plays a central role in metastasis. Successful migration involves a complex interplay between receptors, signalling molecules, adhesion molecules and cytoskeletal proteins (Vicente-Manzanares and Horwitz, 2011). One example of such a protein is vimentin. In addition to migration, it is also highly involved in invasion, adhesion as well as various other signal transduction pathways in cancer cells. Vimentin, an intermediate filament abundant in cells with mesenchymal characteristics, regulates the interaction between cytoskeletal proteins such as cytokeratins (keratin containing intermediate filaments) and adhesion molecules including P-cadherin (Dai *et al.*, 2016). In order to migrate, cells also rely heavily on the actin cytoskeleton which aids in the formation of protrusions (Vicente-Manzanares and Horwitz, 2011).

Metastatic cells can either migrate individually or more commonly, as a cluster or sheet of cells. Individual migrating cells and cell clusters usually have a leading edge and a trailing edge communicating with each other (Kramer *et al.*, 2013; Welch and Hurst, 2019). Cell migration was the first metastatic process assessed in response to treatments using the relatively straightforward wound healing/scratch assay. The creation of a wound in a cell monolayer initiates the directional movement of cells without the need for a chemoattractant. Cells at the edges of the wound will rearrange their microtubules and Golgi apparatus, polarising themselves to form a leading edge (Cory, 2011), and initiate cell movement to ensure wound closure.

Very little migration was seen for MCF-7 cells over the 24 hr period (Figures 3.3 and 3.5A). Nonetheless, three of the complexes, UJ92, UJ116 and UJ118 did show a statistically significant (albeit minimal) reduction in migration compared to the VC. Considering that the MCF-7 cells exhibit a very low metastatic potential (Comşa *et al.*, 2015; Dai *et al.*, 2017), extending the incubation period might have shown a more significant difference. This was done by Xie *et al.* (2015) were an incubation period of up to 60 hr was used to assess the inhibitory effects of a nucleoside analogue, NZ51, on the migration of MCF-7 cells. In this

study, wounds made in control MCF-7 samples were completely filled after 60 hr of migration (Xie *et al.*, 2015).

Surprisingly, the difference in wound widths between 0 and 24 hr for the highly metastatic MDA-MB-231 cells were even less noticeable (Figure 3.4) than those of MCF-7 cells. When combining the data from all three biological repeats, however, it became apparent that the various treatment conditions had a more substantial impact on these cells (Figure 3.5B). UJ3 and UJ50 showed the largest change while UJ2 and UJ115 resulted in a reasonable reduction in MDA-MB-231 cell migration. Compared to the UC cell population, DMSO treatment alone seemed to have influenced MDA-MB-231 cell migration with UC populations showing less than 40% of the amount of wound closure compared to the VC, almost as if the presence of DMSO itself induced a stress response and somehow prompted cells to migrate faster.

Although not much difference in wound width can be seen on the images after 24 hr of migration, what is apparent from the photographs is one of the inherent flaws of the manual creation of wounds, namely the large variation in the width of the wounds. The scratch assay is a commonly used, simple and cost-effective assay to assess the 2D migration of cells (Kramer *et al.*, 2013). This assay is also however associated with a high variance and low reproducibility (Stoellinger and Alexanian, 2022) as evident from the large error bars in Figure 3.5A and B. Automated methods for creating wounds are available, although these are much more expensive compared to manual methods. Another variation of the scratch assay that might assist in reducing the large variability is the use of silicone inserts. These inserts are placed in culture well plates before the addition of cells. After a brief incubation period to allow cells to attach to the plate, the inserts are removed and cells are left to migrate to cover the cell-free area (Kramer *et al.*, 2013).

Another concern of the scratch assay is the occurrence of cell proliferation over the incubation period allowed for migration which may also contribute to the closing of the wound (Glenn *et al.*, 2016). The extent to which the proliferation of MCF-7 and MDA-MB-231 cells has contributed to the closure of the wound in this study was not accounted for when interpreting the results. In order to negate the effects of cell proliferation during migration, cells can be treated with sub-lethal doses of mitomycin C to inhibit proliferation (Glenn *et al.*, 2016; Poullot *et al.*, 2013).

The scratch assay has been used a number of times to demonstrate the anti-migratory potential of several complexes. A study done with a compound found in medicinal herbs,

rhaponticin, was assessed for its potential anti-metastatic activity on malignant BC cells. This compound has previously been shown to be useful in the treatment of a number of diseases including allergies and diabetes and showed evidence of the induction of apoptosis in tumour cells (Kim and Ma, 2018). The scratch assay, performed by Kim and Ma (2018) showed that a sub-lethal dose of 100 µM of rhaponticin inhibited the migration of MDA-MB-231 cells by almost 50% after 18 hr of treatment (Kim and Ma, 2018). When comparing this to the findings in Figure 3.5B, UJ3 and UJ50 showed a decrease in migration of 74% and 62%, respectively after 24 hr, at a concentration of only 2.5 µM.

Another metal-based complex, Pt(O,O'-acac)(γ-acac)(DMS), led to a reduction in migration of MCF-7 cells by 53% after only 11 hr of treatment at a remarkable concentration of only 0.5 µM (Muscella *et al.*, 2010). In another study, the anti-metastatic effects of actein, which was also previously shown to inhibit BC cell growth *in vitro*, was compared between MCF-7 and MDA-MB-231 cells. Actein is a natural compound found to be effective against several diseases including osteoporosis and malaria. With the use of the scratch assay, actein at 40 µM showed roughly a 20% difference in wound area in MDA-MB-231 cells after 22 hr of treatment compared to control populations. Like with this study, a very small difference between treated and untreated groups of MCF-7 cells was found, however actein at concentrations of 50 and 100 µM significantly reduced the migration of MCF-7 cells by roughly 10% after 24 hr. Even more interesting is that these effects were confirmed through *in vivo* analysis using zebrafish embryos. Actein at a concentration of 60 µM resulted in a decrease of 74% in the number of embryos containing migrated cells compared to untreated groups, 5 days after injection of MDA-MB-231 cells (Wu *et al.*, 2018).

Several contradicting findings regarding the anti-metastatic potential of CDDP have been published over the years (Karam *et al.*, 2010; Maiuthed and Chanvorachote, 2014; Raudenska *et al.*, 2019; Shrikhande *et al.*, 2015; Zhang *et al.*, 2020). Contrary to the increase in migration of lung cancer cells found by Maiuthed and Chanvorachote (2014), here CDDP treatment showed a decreased migratory effect on both MCF-7 and MDA-MB-231 cells with an impressive 53% decrease in MDA-MB-231 cell migration (Figure 3.5B). Similarly, Zhu *et al.* (2020) found that CDDP at a concentration of 80 nM significantly decreased the migration of MCF-7 cells after 24 hr, while Whang *et al.* (2021) found 10 µM of CDDP to reduce the migration of MCF-7 and MDA-MB-231 cells after only 3 hr. Additional reports where CDDP was shown to reduce cancer cell migration include a study conducted by Raudenska *et al.* (2019) which used the scratch assay to show that both CDDP and docetaxel reduced

migration in prostate cancer cell lines. In another study performed by Karam *et al.* (2010), CDDP was found to reduce the migration of three different ovarian cancer cell lines. It thus seems that the metastasis-related effects of CDDP are very much dependent on the type of cancer.

Invasion is the movement of cells through a 3D medium along with the need for a structural reorganisation and/or degradation of the medium it is moving through. Both adhesion and migration are necessary for invasion to occur (Kramer *et al.*, 2013). The ECM consists of proteins (of which collagens are the most common) and glycoproteins such as fibronectin and laminins. It also serves as a storage site for growth factors and regulatory proteins (Welch and Hurst, 2019). The ECM is important in creating a structural support for tissues and organs and furthermore, plays a role in regulating the cell cycle, facilitating cell migration, distributing growth factors and participates in apoptosis (Cabral-Pacheco *et al.*, 2020). ECM remodelling shown to occur during invasion of BC includes organisational alterations to collagen type I and crosslinking of fibrillar collagen (Chitty *et al.*, 2019).

Transwell® inserts were used to assess the invasive ability of MCF-7 and MDA-MB-231 cells in response to the treatments. With this assay, cells are separated from a chemoattractant solution by a porous membrane. When the inserts are used as is, this assay can be used to assess the migratory ability of cells. Here, however, inserts were covered with a thin layer of collagen type I before the addition of cells. The presence of ECM components mimic *in vivo* conditions, with the idea that the openings in the ECM extract is much smaller than the size of a cell, leading to the cells having to degrade the ECM before they can migrate through the porous membrane through chemotaxis (Marshall, 2011). Chemotaxis is the movement towards a soluble chemoattractant (Welch and Hurst, 2019) which in this case, was FCS. As soon as cells have passed through the porous membrane, they will attach to the bottom of the membrane allowing for quantification (Falasca *et al.*, 2011).

An interesting trend was found with the invasion of cells through collagen type I. For both cell lines, UJ1, UJ2, UJ3 and UJ92 resulted in a very slight reduction (between 10% and 20%) in invasion (Figure 3.6). This reduction was however not statistically significant for treatment with UJ3 in MCF-7 cells. UJ50 showed the greatest significant reduction of invasion in MDA-MB-231 cells (40% reduction, $P < 0.001$) while its effects were not significant in MCF-7 cells. UJ102 showed a negligible effect on invasion in both MCF-7 and MDA-MB-231 cells. The finding of UJ115, UJ116 and UJ118 causing a significant increase

of 11%, 27% and 60%, respectively, in MDA-MB-231 cell invasion was an unexpected finding. UJ116 and UJ118 also increased the invasive abilities of MCF-7 cells through collagen I, however, only the effects of UJ118 were significant ($P < 0.01$). Taking into account, however, the large statistically significant difference between the % invasion of the UC and the VC (Figure 3.6) for both MCF-7 and MDA-MB-231 cells, it seems that DMSO rather than any of the silver(I) phosphine complexes was the biggest contributor to a reduction in invasion through collagen.

CDDP treatment slightly increased the invasive abilities of both cell lines (Figure 3.6); however, the effect was only significant in MDA-MB-231 cells ($P < 0.05$). This increase in invasion of MCF-7 cells was seen despite the cytotoxic effect of CDDP on MCF-7 cells at 48 hr (Figure 3.1A) mentioned earlier. The observed increase in invasion following treatment with CDDP is consistent with the findings of Maiuthed and Chanvorachote (2014) who reported increased metastasis with CDDP treatment in lung cancer cells. In contrast however, Zhu *et al.* (2020) found that 80 nM (vs. 12.5 µM used in this study) of CDDP significantly decreased the invasion of MCF-7 cells after 24 hr. In addition, Karam *et al.* (2010) and Raudenska *et al*. (2019) found a reduction in the *in vitro* invasion of ovarian cancer cells and prostate cancer cells, respectively as a result of CDDP treatment, again pointing to a strong correlation between the type of cancer (and possibly also the treatment dose), and the metastasis-related effects of CDDP which deserves further investigation.

Comparing the results found here to the same compounds described above showing an anti-migratory effect, at 100 µM, rhaponticin induced a reduction in invasion of almost 90% when using the Transwell® assay with FCS as a chemoattractant (Kim and Ma, 2018). Similarly, 20 µM of actein treatment resulted in just over half the number of MDA-MB-231 cells invaded compared to untreated populations while the results at 40 µM did not reach statistical significance. In addition, an actein concentration of 100 µM led to a 64% decrease in the invasion of MCF-7 cells (Wu *et al.*, 2018).

With all the above-mentioned examples, Matrigel® was used as the ECM component covering the porous membrane. Matrigel® is composed of laminins, perlecan and collagen type IV that was extracted from Englebreth-Holm-Swarm mouse sarcoma (Shaw, 2005). Even though Matrigel® is not an exact representation of all the particulars of a regular basement membrane, this is a very widely used matrix preparation and *in vitro* findings where this extract was used was confirmed with *in vivo* experiments (Shaw, 2005). In an

interesting study using four ovarian cancer cell lines, the use of Matrigel® and collagen type I as ECM barriers for Transwell® assays were compared. This study found that invasion through collagen type I required MMP activity whereas invasion through Matrigel® coated Transwells® occurred even in the presence of MMP inhibitors. They ascribed this to the fact that although the main components of the basement membrane are reflected in the composition of Matrigel®, their amounts and the interactions between them are not. The Matrigel® had fewer cross-links than *in vivo* basement membranes which most likely made it easier for cells to traverse without the need for proteolytic degradation. Since proteolytic action forms an important part of the invasion, these researchers concluded that collagen I obtained through acid extraction was better to use when invasion is investigated. Importantly, they highlighted that these studies were carried out on ovarian cancer cell lines only and that it may differ for other cancer types (Marshall, 2011; Sodek *et al.*, 2008). The reason for using collagen instead of Matrigel® in this study, however, was purely cost-related. Matrigel® is considerably more expensive compared to collagen type I extract. In addition, the collagen extract was also used for the assessment of adhesion and later for the evaluation of collagenase activity, making it more versatile in this particular study.

Transwell® assays also have their own drawbacks. Firstly, the dyes used to stain cells for quantification of migration or invasion may also stain the pores of the membrane which may influence the quantification of results (Stoellinger and Alexanian, 2022). In addition, cells remaining on top of the membrane cannot microscopically be distinguished from the invaded cells on the bottom of the membrane. The cells still present in the upper compartment, therefore, must be removed manually before quantification of cells attached to the bottom of the porous membrane (Stoellinger and Alexanian, 2022). According to Stoellinger and Alexanian (2022) however, these cells should not be simply ignored, since several factors including cell adhesion, proliferation and viability of the cells on top especially in long-term assays can influence invasion. It is therefore better to count both the number of cells on the top and on the bottom of the membrane and then represent invasion as a percentage of the total number of cells present in each insert (Stoellinger and Alexanian, 2022). This abovementioned step was omitted in this study and the results in Figure 3.6 thus only represent the cells that were present on the bottom of the insert.

Adhesion plays an important role in various aspects of metastasis. Adhesion of cells is needed for both migration and invasion to occur (Kramer *et al.*, 2013; Vicente-Manzanares and Horwitz, 2011) and is regulated by the formation of focal adhesion complexes between

the cell membrane and the ECM components (Wang *et al.*, 2020). Cell adhesion is also involved in the detachment of cells from the primary tumour, intravasation, the forming of cell clusters during movement through circulation, arresting in circulation, extravasation and establishment of a secondary colony (Chitty *et al.*, 2019; Hapach *et al.*, 2019). As a predominant component of the basement membrane (Muscella *et al.*, 2010), collagen type I was used here to investigate the effects of treatments on cell adhesive abilities.

Quite a few of the complexes (UJ1, UJ3, UJ50, UJ92, UJ102, UJ116 and UJ118) significantly reduced the adhesion of MCF-7 cells (Figure 3.7A), while UJ50, UJ92, UJ102 and UJ115 significantly reduced the adhesion of MDA-MB-231 cells (Figure 3.7B). UJ50, UJ92 and UJ102, however, are the only three complexes resulting in a significant reduction in the adhesion of both cell lines.

Adhesion assays are less commonly performed in metastatic studies compared to migration and invasion assays. Nonetheless, demethoxycurcumin was found to decrease both migration and invasion of MDA-MB-231 cells and was also found to significantly reduce their adhesion to Matrigel®, fibronectin and laminin at a sub-lethal dose of 15 µM (Yodkeeree *et al.*, 2010). In another study, bamboo shavings, used in China and Korea as traditional medicine for hypertension, were found to reduce the adhesion of human fibrosarcoma (HT1080) cells to fibronectin and collagen type I by more than 60% at the maximum tested dose of 250 µg/mL. Migration and invasion of HT1080 cells were also significantly reduced at this concentration (Kim *et al.*, 2013a). Adhesion effects of actein on MDA-MB-231 cells was evaluated against collagen type I, II and IV, fibronectin, laminin, tenascin and vitronectin, however, only 40 µM treatment significantly reduced adhesion to collagen type II and IV (Wu *et al.*, 2018).

Due to the heterogeneity of the different subpopulations of cells in a tumour, different cells can carry out the different steps of metastasis with different degrees of success. The acquired mutations might make some cells more competent at performing one step compared to others. This significantly complicates treating this wide variety of cells since a treatment that may lead to a decrease in one aspect of metastasis might not lead to an overall inhibition of the metastatic process (Hapach *et al.*, 2019). For this reason, we believe the more aspects of metastasis one complex can reduce simultaneously, the more potential that complex would have as an anti-metastatic drug and consequently the harder it would be for cells to acquire resistance against these drugs.

Gandalovičová *et al.* (2017) used the term "migrastatics" to describe a class of drugs that can interfere with cell invasion that can be used together with cytostatic drugs. The goal of these drugs would be to inhibit local invasion and therefore prevent metastasis. Considering the importance of migration and adhesion in invasion, results shown here reveal definite contenders as migrastatic drugs. Of the results obtained thus far, the strongest candidates are UJ92 for the MCF-7 cell line and UJ50 for the MDA-MB-231 cell line, each resulting in a significant reduction of migration, invasion and adhesion (Figure 3.5A and B, 3.6 and 3.7A and B).

4.4 Inhibition of colony formation could help prevent the formation of metastases

The question of why cancer cells would leave the primary tumour is central to the study of metastasis. This can be partially answered by recent findings that show that hypoxic conditions can induce changes in gene expression via hypoxia inducible factor (HIF) that may increase the metastatic potential of tumour cells (Welch and Hurst, 2019). HIF participates in cancer angiogenesis, energy metabolism, EMT and invasion and tumours containing larger anoxic and hypoxic areas tend to be associated with increased metastasis (Fares *et al.*, 2020). Furthermore, one of the reasons that radiation therapy and anti-angiogenesis treatments have been associated with an increased occurrence of metastasis is believed to be due to the resultant hypoxia of these treatments (Sleeman and Steeg, 2010). Still, those cells that do manage to escape from the primary tumour and survive in circulation must now move on to colonisation of the distant site in order to metastasize.

Not all cells that leave the primary tumour and circulate throughout the body or even arrest at a distant site have the potential to form macroscopic secondary masses. Colonisation is therefore a very important final step in the metastatic cascade (Welch and Hurst, 2019). Another major hurdle in anti-metastatic therapy is thus the ability to predict which cells will eventually develop into macroscopic secondary tumours (Riggio *et al*., 2021). This will not only introduce new therapeutic targets but may also reduce the need for additional adjuvant treatments, consequently reducing the side-effects associated with them (Riggio *et al*., 2021).

Research has shown that most primary tumours, and metastatic secondary tumours, originate from a single cell (Fidler and Kripke, 2015; Welch and Hurst, 2019). The colony-forming abilities of MCF-7 and MDA-MB-231 cells in response to silver(I) phosphine treatments were thus investigated under anchorage-dependent and -independent conditions.

The drastic observable difference in the extent of colony formation between MCF-7 and MDA-MB-231 cells even after MCF-7 cells were incubated for twice as long, is again a representation of the differences in aggressiveness of these two cell lines (Figure 3.8A and B; UC). The colony formation assay assesses the long-term proliferative abilities of cells in response to treatments. Cells that were treated with silver(I) phosphine complexes for 24 hr were removed from plates, re-plated as a single-cell suspension and incubated to proliferate. UJ1, UJ3, UJ102 and UJ115 all significantly decreased the ability of MCF-7 cells to proliferate, each leading to a reduction ≥ 50% (Figure 3.9A). For MDA-MB-231 cells, UJ3, UJ50, UJ102, UJ115 and UJ116 significantly reduced colony formation with UJ3 and UJ115 showing the greatest effect with a reduction of > 60% (Figure 3.9B).

The most impressive reduction in colony formation was, however, in MDA-MB-231 cells after being treated with CDDP with a decrease greater than 80% (Figure 3.9B). CDDP exerts its effects through binding to DNA. The resultant DNA damage then leads to 1) the activation of p53, 2) the formation of the apoptosome through the release of cytochrome c, and 3) activation of pro-caspase 9, eventually leading to apoptosis. In addition, CDDP may also result in cell death through the production of ROS (Lucaciu *et al.*, 2022). Conversely, CDDP resistance occurs when the number of DNA molecules exceeds those of the available platinum ions reducing the number of Pt-DNA adducts. Thus, failure to initiate apoptosis allows DNA repair pathways to reverse the DNA damage caused by CDDP. Lower levels of platinum ions can be the result of decreased amounts of transporter proteins responsible for the cellular intake of CDDP as well as the increased presence of proteins responsible for the efflux of CDDP from the cell (Lucaciu *et al.*, 2022). Even though cells in this study were treated with concentrations of CDDP not high enough to induce cytotoxicity, it still had the ability to interfere with MDA-MB-231 cell proliferation (Figure 3.9B), possibly related to its DNA damaging effects. Recent findings have also shown CDDP to have an effect on the cytoskeleton, leading to an increase in the cells' rigidity which might contribute to its anti-proliferative and anti-metastatic effects (Raudenska *et al.*, 2019). Like the findings with MDA-MB-231 cells in this study, CDDP treatment was also found to reduce colony formation completely in three different prostate cancer cell lines (Raudenska *et al.*, 2019). Interestingly, CDDP treatment did not show the same inhibition of colony formation on MCF-7 cells. This could potentially be as a result of the treatment dose of CDDP (12.5 µM) being too low to exert any substantial inhibition of MCF-7 cell proliferation or as a consequence of the longer duration of the experiment (14 days), possibly hinting at the

inhibitory effects of CDDP on MCF-7 cell proliferation being reversible. These hypotheses would however require additional investigation.

In contrast to the effects observed with UJ1, UJ3, UJ102 and UJ115 treatment, the platinum complex Pt(O,O'-acac)(γ-acac)(DMS) completely inhibited the colony forming abilities of MCF-7 cells at 0.5 µM (Muscella *et al.*, 2010). When compared to the reduction in colony formation that UJ3 (62%), UJ50 (40%), UJ102 (34%), UJ115 (62%) and UJ116 (33%) resulted in, treatment with rhaponticin led to a 70% reduction in colony formation of MDA-MB-231 cells (Kim and Ma, 2018). In another study, bamboo shavings evaluated by Kim *et al.* (2013a) for their anti-metastatic effects, led to > 60% reduction in colony formation of HT1080 fibrosarcoma cells at a dose of 50 µg/mL, while colony formation was almost completely inhibited at 250 µg/mL. In addition to attenuating migration and invasion of both MCF-7 and MDA-MB-231 cells, aloperine, also suppressed the colony formation of both MCF-7 and MDA-MB-231 cells (Tian *et al.*, 2018). Aloperine, extracted from Chinese medicine, is known for its anti-inflammatory, anti-cancer, immunosuppressive and cardiovascular protective effects (Han *et al.*, 2021).

Another unexpected finding was the increase in colony-forming abilities by silver(I) complexes UJ2 (not significant), UJ92 (not significant), UJ116 ($P < 0.05$) and UJ118 (not significant) for MCF-7 cells (Figure 3.9A). An increase in colony formation was also seen for UJ2, UJ92 and UJ118 for MDA-MB-231 cells (Figure 3.9B), however, these were not statistically significant. Despite the effect of UJ116 on MCF-7 cells to be the only statistically significant result, this observation may be cause for concern, especially since UJ116 and UJ118 also increased the invasive abilities of both cell lines (Figure 3.6). Comparing these findings to the previously evaluated effects of these complexes we observed UJ2, UJ92 and UJ116 showing fairly good anti-metastatic potential in MCF-7 cells until this point, with UJ92 leading to a significant decrease in migration, invasion and adhesion. Similarly, when looking at MDA-MB-231 cells, UJ2 and UJ92 also showed some anti-metastatic potential, each reducing migration and invasion or invasion and adhesion, respectively. Considering the finding that some chemotherapeutics may increase the aggressiveness and metastatic abilities of certain cancer cells (Maiuthed and Chanvorachote, 2014; Sun *et al.*, 2022), perhaps the finding of an increase in metastasis on a particular cancer type could be just as important as finding an inhibition of metastasis when considering potential drugs for clinical use. This emphasises the importance of considering all aspects of the metastatic process when assessing the efficacy of anti-metastatic drugs, rather than focusing on one aspect alone. The

fact, however, that these findings were observed through *in vitro* experiments should also be kept in mind. Cells growing on plastic culture dishes in a monolayer can represent the *in vivo* environment only to a certain extent.

Herein lays one of the major drawbacks of experiments performed on plastic culture dishes. Differences have been found between the expression of genes and the presence of proteins between cells grown in anchorage-dependent and -independent conditions. Also, great differences in IC_{50} values of a particular treatment have been found between cells under adherent and non-adherent conditions (Lau *et al.*, 2021). It is thus strongly recommended that any reduction in *in vitro* metastatic ability should be confirmed *in vivo* as well before making any official conclusions.

Of all the assays performed thus far, the anchorage-independent growth of cells in soft agar may be the most rigorous assessment of metastatic ability. The soft agar assay is often used as a bridge between *in vitro* and *in vivo* studies (Lau *et al.*, 2021) since the growth of cancer cells in soft agar is a more accurate representation of *in vivo* tumour growth in animal studies (Welch and Hurst, 2019). The growth of cells in soft agar, however, is much easier, more rapid and cost-effective while eliminating many of the ethical concerns associated with animal studies (Lau *et al.*, 2021). MCF-7 or MDA-MB-231 cells (1×10^4 cells in total) were mixed with an agarose-DMEM mixture and the number of colonies formed after incubation was counted and expressed as a percentage of the VC. UJ2 and UJ116 both significantly reduced the number of colonies in MCF-7 cells after 14 days of incubation (Figure 3.12), while UJ92, UJ102, UJ115 and UJ116 all significantly reduced the number of colonies formed after 7 days of incubation for MDA-MB-231 cells (Figure 3.13). A large observable difference in colony sizes was seen between treated and VC populations for MDA-MB-231 cells (Figure 3.11). Consequently, the average area of the counted colonies of MDA-MB-231 cells was also determined. A significant reduction in average colony area was found for UJ3, UJ50 and UJ115 (Figure 3.14).

The difference in the colour of the growth media between MDA-MB-231 cell populations can be an indication of the extent of cell growth in the sample. Phenol red or phenolsulfonphthalein is a pH indicator often added to cell culture media (Weiskirchen *et al.*, 2023). This indicator is yellow at an acidic pH, red at a neutral pH and fuchsia at an alkaline pH. These colour changes can occur as a result of a decrease in pH of the culture media due to the accumulation of waste products from cell growth or the presence of contaminants

(Weiskirchen *et al.*, 2023). During cell growth and proliferation, the production and accumulation of lactate, a by-product of glycolysis, leads to a reduction in the pH of the culture media resulting in the media turning orange then yellow (Sharma *et al.*, 2020). The yellow colour observed for the UC as well as UJ92 and UJ118 treated samples may be indicative of a large amount of cell growth. For UJ118, this corresponds to the findings of an average increased number of colonies (Figure 3.13) and the increase in average colony area (Figure 3.14) compared to the VC. The yellow media colour for UJ92 was unexpected since it was found that there was a significant reduction in the average number of colonies formed compared to the VC (Figure 3.13). The average colony area, however, increased when compared to the VC (Figure 3.14). It thus seems that although the number of colonies formed from UJ92 treated cells was less, the colonies that did form were on average larger than those of the VC, possibly resulting in the yellow colour of the media and alluding to an increase in the rate of cell proliferation. The pink coloured spent media of UJ50, UJ115, UJ116 and CDDP treated samples represents the least amount of cell growth of all the treatment conditions. This corresponds to the findings of a significant reduction in the number of colonies (UJ115, UJ116 and CDDP; Figure 3.13) as well as the average colony area (UJ50, UJ115 and CDDP; Figure 3.14) of these four treatment conditions. Once again, CDDP greatly reduced colony formation in soft agar for both cell lines corresponding to its reduction in anchorage-dependent colony formation of MDA-MB-231 cells which may be due to its effects on DNA (Lucaciu *et al.*, 2022); however, additional studies are required to confirm this.

Another mechanism that might be involved in the limited growth of cells in soft agar is anoikis, a mode of cell death induced when cells detach from each other or the ECM (Chitty *et al.*, 2019). Resistance to anoikis is an important characteristic enabling malignant cells that have detached from the primary tumour to survive until settling at a secondary site (Lau *et al.*, 2021). Pt(O,O'-acac)(γ-acac)(DMS) was found to reduce MCF-7 colony formation in soft agar at 0.25 µM by a remarkable 73%, while it was completely inhibited at 0.5 µM. Further evaluation revealed that this was due to the induction of anoikis (Muscella *et al.*, 2010).

Whether treatment with the silver(I) phosphine complexes decreased the growth of MCF-7 and MDA-MB-231 cells in soft agar by reducing their ability to resist anoikis would require additional studies. This may be done with the use of the low adherence and re-attachment assay (LARA). Initially, cells are added to low adherence culture plates and incubated for between 4 and 48 hr. After this, the cells are removed and added to normal culture plates and

incubated to allow attachment. Cells that have adhered to normal culture plates may then be quantified through staining with CV. Only those cells that have survived under the low adherent conditions (i.e. cells that have resistance to anoikis) will be able to attach to the normal cell culture plate and subsequently be quantified (Joussaume *et al.*, 2020). An alternative method makes use of flow cytometry and staining with propidium iodide (PI) and fluorescein isothiocyanate (FITC)-Annexin V. With this assay, termed the low adherence flow cytometry analysis (LAFCA) assay, cells are incubated in low adherence cell culture plates for 24 hr after which they are stained with the abovementioned fluorescent dyes. Cells that were able to resist anoikis (i.e. survive under low adherence conditions) will not be stained by either PI or FITC-Annexin V (Joussaume *et al.*, 2020).

Another metal-based complex containing gold(I), auranofin, significantly reduced the number of colonies formed by MDA-MB-231 cells in soft agar by more than 60% at a dose of 0.5 µM (Kim *et al.*, 2013b). Like UJ3 and UJ50 on MDA-MB-231 cells, lunasin treatment did not reduce the number of colonies formed in soft agar for H460 lung cancer cells, but a decrease in colony size was detected (McConnell *et al.*, 2015). Bamboo shavings attenuated the growth of HT1080 human fibrosarcoma cells in soft agar and showed evidence of a decrease in colony size at concentrations of 50 – 250 µg/mL. These studies were repeated in B16F10 murine melanoma cells with a similar reduction in colony formation in soft agar as well as a decrease in colony size along with a reduction in migration and invasion. The *in vivo* studies corroborated these findings where the ability of B16F10 cells to form metastasis in the lungs of mice after injection of an aqueous extract of the bamboo shavings, was significantly reduced (Kim *et al.*, 2013a).

Naturally, the soft agar assay is not without its limitations. There are arguments to be made against this assay that states that cell growth in soft agar is not completely anchorage-independent since cells are indeed attached to carbohydrate moieties within the agar (Welch and Hurst, 2019). An interesting improvement to the soft agar assay that resolves some of the limitations associated with subsequent molecular studies of cells grown in soft agar has been described by Lau *et al.* (2021). They have developed an efficient extraction protocol that allows proteins, DNA and RNA to be isolated directly from colonies formed in agar (Lau *et al.*, 2021).

Collectively looking at the research exploring the potential anti-metastatic activity of compounds, many potential drugs are natural compounds isolated from plants. A very

popular metal in cancer therapy, however, that deserves special mention is ruthenium. By exploiting the transferrin transporter system, ruthenium complexes can reach higher concentrations in cancerous cells compared to normal cells (Lucaciu *et al.*, 2022). Once inside the cell, Ru(III) is reduced to Ru(II) as a result of the lower pH and oxygen levels within cancerous cells, thereby further limiting their cytotoxic effects to hypoxic tumours that are typically resistant to other forms of chemotherapy and radiation (Lucaciu *et al.*, 2022). These ruthenium-based complexes are believed to exert their effects through binding to DNA and inducing cell cycle arrest and apoptosis. In addition, they may also act through the generation of ROS and inhibition of protein kinases (González-Ballesteros *et al.*, 2022). Several ruthenium-based complexes have been developed and assessed for their potential anti-metastatic effects, four of which have reached clinical trials, the chemotherapeutic drugs NAMI-A, KP1339 and KP1019 along with TLD1433 used in photodynamic therapy (Coverdale *et al.*, 2019; González-Ballesteros *et al.*, 2022). What makes ruthenium drugs even more interesting is the fact that some of these complexes including NAMI-A and another complex, RAPTA-C, show very little cytotoxicity towards tumours. These complexes have shown a more significant effect as anti-metastatic drugs preferentially exerting their effects on cells with metastatic abilities (Bergamo and Sava, 2015; Lu *et al.*, 2016; Lucaciu *et al.*, 2022).

When the anti-metastatic effects of NAMI-A were tested on MDA-MB-231 cells, it was found to reduce invasion by 70%, decrease cell adhesion by 60%, decrease cell migration and reduce MMP-9 activity in these cells at a sub-lethal dose of 100 μM (Brescacin *et al.*, 2015). Furthermore, a biphosphine bipyridine ruthenium complex was found to reduce migration, decrease invasion by 80% and lead to a 60% reduction in MMP-9 activity of MDA-MB-231 cells at a non-toxic concentration of 20 μM. In addition, this complex also reduced MDA-MB-231 cell adhesion to collagen type I by 35% at the same concentration (Popolin *et al.*, 2017).

Other metal-based complexes demonstrating some anti-metastatic activity include gold (Au) containing complexes, AuL6 and AuL7, which inhibited tubulin polymerisation in MDA-MB-231 cells. In addition, a zinc-containing complex inhibited migration and EMT in MDA-MB-231 cells along with reducing vimentin and β-integrin. A few copper-containing complexes also showed evidence of inhibiting migration and invasion along with decreasing MMP-2 and -9 levels in MCF-7 as well as MDA-MB-231 cells (González-Ballesteros *et al.*, 2022).

Another interesting development is the synthesis of bimetallic complexes containing both Pt(IV) and Ru(II). These complexes have been created to target both metastasis and drug resistance at the same time. Abbreviated as 'ruthplatins', these complexes have shown great toxicity in several CDDP-resistant cells by inducing cell cycle arrest. In addition, these complexes showed anti-metastatic activity against MDA-MB-231 cells as well as A549 lung cancer cells (Ma *et al.*, 2016).

4.5 Anti-metastatic mechanism of action of silver(I) phosphine complexes

There are a multitude of proteins involved in the metastatic process and answering the important question of "how cancer metastasizes" can lead to the identification of therapeutic targets. Many proteins important to this process have been identified and studied. For example, transcription factors of EMT, including CDH1, CLDN3 4 and 7, SNAI1 and 2, TWIST1 and 2, and ZEB1 and 2 (Dai *et al.*, 2016). Interestingly, an association between EMT and the development of chemotherapeutic resistance has also been found where EMT was induced through the up-regulation of EMT transcription factors in drug-resistant BC cells (Seo *et al.*, 2021). Also playing a major role in metastasis is tumour necrosis factor (TNF), an important cytokine in the angiogenesis pathway. TNF contributes to metastasis through the regulation of the expression of pro-angiogenic factors and the stimulation of the proliferation of endothelial cells. It is also involved in increasing the motility and metastatic abilities of cancer cells by up-regulating the expression of adhesion molecules (Aznag *et al.*, 2018). Furthermore, the preparation of a premetastatic niche in BC patients facilitating metastasis to the lung and bone is created because of the release of lysyl oxidase (LOX) and LOX-like proteins driven by HIF (Fares *et al.*, 2020). Also, corresponding to the hallmark of altered metabolism as stated by Hanahan and Weinberg (2011), metastatic cells show increased expression of mono-carboxylate transporter 1 (MCT1) which increases the transport of lactate that metastatic cells can use as a source of energy (Fares *et al.*, 2020). An interesting study looking at BC in mice showed that there was a correlation between the activity of asparagine synthetase and the metastatic ability, to the extent that when the levels of asparagine was reduced, there was a corresponding reduction in the development of metastases (Fares *et al.*, 2020).

Any one or more of these abovementioned proteins could be the target of anti-metastatic drugs. The anti-migratory and anti-invasive effects of actein for example, was found to be as

a result of inhibition of the EGFR / AKT pathway and a reduction in expression of nuclear factor kappa B (NF-κB) and the chemokine receptor, C-X-C motif chemokine receptor 4 (CXCR4). NF-κB inhibition has been associated with a reduction in invasion and metastasis while the reduction in adhesion of actein on MDA-MB-231 cells was believed to be caused by the inhibition of integrin α2 and β1 (Malakouti *et al.*, 2022; Wu *et al.*, 2018; Yodkeeree *et al.*, 2010). The platinum-based complex, Pt(O,O'-acac)(γ-acac)(DMS), was found to exert its effects through the generation of ROS and inhibition of Src, an important tyrosine kinase protein involved in metastasis (Muscella *et al.*, 2010). The reduction in migration, invasion and adhesion by demethoxucurcumin was found to be due in part to a reduction in the level of the adhesive molecule ICAM-1 as well as CXCR4. A reduction in ICAM-1 levels results in decreasing invasion and metastasis in BC cells, while CXCR4 may be involved in the organotropism of metastatic BC cells (Yodkeeree *et al.*, 2010). The anti-metastatic activity of rhaponticin was found to be due to the inhibition of HIF accumulation, concomitant with an increase in its degradation (Kim and Ma, 2018). HIF is also involved in EMT (Fares *et al.*, 2020), and consequently the reduction of HIF was accompanied by a reduction in EMT transcription factors including Slug, SNAI1, ZEB1 and vimentin (Kin and Ma, 2018).

Similarly, the increased effects of doxorubicin on metastasis were found to be due to an increase in the activity of NF-κB and an increase of CXCR4 (Malakouti *et al.*, 2022). The mechanism by which CDDP increased the migration of H460 lung cancer cells was found to be due to an up-regulation of focal adhesion kinase (FAK) and AKT, proteins involved in the regulation of metastasis. In addition, there was also an up-regulation in various integrins responsible for inducing the increase in migration of H460 cells in response to CDDP treatment (Maiuthed and Chanvorachote, 2014).

Naturally, the all-important MMPs are often involved in an anti-metastatic mechanism of action. MMPs have been the subject of widespread research as a therapeutic target in the fight against cancer. Various classes of MMP inhibitors have been developed and progressed to clinical trials with varying degrees of success; however, none of these have been used in the clinical setting to date (Cabral-Pacheco *et al.*, 2020). The first class consisted of compounds that inhibit MMP activity by mimicking the structure of MMP substrates and those that chelate the zinc ion needed for catalytic activity. This class includes the hydroxamate-based inhibitors batimastat, marimastat and ilomastat (Cabral-Pacheco *et al.*, 2020). A second class consists of hydroxamate-based inhibitors that are more specific than their predecessors and includes cipemastat and prinomastat. Several members of these two classes were shown to be

ineffective and caused multiple side-effects including muscoskeletal toxicity believed to be due to the chelation of key metals necessary for the functioning of other proteins along with inhibition of metabolic pathways due to their non-specific nature (Cabral-Pacheco *et al.*, 2020). A third class of compounds designed to circumvent the drawbacks of previous MMP inhibitors include rebimastat, tanomastat and Ro 28-2653, however, these drugs also produced numerous side-effects or did not show sufficient effectiveness to justify further research (Cabral-Pacheco *et al.*, 2020). The continued investigation developed several other classes of MMP inhibitors using antibodies, endogenous MMP inhibitors or drugs that target alternate binding sites. However, due to the dual role of TIMPs occasionally activating MMP activity instead of leading to inhibition, their success as therapeutic targets has been minimal (Cabral-Pacheco *et al.*, 2020).

The popularity of MMPs as therapeutic targets for an anti-metastatic mechanism of action prompted us to investigate the effects of silver(I) phosphine treatments on the expression of MMP-2 and -9 in MCF-7 and MDA-MB-231 cells. Focusing on the complexes that showed the most potential as inhibitors of metastasis for each of the two BC cell lines, proteins were extracted from treated cells and their levels detected through western blot analyses. These complexes included UJ1, UJ3 and UJ102 for MCF-7 cells and UJ3, UJ50 and UJ102 for MDA-MB-231 cells (Chapter 3, section 3.6 and Table 3.1).

A correlation between the aggressiveness and metastatic ability of various cancer types and MMP-2 and -9 has been reported. Higher levels of both MMPs have also been found in BC cells and the surrounding non-malignant cells (Li *et al.*, 2017; Muscella *et al.*, 2010; Tian *et al.*, 2018; Zhou *et al.*, 2014). Contrary to what was expected, western blot analyses revealed that intracellular MMP-2 levels were increased as a result of silver(I) phosphine treatment in MCF-7 (UJ1 and UJ3, not significant; Figure 3.15B) and MDA-MB-231 (UJ3 (not significant) and UJ50 ($P < 0.05$ for pro-MMP-2); Figure 3.15D) cells. UJ102 resulted in a negligible change in MMP-2 levels in both cell lines (Figure 3.15B and D). These findings urged the investigation into MMP-2 and -9 activities present in the conditioned media of cells, which can be detected by gelatin zymography at 72 and 92 kDa, respectively (Kim *et al.*, 2013a; Muscella *et al.*, 2010). Only UJ3 treatment in MDA-MB-231 cells showed a significant decrease in MMP-2 activity (Figure 3.16B). Therefore, despite leading to an increase in the overall accumulated protein levels of MMP-2, the anti-metastatic activities of UJ3 may at least partially be ascribed to a reduction in extracellular MMP-2 activity.

Numerous compounds with anti-metastatic potential have been found to reduce the expression levels and/or activities of MMPs including demethoxycurcumin which reduced MMP-9 levels in MDA-MB-231 cells (as determined with gelatin zymography) (Yodkeeree *et al.*, 2010). Using the same method, Pt(O,O'-acac)(γ-acac)(DMS) also showed evidence of reducing the levels and activity of MMP-2 and -9 in MCF-7 cells (Muscella *et al.*, 2010). Similar results were reported for human neuroblastoma cells (SH-SY5Y) treated with Pt(O,O'-acac)(γ-acac)(DMS) (Muscella *et al.*, 2014). Moreover, MMP-2 and -9 expression levels were decreased in both MCF-7 and MDA-MB-231 cells as a result of treatment with aloperine detected through western blot analyses (Tian *et al.*, 2018). Actein treatment at 40 μM was found to decrease the expression of MMP-2 and -9 and reduce MMP-9 activity in MDA-MB-231 cells while no significant change in MMP-2 activity was observed (Wu *et al.*, 2018). Similar to the findings for UJ3 treatment in MDA-MB-231 cells, Ma *et al.* (2017) found 24 hr treatment of the anti-metastatic compound benzyl isothiocyanate at a concentration range of 0.5 – 2 μM to increase the levels of both MMP-2 and -9 in A375.S2 human melanoma cells as shown through western blot analyses. Subsequent gelatin zymography, however, revealed a decrease in MMP-2 activity at 1 and 2 μM treatment. These authors, however, did not elaborate on the potential causes or implications of these findings.

No MMP-9 expression or activity could be detected in either cell line through western blot analyses or gelatin zymography, respectively. There are many conflicting reports regarding MMP-2 and -9 expression levels and activity in BC cell lines *in vitro*. In addition to the findings mentioned above, Mabasa *et al.* (2021) reported MMP-2 activity through gelatin zymography, however, they did not find any MMP-9 activity in MCF-7 cells. Both MMP-2 and -9 activity however was found in MCF-7 cells through gelatin zymography by Etique *et al.* (2006). In contrast, Gest *et al.* (2013) found MMP-9 activity in MDA-MB-231 cells but not MMP-2 activity through gelatin zymography. In other studies, Kim *et al.* (2013) and Kim and Ma (2018) both used phorbol 12-myristate 13-acetate (PMA) to stimulate MMP activity before assessing the anti-metastatic effect of bamboo shavings and rhaponticin, respectively on MMP-2 and -9. Another commonly used addition to the protocol for zymography includes first concentrating MMP proteins present in the conditioned media before separating the proteins through electrophoresis (Toth and Fridman, 2001). Perhaps more concentrated samples could have led to the observation of MMP-9 expression and activity for MCF-7 and MDA-MB-231 cells in this study.

Contrastingly, in another interesting study, no MMP-9 activity was detected in MDA-MB-231 cells, however, when the cells were cultured on fibronectin, MMP-9 activity was detected through gelatin zymography (Maity *et al.*, 2011). When the researchers repeated these experiments with MDA-MB-231 cells grown on collagen type IV, again no MMP-9 activity was detected by them. The authors concluded that certain signalling pathways were activated through specific interactions between cell surface integrins and fibronectin which was necessary to activate the expression of MMP-9 in MDA-MB-231 cells (Maity *et al.*, 2011). In an even earlier study conducted by Balduyck *et al.* (2000), similar observations to Maity *et al.* (2011) were made. When Balduyck *et al.* (2000) cultured MDA-MB-231 cells on plastic culture dishes; they could not detect any mRNA for MMP-9. However, when they cultured MDA-MB-231 cells on a thin layer of Matrigel®, MMP-9 expression was induced, and its activity was detected through zymography. On the other hand, Balduyck *et al.* (2000) also found that cell lines with less metastatic potential including MCF-7 cells did not express MMP-1, -3, -9 or -13 at all.

To summarise, the observations made in this study where MMP-9 was not detected in MCF-7 cells through western blot analyses or zymography, corresponds with the findings of Balduyck *et al.* (2000) and Mabasa *et al.* (2021) who were also unable to detect any MMP-9 expression in the same cell line. In addition, our lack of finding MMP-9 expression and activity in MDA-MB-231 cells corresponds to the findings of both Balduyck *et al.* (2000) and Maity *et al.*, (2011) findings where MMP-9 was only found through specific interaction of cells with components of the ECM. Our findings, however, do not correspond to other studies mentioned before where MMP-9 was detected in MCF-7 and MDA-MB-231 cells with or without the presence of the inducer PMA.

Collagen zymography (Figure 3.17) showed similar results to gelatin zymography (Figure 3.16) where only UJ3 treatment resulted in a significant reduction of a 70 kDa collagenase in MDA-MB-231 cells (Figure 3.17B). There are three different known collagenases, MMP-1, -8 and -13. MMP-1 can be present in a 57 kDa major form or a 61 kDa minor glycosylated form and preferentially cleaves collagen type III. MMP-8 is 64 kDa with a 75 kDa glycosylated form which more readily cleaves collagen type I. Lastly, MMP-13 is a 48 kDa enzyme that preferentially cleaves collagen type II (Klein and Bischoff, 2011). Based on these values, the 70 kDa collagenase found in MDA-MB-231 conditioned media through collagen type I zymography is most likely MMP-8 (Figure 3.17).

In general, MMPs are associated with aiding the process of metastasis, however, MMP-8 or collagenase-2 is an interesting exception in some cancer types. In a paper written by Juurikka *et al.* (2019), the often-contradictory reports regarding MMP-8 were compared. The authors found that MMP-8 can both serve a protective as well as a harmful role in cancer metastasis but that this is highly dependent on the cancer type. In cancers of the breast, skin and tongue, MMP-8 was found to inhibit invasion and decrease metastasis while the opposite effect was found for cancers of the liver and stomach. Juurikka *et al.* (2019) also reported that some studies found MCF-7 cells to not show any evidence of the presence of MMP-8. This corresponds to what was found in this study with the absence of collagen activity in MCF-7 conditioned media. On the contrary, MMP-8 activity was detected in the highly metastatic BC cell lines including MDA-MB-435, MDA-MB-468 and MDA-MB-231. However, it was observed that in cell lines expressing MMP-8, the metastatic ability was less in *in vivo* mice studies, suggesting a protective role of MMP-8 against metastasis *in vivo* (Juurikka *et al.*, 2019). The seemingly contradictory finding where UJ3 showed anti-metastatic effects on MDA-MB-231 cells in reducing migration, invasion and colony formation *in vitro* (Table 3.1), concurrent with a decrease in MMP-8 activity (Figure 3.17B) should rather be further evaluated before definite conclusions can be drawn. This may be done with the help of western blot analyses or through MMP-8 mRNA studies.

Since no obvious mechanism of action was found for UJ1, UJ3 and UJ102 in MCF-7 cells or for UJ50 and UJ102 in MDA-MB-231 cells, there are several other proteins that may be evaluated instead of MMPs. Anillin, an important scaffolding protein, has been found to be overexpressed in BC as well as several other cancer types including colon, gastric, lung, liver and pancreatic cancer. It was also found that there is a correlation between the expression of anillin and BC metastatic potential since higher levels of anillin were found in more invasive BC cell lines such as MDA-MB-231, MDA-MB-468 and BT549 compared to the less invasive MCF-7 and BT474 cell lines. A recent study has found anillin to be important in the *in vitro* migration, invasion and anchorage-independent colony-forming abilities of BC cells and depletion of anillin decreased the *in vivo* metastasis of BC (Wang *et al.*, 2020). Studies involving the relationship between anillin expression and metastasis in MDA-MB-231 cells found that the knockdown or the overexpression of anillin did not have any effect on the anchorage-dependent growth abilities of cells. However, decreased levels of anillin were found to decrease the ability of MDA-MB-231 cells to form colonies in soft agar (Wang *et al.,* 2020). Since a decrease in anillin was also showed to reduce migration and invasion of

MDA-MB-231 cells (Wang *et al.*, 2020), this could be an interesting protein to look at in establishing the anti-metastatic mechanism of UJ50 and UJ102 in MDA-MB-231 cells.

Another protein worth considering as a target of silver(I) phosphine treatment could be the urokinase plasminogen activator (uPA). Increased levels of uPA cause the plasmin levels to increase which contributes to the degradation of the ECM. Plasmin in turn can then activate growth factors including VEGF involved in metastatic signalling pathways (Mali *et al.*, 2017). The anti-metastatic activity of demethoxucurcumin was found to be due to a reduction in uPA and its receptor (uPAR), along with an increase in the uPA inhibitor (Yodkeeree *et al.*, 2010). Similarly, the anti-metastatic effects of enterolactone were due to a decrease in uPA in MDA-MB-231 cells (Mali *et al.*, 2017).

In fact, there are several additional proteins involved in the metastatic cascade of BC cells that can be investigated to establish a mechanism of action of the silver(I) phosphine complexes. Since the assays conducted in this study (only looking at one protein at a time) to establish an anti-metastatic mechanism of action are quite laborious and time-consuming it is proposed to rather consider either a proteomic or metabolomic approach. Through these, any changes in protein or metabolite profiles as a results of silver(I) phosphine treatment can be evaluated simultaneously (Hart, 2005).

4.6 Anti-metastatic control treatments

CDDP was used in this study as a comparative benchmark for metal-based complexes since it is considered to be the golden standard of metal-based chemotherapeutic drugs (Ma *et al.*, 2016) and is also frequently used in the treatment of mBC (Zhu *et al.*, 2020). Despite its effectiveness, this platinum containing drug is however associated with multiple systemic side-effects (Lucaciu *et al.*, 2022) making the search for alternative metal-based treatments with superior qualities crucial. Previous studies conducted on this particular class of silver(I) phosphine complexes have also compared the effects of the silver(I) phosphine complexes to CDDP where great promise for these complexes have been shown against oesophageal cancer and BC (Engelbrecht *et al.*, 2018; Ferreira *et al.*, 2015; Human *et al.*, 2015; Human-Engelbrecht *et al.*, 2017; Potgieter *et al.*, 2017). In addition, at a concentration of 10X less that the tested dose of CDDP, these silver(I) phosphine complexes have shown great promise against cell lines representing cancer of the cervix (HeLa), colon (HT-29) and liver (Hep-G2) while showing partial success towards cancer of the lung (A549), pancreas (MIA PaCa2),

prostate (PC3) and skin (MeWo) (M.J. Cronjé, personal communication, Aug 17, 2023), illustrating the potential of these metal-based complexes as an alternative to CDDP.

The highest non-toxic concentrations of silver(I) phosphine complexes were used for the subsequent anti-metastatic studies. Keeping in line with this reasoning, the same was done for CDDP. These studies were performed by fellow researchers Dr. Kim Roberts (Roberts, 2023) and Dr. Zelinda Engelbrecht (Z Engelbrecht, personal communication, May 30, 2021). The highest concentrations of CDDP that was not toxic to MCF-7 and MDA-MB-231 cells were 12.5 µM and 25 µM, respectively (Figure 3.1A and B). These concentrations were 10X that of the highest sub-lethal concentrations found for the silver(I) phosphine complexes (Figure 3.1A and B). As explained in Section 4.2, the similar sub-lethal concentrations of silver(I) phosphine complexes were chosen for each cell line to attempt to eliminate the effects of varying DMSO concentrations used as the VC. Since CDDP was prepared in a 0.9% NaCl solution and not DMSO, the same doses used for silver(I) phosphine complexes were not used for CDDP.

All of the findings of this study were presented as a percentage value of the VC (including CDDP). Taking into consideration the large significant difference between the VC and UC cell samples in Figure 3.5B, Figure 3.6, Figure 3.7B and Figure 3.15D, it would seem that DMSO had a greater effect on several metastasis-related phenotypes that initially expected.

To summarize, in MDA-MB-231 cells, the migration of UC populations was significantly less than that of the VC (Figure 3.5B) and the adhesion of UC MCF-7 and MDA-MB-231 cells was considerably less compared to the VC (Figure 3.7A and B). In contrast, the invasive abilities of UC populations of both cell lines were significantly increased compared to VC populations (Figure 3.6). It thus seemed that low doses of DMSO (MCF-7: 0.125%; MDA-MB-231: 0.25%) increased migration and adhesion in MDA-MB-231 cells and increased adhesion in MCF-7 cells, but decreased MCF-7 and MDA-MB-231 cell invasion.

DMSO, a widely used solvent for drugs (Wang *et al.*, 2012) is considered to be an antioxidant at low concentrations while being pro-oxidant at high concentrations (Dludla *et al.*, 2018). However, low doses of DMSO, ≤ 3.7%, were previously found to initiate oxidative stress in MCF-7 cells detected as an increase in the activity of ROS and increased apoptosis compared to untreated cells (Sangweni *et al.*, 2021). DMSO at 10%, 5%, 2.5% as well as 1.25% was found to be cytotoxic and inhibit the *in vitro* proliferation of MCF-7 and MDA-MB-231 cells while DMSO at a concentration of 0.6% was toxic to MCF-7 but not

MDA-MB-231 cells. Concentrations of 0.3% and 0.15% were not toxic to either BC cell line (Nguyen *et al.*, 2020). *In vivo*, low doses of DMSO (0.5 – 1 mg/g) were found to suppress the growth of BC in mice (Deng *et al.*, 2014). Furthermore, DMSO doses of 1% and 2% were found to inhibit the migration, invasion and colony-forming abilities of CL1-5 human lung adenocarcinoma cells concurrent with an up-regulation of E-cadherin (Wang *et al.*, 2012). In addition to being an important solvent, DMSO even at very low concentrations seems to have its own effect on cell behaviour which should not be ignored and investigated in more detail.

When taking all of these factors into account, the interpretation of the anti-metastatic effects of CDDP on MCF-7 and MDA-MB-231 cells as conducted in this study becomes somewhat complicated. CDDP significantly decreased migration (Figure 3.5B), increased invasion (Figure 3.6), and decreased anchorage-dependent colony formation (Figure 3.9B) in MDA-MB-231 cells while significantly decreasing anchorage-independent colony formation (Figure 3.12 and 3.13) in both cell lines, while not showing any significant effects on the rest of the metastatic parameters tested. For the purpose of this study, CDDP might not have been the best treatment to use as an anti-metastatic control. Perhaps another drug used for the treatment of mBC as listed in Table 1.3 might have been a better option.

In addition, thiazolidinediones, which are ligands of nuclear receptors, reduces the function of several inflammatory transcription factors such as NF-κB. These drugs, including pioglitazone, can inhibit the invasion and metastasis of BC cells (Malakouti *et al.*, 2022). Chondramide, cytochalasin D and latrunculin A, drugs that target actin polymerization, have been found to inhibit invasion in MDA-MB-231 cells, while blebbistatin was found to inhibit the *in vitro* invasion of MCF-7 and MDA-MB-231 cells through inhibiting the activity of myosin II (Gandalovičová *et al.*, 2017). Perhaps one of these complexes might have been a better alternative to CDDP for this study.

On the other hand, the inclusion of assay specific active controls for each assay might have been even more informative. For example, Almeida *et al.* (2019) suggested the use of either colchicine or paclitaxel, compounds with anti-microtubule activity, as controls for the inhibition of migration for the scratch assay. In addition, cytochalasin D, another inhibitor of cell migration through actin depolymerisation was used by Glenn *et al.* (2016). The use of oxidized streptolysin O was investigated by Hall *et al.* (2011) as a potential inhibitor of cell invasion. It was found that this compound significantly inhibited the *in vitro* invasion of MDA-MB-231 cells through Matrigel® (Hall *et al.*, 2011). To inhibit the *in vitro* colony

formation of cells, Rundén-Pran *et al.* (2022) suggested the use of chlorpromazine hydrochloride or staurosporine.

The inclusion of positive controls is especially important in the detection of MMPs through western blot and zymography. No MMP-9 was detected in either MCF-7 or MDA-MB-231 cells through the use of western blot, however, whether this was a consequence of the lack of detectable levels of MMP-9 present in these cell lines or perhaps due to experimental factors (e.g. low concentration of MMP-9 in loaded protein sample) or the choice of antibody is not clear. The same argument can be made for the zymography analysis where no MMP-2 or -8 activity was detected in MCF-7 cells and no MMP-9 activity was detected in either cell line. Empty western blot and zymography images were not included in the results since no visible bands were present. Tajhya *et al.* (2017) recommends the inclusion of recombinant MMPs as control samples when conducting experiments on *in* vitro cellular MMPs. In addition, control treatments known to reduce the expression or activity of MMP-2 and -9 could have been included. As a control treatment for western blot, this may include NS-398, a cyclooxygenase-2 inhibitor, which was found to reduce mRNA levels of MMP-2 and -9 in BC cells *in vitro* (Larkins *et al.*, 2006). Pre-treatment with batimastat or prinomastat, both inhibitors of MMP activity may have been included as controls for MMP zymography analysis (Benjamin and Khalil, 2012).

4.7 Final note

Metastases or distant secondary masses consist of cells that although they originate from the primary tumour, are cells that are biochemically and genetically different from those cells of the primary tumour. Metastatic cells have gone through a series of transformations enabling them to establish metastases (Riggio *et al.*, 2021; Welch and Hurst, 2019). Where metastasis is concerned, not all cancer cells are considered equal. Metastatic traits (migration, invasion and loss of adhesion to the primary tumour etc.) may be acquired in any order but the acquisition of all metastatic traits is necessary for the completion of the metastatic cascade. These cells can subsequently proliferate and pass these traits on to their daughter cells (Welch and Hurst, 2019). What makes this process even more complex is the ability of a metastasized (secondary) tumour to metastasize further, forming tumour masses throughout the body (Welch and Hurst, 2019).

Future development of anti-metastatic treatments would need to centre on improving our identification and understanding of those characteristics, whether it is certain genes or groups

of genes or phenotypic markers, which distinguish metastatic cells from other cells so that they could be effectively targeted. These treatments would likely have to involve targeting more than one characteristic simultaneously (Wang and Huang, 2017). An example of such a phenotypic marker is the discovery of the presence of a perinuclear compartment in cancer cells which shows a correlation with the metastatic ability of several prostate cancer types (Wang and Huang, 2017).

Patients are often over-treated with drugs after surgical removal of the primary tumour, in an understandable attempt to prevent the formation of macro-metastases. However, this may lead to lifelong side-effects (Ganesh and Massagué, 2021), emphasising the need for a better understanding of metastatic spread so that more specific treatment strategies can be developed. Interesting findings using immune checkpoint inhibitors have been found in TNBC mice studies. When these inhibitors were administered prior to the surgical removal of the primary tumour, patients showed improved outcomes due to the removal of micro-metastases by the immune system, compared to those patients who received the treatment post-surgery (Ganesh and Massagué, 2021). Another interesting form of immune therapy for hormone receptor-positive mBC has shown great promise in an on-going clinical trial. Tumour infiltrating lymphocytes reactive against certain mutations are extracted from a patient, multiplied and then re-administered creating an effective immune response (Zacharakis *et al.*, 2022). In another recent study, a peptide was developed that can inhibit the interaction between proline-rich tyrosine kinase 2 (Pyk2) and its substrate cortactin, proteins which participate in cancer metastasis through the formation of invadopodia (Twafra *et al.*, 2023).

The research conducted here is naturally not without limitations, the foremost one being the lack of *in vivo* studies regarding the anti-cancer as well as the anti-metastatic effects of the silver(I) phosphine complexes. Even though a few of the complexes did show preliminary potential, the *in vitro* metastatic parameters evaluated in this study represent only a few important steps of metastasis and does not by any means encompass the entire complexity of the metastatic cascade or the involvement of the tumour environment. In addition, only two BC cell lines representing two of the BC subtypes (luminal A and TNBC) were evaluated. This falls far short of representing the large variety of BCs that exists and do not answer the question of whether the anti-metastatic effects seen here are specific to the BC subtype, especially since the different complexes did not have a similar effect on MCF-7 and MDA-MB231 cells. An evaluation of the effects of the silver(I) phosphine complexes on the

expression and activity of certain MMPs did not provide much insight into a potential anti-metastatic mechanism of action. A more comprehensive genomic, proteomic or metabolomic study of the *in vitro* effects of these sub-lethal doses of silver(I) phosphine complexes on BC cell lines is thus needed.

Of the class of silver(I) phosphine complexes synthesised, UJ50, UJ92, UJ102, UJ115, UJ116 and UJ118 were originally chosen for this research due to their cytotoxic effect when tested on MCF-7 and MDA-MB-231 cells (Appendix D). The discovery that certain ruthenium complexes are more efficient at inhibiting metastases rather than acting as cytotoxic agents (Lucaciu *et al.*, 2022), suggests that additional silver(I) phosphine complexes could be evaluated for their potential anti-metastatic action, not only against BC but other cancer types as well.

Another interesting factor to look at would be the result of treatment with a cocktail of the different silver(I) phosphine complexes showing anti-metastatic activity. The synergistic effect of multiple complexes, each inhibiting key steps of metastasis on their own may show a greater potential than either one on its own could.

In addition, considering that MMP inhibitors have thus far not achieved much success in the clinical setting, anti-metastatic treatments (like UJ50 and UJ102) that work independently of these proteins might offer an advantageous alternative.

To end off, even though metastasis may be more difficult to treat compared to the primary tumour, metastatic cells are still able to respond to several different therapies. Welch and Hurst (2019) therefore concluded their review on metastasis by stating that instead of referring to metastasis as being incurable, we should rather refer to it as “currently incurable” and keep the hope alive that a cure may still be developed in future.

Conclusions

The main aim of this study was to investigate whether silver(I) phosphine complexes could reduce the metastatic potential of two BC cell lines *in vitro*. MCF-7 and MDA-MB-231 cells were treated with a selection of nine related silver(I) phosphine complexes and various metastatic parameters were evaluated in response to the treatments.

Of the nine complexes tested, some showed early potential in reducing key aspects of metastasis *in vitro* in both the minimally invasive MCF-7 cell line as well as the highly invasive MDA-MB-231 cell line. UJ1, UJ92, UJ116 and UJ118 all resulted in a significant reduction in more than one feature of metastasis including migration, invasion and adhesion of MCF-7 cells. The same was found for UJ2, UJ3, UJ50, UJ92 and UJ115 for the MDA-MB-231 cell line. Findings also showed that three of the complexes, UJ115, UJ116 and UJ118, partially increased the abilities of cells to invade through collagen type I towards a chemoattractant. This poses the concern that these complexes might contribute to the development of metastasis at sub-toxic concentrations as seen with some commonly used chemotherapeutic drugs. It would be important to evaluate this further before proposing these as potential anti-metastatic agents.

The above mentioned *in vitro* effects also require further investigation both *in vitro* and *in vivo* since limitations of the experiments performed in this study could affect the interpretation of the results. For instance, the proliferative effects of cells contributing to wound closure during the scratch assay and in the Transwell® invasion assay was not accounted for and cannot be ignored. In addition, although making up a large part of the ECM, collagen alone does not represent the entirety of the ECM *in vivo*. For this reason the invasion through and adhesion to other components of the ECM including collagen type II and IV, fibronectin, laminin and vitronectin should also be assessed.

Once disseminated from the primary tumour, cells must colonize to a new environment to form secondary metastases. This aspect of the metastatic process was also studied by assessing the abilities of MCF-7 and MDA-MB-231 cells to proliferate and form colonies in response to silver(I) phosphine treatments. The ability of MCF-7 cells in single suspension to form colonies on plastic culture dishes was significantly decreased by UJ1, UJ3, UJ102 and UJ115. A similar significant decrease was seen in response to treatment with UJ3, UJ50, UJ102, UJ115 and UJ116 for MDA-MB-231 cells. In contrast, UJ116 showed a tendency to significantly increase colony formation in MCF-7 cells. In addition, the growth of cells in soft agar was used to evaluate whether silver(I) phosphine treatment might reduce the abilities of cells to survive and proliferate

in a semi-solid medium independent of being attached to a culture dish. UJ2 and UJ116 both significantly reduced the number of colonies formed for MCF-7 cells, while UJ92, UJ102, UJ115 and UJ116 significantly reduced the number of colonies formed for MDA-MB-231 cells. In addition, UJ3, UJ50 and UJ115 resulted in significantly smaller colonies for MDA-MB-231 cells compared to the VC. These findings suggest a possible role of these complexes to reduce the formation of secondary metastases of BC from disseminated cells *in vitro*.

The positive findings of a significant reduction in metastasis *in vitro* prompted the investigation into the protein targets of the anti-metastatic action of the silver(I) phosphine complexes. Taking into account all of the findings, both statistically significant and trending, albeit non-significant, the complexes with the most potential were selected for each cell line. Complexes were selected based on their abilities to significantly reduce more than one aspect of metastasis while not showing any propensity to increase any of the evaluated steps. Further analysis was thus conducted on UJ1, UJ3 and UJ102 for MCF-7 cells and UJ3, UJ50 and UJ102 for MDA-MB-231 cells.

Considering the significance of MMPs in metastasis and their popularity as therapeutic targets of anti-metastatic drugs, the levels of MMP-2 and MMP-9 were assessed in response to treatments. A non-significant increase in intracellular MMP-2 levels was found as a result of UJ1 and UJ3 treatment in MCF-7 cells and UJ3 treatment in MDA-MB-231 cells. On the contrary, a significant increase in pro-MMP-2 levels was found for MDA-MB-231 cells in response to treatment with UJ50 as revealed through western blot analyses. No levels of MMP-9 accumulation were found in either cell line at amounts that were detectable through western blot analyses, despite varying the experimental conditions. These outcomes, being different to what was expected, encouraged the evaluation of MMP activity in conditioned media of MCF-7 and MDA-MB-231 treated cells through zymography. Conditioned media of MCF-7 cells did not show any MMP activity detectable through zymography with the use of gelatin, collagen or casein as a substrate. The evaluation of the effect of silver(I) phosphine treatment on MCF-7 MMP activity was thus inconclusive. With the use of zymography, only UJ3 treatment was shown to significantly reduce MMP-2 and potentially MMP-8 activity in conditioned media of MDA-MB-231 cells, while no casein degrading activity was detected.

Taken together, the findings of this study show that in addition to their toxic effects at higher concentrations, as revealed through previous research, silver(I) phosphine complexes also have *in vitro* anti-metastatic effects at low concentrations against two malignant BC cell lines. While the mechanism of action of these anti-metastatic effects remains to be determined, it seems to be for

the most part, except for UJ3 on MDA-MB-231 cells, independent of MMP activity. Further investigation is, however, needed to confirm this.

The inclusion of active controls for each of the various experiments conducted as well as a more detailed investigation into the effects of DMSO on various metastatic phenotypes *in vitro* would greatly assist in interpreting the findings of this study. Similarly, the inclusion of *in vivo* or at least 3D cell culture studies would have been a useful addition to confirm the *in vitro* findings. Nonetheless, these findings do warrant further investigation into the potential of silver(I) phosphine complexes as possible anti-metastatic drugs for malignant BC.

Future studies

The work conducted here served as a preliminary study to establish whether silver(I) phosphine complexes had any potential to be used as anti-metastatic drugs at sub-lethal doses on two malignant human BC cell lines. The findings presented here could lead to a whole new set of projects involving anti-metastatic drug discovery.

- Firstly, dose-response *in vitro* studies can be carried out using the selected silver(I) phosphine complexes with the most anti-metastatic potential as was found in this study.
- This study can be expanded to include additional BC cell lines for a more comprehensive study of the potential anti-metastatic effects of silver(I) phosphine complexes on a specific molecular subtype of BC. This may involve the inclusion of additional triple negative (e.g. BT20, MDA-MB-468) or luminal A (e.g. MDA-MB134, T47D) BC cell lines (Dai *et al.*, 2017).
- The potential toxicity of the concentrations of the silver(I) phosphine complexes used in this study against a normal breast epithelial cell line e.g. MCF10A should be evaluated to ensure the safety of these complexes and treatment doses on non-malignant breast tissue.
- Instead of studying protein levels through western blot, the expression of certain proteins suspected to be involved in the anti-metastatic effects of the silver(I) phosphine complexes (e.g. MMPs, anillin, TNF, uPA or EMT associated proteins) could be silenced through RNA interference studies to see whether the anti-metastatic effect is lost.
- In contrast to studying individual genes or proteins, however, an "-omics" approach (genomics, proteomics or metabolomics) could be employed. Possible changes in large amounts of mRNA, proteins or metabolites in response to treatments could be investigated simultaneously to see which proteins or signalling pathways are targeted.
- Genomic, proteomic and metabolomic studies performed on cases where a specific treatment was found to increase certain metastatic parameters of MCF-7 or MDA-MB-231 cells could also be informative. This could lead to further insights into how commonly used chemotherapeutic drugs may lead to the aggravation of metastatic spread as well as possible ways to overcome this.

- 3D cell culture studies are gaining a lot of popularity due to their more accurate representation of *in vivo* environments compared to 2D monolayer cell cultures (Edmondson *et al.,* 2014). Tumour spheroids using the MCF-7 and MDA-MB-231 cell lines could be constructed. A 3D tumour spheroid invasion assay can then be used to evaluate the anti-metastatic effects of the silver(I) phosphine complexes in 3D cultures (Vinci *et al.,* 2015).
- Another field of cell culture that could contribute greatly to metastatic research is the construction of co-cultures which adds some of the complex interactions between cancer cells and other cell types into the investigation. One such study used the co-culture of BC cells and bone marrow stromal cells to investigate key factors involved in the organotropism displayed by ER-positive BC cells to metastasize to the bone (Arrigoni *et al.*, 2016). Mi *et al.* (2016) suggested the use of MDA-MB-231 cells and non-malignant breast cells e.g. HMEpiC (human mammary epithelial cells) in a co-culture system to investigate the effects of normal cells on the migration of BC cells. In addition, the interaction between BC cells and immune cells in drug screening studies can be investigated by co-culturing BC cell lines with BC patient-derived immune cells (Saraiva *et al.*, 2020).
- In addition to mBC cell lines, using the *in vitro* anti-metastatic assays carried out in this study, the research could be expanded to include many other highly metastatic cancer types using cell lines representing cancer of the prostate, lung, liver, colon and kidneys.
- This study could be expanded to include additional members of the class of silver(I) phosphine complexes (different ligands or ligand ratios) to evaluate their *in vitro* anti-metastatic potential.
- Lastly, animal studies to evaluate the toxicity as well as the anti-metastatic effects of the silver(I) phosphine complexes *in vivo* need to be performed. To date *in vivo* toxicity studies carried out on rats and xenograft mouse models have only been performed on three of the silver(I) phosphine complexes (unpublished data).

References

Aiello, N.M., Maddipati, R., Norgard, R.J., Balli, D., Li, J., Yuan, S., Yamazoe, T., Black, T., Sahmoud, A., Furth, E.E., Bar-Sagi, D., Stanger, B.Z., (2018), EMT subtype influences epithelial plasticity and mode of cell migration, *Developmental Cell*, 45(6): 681-695, e4. doi: 10.1016/j.devcel.2018.05.027

Almeida, V.M., Bezerra, M.A., Nascimento, J.C. and Amorin, L.M.F., (2019), Anticancer drug screening: standardization of *in vitro* wound healing assay, *Jornal Brasileiro de Patologia e Medicina Laboratorial*, 55(6): 606-619

Anderson, R.L., Balasas, T., Callaghan, J., Coombes, R.C., Evans, J., Hall, J.A., Kinrade, S., Jones, D., Jones, P.S., Jones, R., Marshall, J.F., Panico, M.B., Shaw, J.A., Steeg, P.S., Sullivan, M., Tong, W., Westwell, A.D. and Rithcie, J.W.A., (2019), A framework for the development of effective anti-metastatic agents, *Clinical Oncology*, 16: 185-204. doi: 10.1038/s41571-018-0134-8

Arrigoni, C., Bersini, S., Gilardi, M. and Moretti, M., (2016), *In vitro* co-culture models of breast cancer metastatic progression towards bone, *International Journal of Molecular Sciences*, 17(9): 1405. doi: 10.3390/ijms17091405

Asif, M., Iqbal, M.A., Hussein, M.A., Oon, C.E., Haque, R.A., Ahamed, M.B.K., Majid, A.S.A. and Majid, A.M.S.A., (2016), Human colon cancer targeted pro-apoptotic, anti-metastatic and cytostatic effects of binuclear Silver(I)-*N*-Heterocyclic carbine (NHC) complexes, *European Journal of Medicinal Chemistry*, 108: 177-187. Doi: 10.1016/j.ejmech.2015.11.034

Aznag, F.Z., Kadmiri, N.E. and Izaabel, E.H., (2018), Tumor necrosis factor-alpha and tumor necrosis factor beta polymorphisims and risk of breast cancer: Review, *Gene Reports*, 12: 317-323. doi: 10.1016/j.genrep.2018.07.018

Badal, A., (2022), The mechanistic action of silver(I) thiocyanate 4-methoxyphenyl phosphine promoting apoptosis in MCF-7 and MDA-MB-231 breast cancer cell lines, M.Sc. Dissertation, University of the Witwatersrand, South Africa

Balduyck, M., Zerimech, F., Gouyer, V., Lemaire, R., Hemon, B., Grard, G., Thiebaut, C., Lemaire, V., Dacquembronne, E., Duhem, T., Lebrun, A., Dejonghe, M-J. and Huet, G., (2000), Specific expression of matrix metalloproteinases 1, 3, 9 and 13 associated with invasiveness of breast cancer cells *in vitro*, *Clinical and Experimental Metastasis*, 18: 171-178.

Barron, P.F., Dyason, J.C., Healy, P.C., Enhelhardt, L.M., Skelton, B.W. and White A.H., (1986), Lewis base adducts of Group 11 metal compounds. Part 24. Co-ordination of triphenylphosphine with silver nitrate – A solid-state cross-polarization magic angle spinning 31P nuclear magnetic resonance, crystal structure and infrared spectroscopic study of Ag(PPh3)*n*NO3(n=1-4), *Journal of the Chemical Society, Dalton transactions*, 1965-1970.

Benjamin, M.M. and Khalil, R.A., (2012), Matrix metalloproteinase inhibitors as investigative tools in the pathogenesis and management of vascular disease, *Exp Suppl*., 103: 209-279. doi: 10.1007/978-3-0348-0364-9_7

Bergamo, A. and Sava, G., (2015), Linking the future of anticancer metal-complexes to the therapy of tumour metastases, *Chemical Society Reviews*, 44: 8818. doi: 10.1039/c5cs00134j

Berners-Price, S.J. and Sadler, P.J., (1988), Structure and bonding, phosphine and metal phosphine complexes: Relationship of chemistry to anticancer and other biological activity, *Bioinorganic Chemistry*, 70: 27-102.

Bhushan, A., Gonsalves, A. and Menon, J.U., (2021), Current state of breast cancer diagnosis, treatment and theranostics, *Pharmaceutics*, 13: 723. doi: 10.3390/pharmaceutics13050723

Brescacin, L., Masi, A., Sava, G. and Bergamo, A., (2015), Effects of the ruthenium-based drug NAMI-A on the roles played by TGF-β1 in the metastatic process, *Journal of Biological Inorganic Chemistry*, 20: 1163-1173. doi: 10.1007/s00775-015-1297-8

Cabral-Pacheco, G.A., Garza-Veloz, I., Castruita-De la Rosa, C., Ramirez-Acuña, J.M., Perez-Romero, B.A., Guerrero-Rodriguez, J.F., Martinez-Avila, N. and Martinez-Fierro, M.L., (2020), The roles of matrix metalloproteinases and their inhibitors in human diseases, *International Journal of Molecular Sciences*, 21: 9739. doi: 10.3390/ijms21249739

Cairncross, L., Parkes, J., Craig, H. and Are C., (updated 10 September 2021), Cancer on the global stage: Incidence and cancer-related mortality in South Africa, https://ascopost.com/issues/september-10-2021/cancer-on-the-global-stage-incidence-and-cancer-related-mortality-in-south-africa, (Accessed 7 November 2022)

Caulfield, S.E., Davis, C.C. and Byers, K.F., (2019), Olaparib: A novel therapy for metastatic breast cancer in patients with a *BRCA1/2* mutation, *Journal of the Advanced Practitioner in Oncology*, 10(2): 167-174. doi: 10.6004/jadpro.2019.10.2.6

Chitty, J.L., Filipe, E.C., Lucas, M.C., Hermann, D., Cox, T.R. and Timpson, P., (2018), Recent advances in understanding the complexities of metastasis [version 2; referees: 3 approved], *F1000Research,* 7(F1000 Faculty Rev): 1169. doi: 10.12688/f1000research.15064.2

Comşa, Ş., Cîmpean, A.M. and Raica, M., (2015), The story of MCF-7 breast cancer cell line: 40 years of Experience in Research, *Anticancer Research,* 35: 3147-3154. PMID: 26026074

Cory, G. (2011), Scratch-wound assay, In Methods in Molecular Biology, vol 769: Cell Migration: Developmental Methods and Protocols, Wells, C.M. and Parsons, M. (eds.), Springer Science + Business Media, Chapter 2. doi: 10.1007/978-1-61779-207-6_1

Coverdale, J.P.C., Laroiya-McCarron, T. and Romero-Canelon, I., (2019), Designing ruthenium anticancer drugs: what have we learnt from the key drug candidates?, *Inorganics,* 7(31). doi: 10.3390/inorganics7030031

Dai, X., Cheng, H., Bai, Z. and Li, J., (2017), Breast cancer cell line classification and its relevance with breast tumour subtyping, *Journal of Cancer,* 8(16): 3131-3141. doi: 10.7150/jca.18457

Dai, X., Xiang, L., Li, T. and Bai, Z., (2016), Cancer hallmarks, biomarkers and breast cancer molecular subtypes, *Journal of Cancer,* 7(10): 1281-1294. doi: 10.7150/jca.13141

De Fries, R. and Mitsuhashi, M., (1995), Quantification of mitogen induced human lymphocyte proliferation: Comparison of alamarBlue™ assay to ^{3}h-thymidine incorporation assay, *Journal of Clinical Laboratory Analysis*, 9(2): 89-95. doi: 10.1002/jcla.1860090203

Deng, R., Wang, S.M., Yin, T., Ye, T.H., Shen, G.B., Li, L., Zhao, J.Y., Sang, Y.X., Duan, X.G., Wei, Y.Q., (2014), Dimethyl sulfoxide suppresses mouse 4T1 breast cancer growth by modulating tumor-associated macrophage differentiation, *Journal of Breast Cancer,* 17(1): 25-32. doi: 10.4048/jbc.2014.17.1.25

Dludla, P.V., Jack, B., Viraragavan, A., Pheiffer, C., Johnson, R., Louw, J. and Muller, C.J.F., (2018), A dose-dependent effect of dimethyl sulfoxide on lipid content, cell viability and oxidative stress in 3T3-L1 adipocytes, *Toxicology Reports,* 5: 1014-1020. doi: 10.1016/j.toxrep.2018.10.002

Dufour, A. and Overall, C.M., (2013), Missing the target: matrix metalloproteinase antitargets in inflammation and cancer, *Trends in Pharmacological Sciences*, 34(4): 233-242. doi: 10.1016/j.tips.2013.02.004

Edmondson, R., Broglie, J.J., Adcock, A.F. and Yang, L.. (2014), Three-dimensional cell culture systems and their applications in drug discovery and cell-based biosensors, *Assay and Drug Development Technologies*, 12(4): 207-218. doi: 10.1089/adt.2014.573

Engelbrecht, Z., (2017), Novel Anticancer silver(I) phosphines proven to target the mitochondrial-mediated cell death pathway in malignant cells, Ph.D. Thesis, University of Johannesburg, South Africa

Engelbrecht, Z., Meijboom, R. and Cronjé, M.J., (2018), The ability of silver(I) thiocyanate 4-methoxyphenyl phosphine to induce apoptotic cell death in esophageal cancer cells is correlated to mitochondrial perturbations, *Biometals*, **31:** 189-202, doi: 10.1007/s10534-017-0051-9

Etique, N., Grillier-Vuissoz, I. and Flament, S., (2006), Ethanol stimulates the secretion of matrix metalloproteinases 2 and 9 in MCF-7 human breast cancer cells, *Oncology Reports*, 15: 603-608. PMID: 16465419

Falasca, M., Raimondi, C. and Maffucci, T., (2011), Boyden chamber, In Methods in Molecular Biology, vol 769: Cell Migration: Developmental Methods and Protocols, Wells, C.M. and Parsons, M. (eds.), Springer Science + Business Media, Chapter 7. doi: 10.1007/978-1-61779-207-6_1

Fares, J., Fares, M.Y., Khachfe, H.H., Salhab, H.A. and Fares, Y., (2020), Molecular principles of metastasis: a hallmark of cancer revisited, *Signal Transduction and Targeted Therapy*, 5:28. doi: 10.1038/s41392-020-0134-x

Feng, Y., Spezia, M., Huang, S., Yuan, C., Zeng, Z., Zhang, L., Ji, X., Liu, W., Huang, B., Luo, W., Liu, B., Lei, Y., Du, S., Vuppalapati, A., Luu, H.H., Haydon, R.C., He, T.C. and Ren, G., (2018), Breast cancer development and progression: Risk factors, cancer stem cells, signalling pathways, genomics and molecular pathogenesis, *Genes and Diseases*, 5: 77-106. doi: 10.1016/j.gendis.2013.05.001

Ferreira, E., (2015), Silver(I) phosphine compounds selectively induce apoptosis in MCF-7 breast cancer cells, Ph.D. Thesis, University of Johannesburg, South Africa

Ferreira, E., Munyaneza, A., Omondi, B., Meijboom, R and Cronjé, M.J., (2015), The effect of 1:2 Ag(I) thiocyanate complexes in MCF-7 breast cancer cells, *Biometals*, **28:** 765-781, doi: 10.1007/s10534-015-9865-5

Fidler, I.J. and Kripke, M.L., (2015), The challenge of targeting metastasis, *Cancer Metastasis Reviews*, 34: 635-641. doi: 10.1007/s10555-015-9586-9

Forbes, N.S., Coffin, R.S., Deng, L., Evgin, L., Fiering, S., Giacalone, M., Gravekamp, C., Gulley, J.L., Gunn, H., Hoffman, R.M., Kaur, B., Liu, K., Lyerly, H.K., Marciscano, A.E., Moradian, E., Ruppel, S., Saltzman, D.A., Tattersall, P.J., Thorne, S., Vile, R.G., Zhang, H.H., Zhou, S. and McFadden, G., (2018), White paper on microbial anti-cancer therapy and prevention, *The Journal for ImmunoTherapy of Cancer* , 6(1): 78. doi: 10.1186/s40425-018-0381-3

Franken, N.A.P., Rodermond, H., Stap, J. and Haveman, J., (2006), Clonogenic assay of cells, *Nature Protocols*, 1(5): 2315-2319. doi: 10.1038/nprot.2006.339

Galea, C.A., Nguyen, H.M., Chandy, K.G., Smith, B.J. and Norton, R.S., (2014), Domain structure and function of matrix metalloprotease 23 (MMP23): role in potassium channel trafficking, *Cellular and Molecular Life Sciences*, 71: 1191-1210. doi: 10.1007/s00018-013-1431-0

Gandalovičová, A., Rosel, D., Fernandes, M., Veselý, P., Heneberg, P., Čermák, V., Petruželka, L., Kumar, S., Sanz-Moreno, V. and Brábek, J., (2017), Migrastatics – anti-metastatic and anti-invasion Drugs: promises and challenges, *Trends in Cancer*, 3(6): 391-406. doi: 10.1016/j.trecan.2017.04.008

Ganesh, K., and Massagué, J., (2021), Targeting metastatic cancer, *Nature Medicine*, 27(1): 34-44. doi: 10.1038/s41591-020-01195-4

Gest, C., Joimel, U., Huang, L., Pritchard, L-L., Petit, A., Dulong, C., Buquet, C., Hu, C-Q., Mirshahi, P., Laurent, M., Fauvel-Lafève, F., Cazin, L., Vannier, J-P., Lu, H., Soria, J., Li, H., Varin, R. and Soria, C., (2013), Rac3 induces a molecular pathway triggering breast cancer cell aggressiveness: differences in MDA-MB-231 and MCF-7 breast cancer cell lines, *BMC Cancer*, 13:63. doi: 10.1186/1471-2407-13-63

Glenn, H.L., Messner, J. and Meldrum, D.R., (2016), A simple non-perturbing cell migration assay insensitive to proliferation effects, *Scientific Reports*, 6: 31694. doi: 10.1038/srep31694

González-Ballesteros, M.M., Mejía, C. and Ruiz-Azuara, L., (2022), Metallodrugs: an approach against invasion and metastasis in cancer treatment, *FEBS Open Bio*, 12: 880-899. doi: 10.1002/2211-5463.13381

Guzmán, C., Bagga, M., Kaur, A., Westermarck, J. and Abankwa, D., (2014), ColonyArea: An ImageJ plugin to automatically quantify colony formation in clonogenic assays, PLoS ONE, 9(3): e92444. doi: 10.1371/journal/pone.0092444

Hall, E.H., Gurel, V., Dahlberg, A.E., McMichael, J. and Brautigan, D.L., (2011), Inhibition of human breast cancer Matrigel invasion by streptolysin O activation of the EGF receptor ErbB1, *Cellular Signalling*, 23(12): 1972-1977. Doi: 10.1016/j.cellsig.2011.07.007

Han, W., Kong, D., Lu, Q., Zhang, W. and Fan, Z., (2021), Aloperine inhibits proliferation and promotes apoptosis in colorectal cancer cells by regulating the circNSUN2/miR-296-5p/STAT3 pathway, *Drug Design, Development and Therapy*, 2021(15): 857-870. doi: 10.2147/DDDT.S288473

Hanahan, D., (2022), Hallmarks of cancer: new dimensions, *Cancer Discovery*, 12: 31-46. doi: 10.1158/2159-B290.CD-21-1059

Hanahan D. and Weinberg R.A., (2000), The hallmarks of cancer, *Cell*, 100: 57-70

Hanahan D. and Weinberg R.A., (2011), Hallmarks of cancer: the next generation, *Cell*, 144: 646-674. doi: 10.1016/j.cell.2011.02.013

Hanna, K. and Mayden, K., (2021), Chemotherapy treatment considerations in metastatic breast cancer, *Journal of the Advanced Practitioner in Oncology*, 12(suppl 2): 6-12. doi: 10.6004/jadpro.2021.12.2.11

Hapach, L.A., Mosier, J.A., Wang, W. and Reinhart-King, C.A., (2019), Engineered models to parse apart the metastatic cascade, *npj Precision Oncology*, 3(20): 1-8. doi: 10.1038/s41698-019-0092-3

Hart, C.P., (2005), Finding the target after screening the phenotype, *Drug Discovery Today: Targets*, 10(7): 513-519. doi: 10.1016/S1359-6446(05)03415-X

Human, Z., Munyaneza, A., Omondi, B., Sanabria, N.M., Meijboom, R. and Cronjé, M.J., (2015), The induction of cell death by phosphine silver(I) thiocyanate complexes in SNO-esophageal cancer cells, *Biometals*, 28: 219-228, doi: 10.1007/s10534-014-9817-5

Human-Engelbrecht, Z., Meijboom, R. and Cronjé, M.J., (2017), Apoptosis-inducing ability of silver(I) cyanide-phosphines useful for anti-cancer studies, *Cytotechnology*, 69: 591-600, doi: 10.1007/s10616-017-0070-y

Humphries, M.J., (2001), Cell adhesion assays, *Molecular Biotechnology*, 18(1): 57-61

Jabłońska-Trypuć, A., Matejczyk, M. and Rosochacki, S., (2016), Matrix metalloproteinases (MMPs), the main extracellular matrix (ECM) enzymes in collagen degradation, as a target for anticancer drugs, *Journal of Enzyme Inhibition and Medicinal Chemistry*, 31(S1): 177-183. doi: 10.3109/14756366.2016.1161620

Jazieh, K., Bell, R., Agarwal, N. and Abraham, J., (2020), Novel targeted therapies for metastatic breast cancer, *Annals of Translational Medicine*, 8(14): 907. doi: 10.21037/atm.2020.03.43

Jenkins, S.R., (2015), Insights into the mechanisms of drug action of a novel silver(I) chemotherapeutic against malignant melanoma cell line, M.Sc. Dissertation, University of Johannesburg, South Africa

Jin, X. and Mu, P., (2015), Targeting breast cancer metastasis, *Breast Cancer: Basic and Clinical Research*, 9(S1): 23-34. doi: 10.4137/BCBCR.S25460

Jolly, M.K., Ware, K.E., Gilja, S., Somarelli, J.A. and Levine, H., (2017), EMT and MET: necessary or permissive for metastasis?, *Molecular Oncology*, 11(7): 755-769. doi: 10.1002/1878-0261.12083

Joussaume, A., Karayan-Tapon, L., Benzakour, O. and Dkhissi, F., (2020), A comparative study of anoikis resistance assays for tumour cells, *Biomedical Journal of Scientific & Technical Research*, 29(2): 22255-22262. doi: 10.26717/BJSTR.2020.29.004767

Justus, C.R., Leffler, N., Ruiz-Echevarria, M. and Yang, L.V., (2014), *In vitro* cell migration and invasion assays, *Journal of Visualized Experiments*, 88: e51046. doi: 10.3791/51046

Juurikka, K., Butler, G.S., Salo, T., Nyberg, P. and Åström, P., (2019), The role of MMP8 in cancer: a systematic review, *International Journal of Molecular Sciences*, 20: 4506. doi: 10.3390/ijms20184506

Kaplan, A., Ciftci, G.A. and Kutlu, H.M., (2017), The apoptotic and genomic studies on A549 cell line induced by silver nitrate, *Tumor Biology*, 39(4). doi:10.1177/1010428317695033

Karam, A.K., Santiskulvong, C., Fekete, M., Eng, C. and Dorigo, O., (2010), Cisplatin and PI3Kinase inhibition decrease invasion and migration of human ovarian carcinoma cells and regulate matrix-metalloproteinase expression, *Cytoskeleton*, 67(8): 535-544. doi: 10.1002/cm.20465

Kim, A., Im, M., Yim, N.H., Jung, Y.P. and Ma, J.Y., (2013a), Aqueous extract of *Bambusae caulis* in *Taeniam* inhibits PMA-induced tumour cell invasion and pulmonary metastasis: suppression of NF-κB activation through ROS signaling, *PLoS ONE*, 8(10): e78061. doi: 10.1371/journal.pone.0078061

Kim, A. and Ma, J.Y., (2018), Rhaponticin decreases the metastatic and angiogenic abilities of cancer cells via suppression of the HIF-1α pathway, *International Journal of Oncology*, 53: 1160-1170. doi: 10.3892/ijo.2018.4479

Kim, N-H., Park, H.J., Oh, M-K. and Kim, I-S., (2013b), Antiproliferative effect of gold(I) compound auranofin through inhibition of STAT3 and telomerase activity in MDA-MB-231 human breast cancer cells, *BMB Reports*, 46(1): 59-64. doi: 10.5483/BMBRep.2013.46.1.123

Klein, T. and Bischoff, R., (2011), Physiology and pathophysiology of matrix metalloproteases, *Amino Acids*, 41: 271-290. doi: 10.1007/s00726-010-0689-x

Korman, D.B., Ostrovskaya, L.A., Bluhterova, N.V., Rikova, V.A. and Fomina, M.M., (2022), Cytotoxicity of silver compounds, *Biophysics*, 67(4): 565-570. doi: 10.1134/S0006350922040108

Kramer, N., Walzl, A., Unger, C., Rosner, M., Krupitza, G., Hengstschläger, M. and Dolznig, H., (2013), *In vitro* cell migration and invasion assays, *Mutation Research*, 752: 10-24. doi: 10.1016/j.mrrev.2012.08.001

Larkins, T.L., Nowell, M., Singh, S. and Sanford, G.L., (2006), Inhibition of cyclooxygenase-2 decreases breast cancer cell motility, invasion and matrix metalloproteinase expression, *BMC Cancer*, 6(181). doi: 10.1186/1471-2407-6-181

Laronha, H. and Caldeira, J., (2020), Structure and function of human matrix metalloproteinases, *Cells*, 9: 1076. doi: 10.3390/cells9051076

Lau, H.Y., Tang, J., Casey, P.J. and Wang, M., (2021), Evaluating the epithelial-mesenchymal program in human breast epithelial cells cultured in soft agar using a novel macromolecule extraction protocol, *Cancers*, 13:807. doi: doi.org/10.3390/cancers13040807

Leber M.F. and Efferth T., (2009), Molecular principles of cancer invasion and metastasis, *International Journal of Oncology*, 34: 881-895. doi: 10.3892/ijo_00000214

Li, H., Qiu, Z., Li, F. and Wang, C., (2017), The relationship between MMP-2 and MMP-9 expression levels with breast cancer incidence and prognosis, *Oncology Letters*, 14: 5865-5870. doi: 10.3892/ol.2017.6924

Lipschitz, S., (2018), Screening mammography with special reference to guidelines in South Africa, *SA Journal of Radiology*, 22(2): 1370. doi: 10.4102/sajr.v22i2.1370

Liu, X., Li, J., Cadilha, B.L., Markota, A., Voigt, C., Huang, Z., Lin, P.P., Wang, D.D., Dai, J., Kranz, G., Krandick, A., Libl, D., Zitzelsberger, H., Zagorski, I., Braselmann, H., Pan, M., Zhu, S., Huang, Y., Niedermeyer, S., Reichel, C.A., Uhl, B., Briukhovetska, D., Suárez, J., Kobold, S., Gires, O., Wang, H.. (2019), Epithelial-type systemic breast carcinoma cells with a restricted mesenchymal transition are a major source of metastasis, *Science Advances*, 5(6): eaav4275. doi: 10.1126/sciadv.aav4275

Lu, H., Blunden, B.M., Scarano, W., Lu, M. and Stenzel, M.H., (2016), Anti-metastatic effects of RAPTA-C conjugated polymeric micelles on two-dimensional (2D) breast tumor cells and three-dimensional (3D) multicellular tumor spheroids, *Acta Biomaterialia,* 32: 68-76. doi: 10.1016/j.actbio.2015.12.020

Lucaciu, R.L., Hangan, A.C., Sevastre, B and Oprean, L.S., (2022), Metallo-drugs in cancer therapy: past, present and future, *Molecules,* 27:6485. doi: 10.3390/molecules27196485

Lukasiewicz, S., Czeczelewski, M., Forma, A., Baj, J., Sitarz, R. and Stanislawek, A., (2021), Breast cancer – epidemiology, risk factors, classification, prognostic markers and current treatment strategies – an updated review, *Cancers,* 13(4287): 1-30. doi: 10.3390/cancers13174287

Ma, Y-S., Hsiao, Y-T., Lin, J-J., Liao, C-L., Lin, C-C. and Chung, J-G., (2017), Phenetyl Isothiocyanate (PEITC) and Benzyl Isothiocyanate (BITC) inhibit human melanoma A375.S2 cell migration and invasion by affecting MAPK signaling pathway *In Vitro, Anticancer Research,* 37: 6223-6234. doi: :10.21873/anticanres.12073

Ma, L., Ma, R., Wang, Z., Yiu, S.M. and Zhu, G., (2016), Heterodinuclear Pt(IV)-Ru(II) anticancer prodrugs to combat both drug resistance and tumor metastasis, *Chemical Communications,* 52: 10735-10738. doi: 10.1039/c6cc04354b

Mabasa, R., Malemela, K., Serala, K., Kgakishe, M., Matsebatlela, T., Mokgotho, M. and Mbazima, V., (2021), *Ricinus communis* butanol fraction inhibits MCF-7 breast cancer cell migration, adhesion, and invasiveness, *Integrative Cancer Therapies*, 20: 1-11. doi: 10.1177/1534735420977684

Maity, G., Choudhury, P.R., Sen, T., Ganguly, K.K., Sil, H. and Chatterjee, A., (2011), Culture of human breast cancer cell line (MDA-MB-231) on fibronectin-coated surface induces pro-matrix metalloproteinase-9 expression and activity, *Tumour Biology,* 32: 129-138. doi: 10.1007/s13277-010-0106-9

Maiuthed, A and Chanvorachote, P., (2014), Cisplatin at sub-toxic levels mediates integrin switch in lung cancer cells, *Anticancer Research,* 34: 7111-7118. PMID: 25503138

Malakouti, P., Mohammadi, M., Boshagh, M.A., Amini, A., Rezaee, M.A. and Rahmani, M.R., (2022), Combined effects of pioglitazone and doxorubicin on migration and invasion of MDA-MB-231 breast cancer cells, *Journal of the Egyptian National Cancer Institute,* 34(13). doi: 10.1186/s43046-022-00110-x

Maldonado, M., Salgado-Aguayo, A., Herrera, I., Cabrera, S., Ortíz-Quintero, B., Staab-Weijnitz, C.A., Eickelberg, O., Ramírez, R., Manicone, A.M., Selman, M. and Pardo, A., (2018), Upregulation and nuclear location of MMP28 in alveolar epithelium of idiopathic pulmonary fibrosis, *American Journal of Respiratory Cell and Molecular Biology*, 59(1): 77-86. doi: 10.1165/rcmb.2017-0223OC

Mali, A.V., Joshi, A.A., Hegde, M.V. and Kadam, S.S., (2017), Enterolactone suppresses proliferation, migration and metastasis of MDA-MB-231 breast cancer cells through inhibition of uPA induced plasmin activation and MMPs-mediated ECM remodelling, *Asian Pacific Journal of Cancer Prevention*, 18(4): 905-915. doi: 10.22034/APJCP.2017.18.4.905

Marshall, J., (2011), Transwell® invasion assays, In Methods in Molecular Biology, vol 769: Cell Migration: Developmental Methods and Protocols, Wells, C.M. and Parsons, M. (eds.), Springer Science + Business Media, Chapter 1. doi: 10.1007/978-1-61779-207-6_1

Martei, Y.M., Dauda, B. and Vanderpuye, V., (2022), Breast Cancer screening in sub-Saharan Africa: a systematic review and ethical appraisal, *BMC Cancer,* 22(203). doi: 10.1186/s12885-022-09299-5

Medici, S., Peana, M., Nurchi, V.M. and Zoroddu, M.A., (2019), Medical uses of silver: history, myths and scientific evidence, *Journal of Medicinal Chemistry*, 62: 5923-5943. doi: 10.1021/acs.jmedchem.8b01439

McConnell, E.J., Devapatla, B., Yaddanapudi, K. and Davis, K.R., (2015), The soybean-derived peptide lunasin inhibits non-small cell lung cancer cell proliferation by suppressing phosphorylation of the retinoblastoma protein, *Oncotarget,* 6(7): 4649-4662. doi: 10.18632/oncotarget.3080

Mi, S., Du, Z., Xu, Y., Wu, Z., Qian, X., Zhang, M. and Sun, W., (2016), Microfluidic co-culture system for cancer migratory analysis and anti-metastatic drugs screening, *Scientific Reports*, 6(35544). doi: 10.1038/srep35544

Muscella, A., Calabriso, N., Ventrugno, C., Urso, L., Fanizzi, F.P., De Pascali, S.A. and Marsigliante, S., (2010), Sublethal concentrations of the platinum(II) complex [Pt(O,O'-acac)(γ-acac)(DMS)] alter the motility and induce anoikis in MCF-7 cells, *British Journal of Pharmacology,* 160: 1362-1377. doi: 10.1111/j.1476-5381.2010.00782.x

Muscella, A., Vetrugno, C., Calabriso, N., Cossa, L.G., De Pascali, S.A., Fanizzi, F.P. and Marsigliante, S., (2014), [Pt(O,O'-acac)(γ-acac)(DMS)] alters SH-SY5Y cell migration and invasion by the inhibition of Na+/H+ exchanger isoform 1 occurring through a PKC-ε/ERK/mTOR pathway, *PLoS ONE,* 9(11): e112186. doi: 10.1371/journal.pone.0112186

Nagase, H., Visse, R. and Murphy, G., (2006), Structure and function of matrix metalloproteinases and TIMPs, *Cardiovascular Research,* 69(3): 562-573. doi: 10.1016/j.cardiores.2005.12.002

Ndagi, U., Mhlongo, N. and Soliman, M.E., (2017), Metal complexes in cancer therapy – an update from drug design perspective, *Drug design, Development and Therapy,* 11: 599-616. doi: 10.2147/DDDT.S119488

Nguyen, S.T., Nguyen, H.T-L. and Truong, K.D., (2020), Comparative cytotoxic effects of methanol, ethanol and DMSO on human cancer cell lines, *Biomedical Research and Therapy*, 7(7):, 3855-3859. doi: 10.15419/bmrat.v7i7.614

Nieto, M.A., Huang, R.Y-J., Jackson, R.A. and Thiery, J.P., (2016), EMT: 2016, *Cell,* 166(1): 21-45. doi: 10.1016/j.cell.2016.06.028

Oyewole-Said, D., Konduri, V., Vazquez-Perez, J., Weldon, S.A., Levitt, J.M. and Decker, W.K., (2020), Beyond T-cells: functional characterization of CTLA-4 expression in immune and non-immune cell types, *Frontiers in Immunology*, 11:608024. doi: 10.3389/fimmu.2020.608024

Ota, A., Tajima, M., Mori, K., Sugiyama, E., Sato, V.H. and Sato, H., (2021), The selective cytotoxicity of silver thiosulfate, a silver complex, on MCF-7 breast cancer cells through ROS-induced cell death, *Pharmacological Reports,* 73(3): 847-857. doi: 10.1007/s43440-021-00260-0

Phaswana-Mafuya, N. and Peltzer, K., (2018), Breast and cervical cancer screening prevalence and associated factors among women in the South African general population, *Asian Pacific Journal of Cancer Prevention,* 19(6): 1465-1470. doi: 10.22034/APJCP.2018.19.6.1465

Popolin, C.P., Reis, J.P.B., Becceneri, A.B., Graminha, A.E., Almeida, M.A.P., Corrêa, R.S., Colina-Vegas, L.A., Ellena, J., Batista, A.A. and Cominetti, M.R., (2017), Cytotoxicity and anti-tumor effects of new ruthenium complexes on triple negative breast cancer cells, *PLoS ONE,* 12(9): e0183275. doi: 10.1371/journal.pone.0183275

Potgieter, K., Engelbrecht, Z., Naganagowda, G., Cronjé, M.J. and Meijboom, R., (2017), Anticancer activity of silver(I) cyclohexyldiphenylphosphine complexes toward SNO cancer cells, *Journal of Coordination Chemistry,* **70(15):** 2644-2658. doi: 10.1080/00958972.2017.1366466

Poullot, N., Pearson, H.B. and Burrows, A., (2013), Investigating metastasis using *in vitro* platforms, Madame Curie Bioscience Database [Internet], Austin (TX): Landes Bioscience, Available from: https://www.ncbi.nlm.nih.gov/books/NBK100379

Quintero-Fabián, S., Arreola, R., Becerril-Villanueva, E., Torres-Romero, J.C., Arana-Argáez, V., Lara-Riegos, J., Ramírez-Camacho, M.A. and Alvarez-Sánchez, M.E., (2019), Role of matrix metalloproteinases in angiogenesis and cancer, *Frontiers in Oncology,* 9:1370. doi: 10.3389/fonc.2019.01370

Raju, S.K., Karunakaran, A., Kumar, S., Sekar, P., Murugesan, M. and Karthikeyan, M., (2022), Silver complexes as anticancer agents: a perspective review, *German Journal of Pharmaceuticals and Biomaterials,* 1(1): 6-28. doi: 10.5530/gjpb.2022.1.3

Raudenska, M., Kratochvilova, M., Vicar, T., Gumulec, J., Balvan, J., Polanska, H., Pribyl, J. and Masarik, M., (2019), Cisplatin enhances cell stiffness and decreases invasiveness rate in prostate cancer cells by actin accumulation, *Scientific Reports,* 9: 1660. doi: 10.1038/s41598-018-38199-7

Reunanen, N. and Kähäri, V., (2013), Matrix metalloproteinases in cancer cell invasion, In Madame Curie Bioscience Database [Internet], Austin (TX): Landes Bioscience, Available from: https://www.ncbi.nlm.nih.gov/books/NBK6598

Ribatti, D., Tamma, R. and Annese, T., (2020), Epithelial-mesenchymal transition in cancer: a historical overview, *Translational Oncology,* 13(6): 100773. doi: 10.1016/j.tranon.2020.100773

Riccardi, C., Musumeci, D., Trifuoggi, M., Irace, C., Paduano, L. and Mentesarchio, D., (2019), Anticancer ruthenium(III) complexes and Ru(II)-containing nanoformulations: an update on the mechanism of action and biological activity, *Pharmaceuticals,* 12: 146. doi: 10.3390/molecules27196485

Riggio, A.I., Varley, K.E. and Welm, A.L., (2021), The lingering mysteries of metastatic recurrence in breast cancer, *British Journal of Cancer,* 124:13-26. doi: 10.1038/s41416-020-01161-4

Roberts, K.E., (2023), Insights into silver(I) phosphine complexes in targeting cell death and metastatic mechanisms in malignant cell lines, Ph.D. Thesis, University of the Witwatersrand, South Africa

Rundén-Pran, E., Mariussen, E., Yamani, N.E., Elje, E., Longhin, E.M. and Dusinska, M., (2022), The colony forming efficiency assay for toxicity testing of nanomaterials – modifications for higher-throughput, *Frontiers in Toxicology*, 4: 983316. doi: 10.3389/ftox.2022.983316

Şahin-Bölükbaşi, S., Şahin, N., Tahir, M.N., Arıcı, C., Çevik, E., Gürbüz, N., Özdemir, I. and Cummings, B.S., (2019), Novel N-heterocyclic carbine silver(I) complexes: Synthesis, structural characterization, and anticancer activity, *Inorganica Chimica Acta*, 486: 711-718. doi: 10.1016/j.ica.2018.11.044

Sangweni, N.F., Dludla, P.V., Chellan, N., Mabasa, L., Sharma, J.R. and Johnson, R., (2021), The implication of low dose dimethyl sulfoxide on mitochondrial function and oxidative damage in cultured cardiac and cancer cells, *Molecules*, 26(23): 7305. doi: 10.3390/molecules26237305

Saraiva, D.P., Matias, A.T., Braga, S., Jacinto, A. and Cabral, M.G., (2020), Establishment of a 3D co-culture with MDA-MB-231 breast cancer cell line and patient-derived immune cells for application in the development of immunotherapies, *Frontiers in Oncology*, 10. doi: 10.3389/fonc.2020.01543

Seo, J., Ha, J., Kang, E. and Cho, S., (2021), The role of epithelial-mesenchymal transition-regulating transcription factors in anti-cancer drug resistance, *Archives of Pharmacal Research*, 44(3): 281-292. doi: 10.1007/s12272-021-01321-x

Sharma, K., Fizet, K.J., Montgomery, K.R., Smeltzer, N.A., Sikorski, M.H., Brown, K.G., Beyke, B.J., Burkhart, R.C., Lynn, A.N. and Grandinetti, G., (2020), A simple colorimetric experiment using mammalian cell culture to study netabolism, *Biochemistry and Molecular Biology Education*, 49(2): 271-277. doi: 10.1002/bmb.21457

Shaw, L.M., (2005), Tumor cell invasion assays, In *Methods in Molecular Biology, vol 294: Cell Migration: Developmental Methods and Protocols*, Guan, J.L. (eds.), Humana Press Inc., Totowa, NJ, page 97-105

Shrikhande, S.S., Jain, D.S., Athawale, R.B., Bajaj, A.N., Goel, P., Kamran, Z., Nikam, Y. and Gude, R., (2015), Evaluation of anti-metastatic potential of cisplatin polymeric nanocarriers on B16F10 melanoma cells, *Saudi Pharmaceutical Journal*, 23: 341-351. doi: 10.1016/j.jsps.2014.08.004

Sim, W., Barnard, R.T., Blaskovich, M.A.T. and Ziora, Z.M., (2018), Antimicrobial silver in medicinal and consumer applications: a patent review of the past decade (2007-2017), *Antibiotics*, 7:93. doi:10.3390/antibiotics7040093

Sleeman, J. and Steeg, P.S., (2010), Cancer metastasis as a therapeutic target, *European Journal of Cancer*, 46(7): 1177-1180. doi: 10.1016/j.ejca.2010.02.039

Sodek, K.L., Brown, T.J. and Ringuette, M.J., (2008), Collagen I but not Matrigel matrices provide an MMP-dependent barrier to ovarian cancer cell penetration, *BMC Cancer*, 8: 223. doi: 10.1186/1471-2407-8-223

Sofyan, N.R.F.M., Nordin, F.J., Razak, M.R.M.A., Halim, S.N.A.A., Khir, N.A.F.M., Muhammad, A., Rajab, N.F. and Sarip, R., (2018), New silver complexes with mixed thiazolidine and phosphine ligands as highly potent antimalarial and anticancer agents, *Journal of Chemistry*, 2018: 8395374. doi: 10.1155/2018/8395374

Somaiah, C., Kumar, A., Mawrie, D., Sharma, A., Patil, S.D., Bhattacharyya, J., Swaminathan, R. and Jaganathan, B.G., (2015), Collagen promotes higher adhesion, survival and proliferation of mesenchymal stem cells, *PLoS One*, 10(12): e0145068. doi: 10.1371/journal.pone.0145068

Stoellinger, H.M. and Alexanian, A.R., (2022), Modifications to the Transwell migration / invasion assay method that eases assay performance and improves the accuracy, *Assay and Drug Development Technologies*, 20(2): 75-82. doi: 10.1089/adt.2021.140

Suarez-Amedo, A., Figueroa, F.T., Clavijo, C., Arbeláez, P., Cruz, J.C. and Muñoz-Camargo, C., (2020), An image J plugin for the high throughput image analysis of *in vitro* scratch wound healing assays, *PLoS ONE*, 15(7): e0232565. doi: 10.1371/journal.pone.0232565

Sun, Y.S., Zhao, Z., Yang, Z.N., Xu, F., Lu, H.J., Zhu, Z.Y., Shi, W., Jiang, J., Yao, P.P. and Zhu, H.P., (2017), Risk factors and preventions of breast cancer, *International Journal of Biological Sciences*, 13(11): 1387-1397. doi: 10.7150/ijbs.21635

Sun, Z., Zhou, D., Yang, J. and Zhang, D., (2022), Doxorubicin promotes breast cancer cell migration and invasion via DCAF13, *FEBS Open Bio*, 12: 221-230. doi: 10.1002/2211-5463.13330

Sung, H., Ferlay, J., Siegel, R.L., Laversanne M., Soerjomataram, I., Jemal, A. and Bray, F., (2021), Global cancer statistics 2020: GLOBOCAN estimates of incidence and mortality worldwide for 36 cancers in 185 countries, *CA: A Cancer Journal for Clinicians*, 71: 209-249. doi: 10.3322/caac.21660

Tajhya, R.B., Patel, R.S. and Beeton, C., (2017), Detection of matrix metalloproteinases by zymography, *Methods in Molecular Biology*, 1579: 231-244. doi: 10.1007/978-1-4939-6863-3_12

Tian, D., Li, Y., Li, X. and Tian, Z., (2018), Aloperine inhibits proliferation, migration and invasion and induces apoptosis by blocking the Ras signalling pathway in human breast cancer cells, *Molecular Medicine Reports,* 18: 3699-3710. doi: 10.3892/mmr.2018.9419

Toth, M. and Fridman, R., (2001), Assessment of gelatinases (MMP-2 and MMP-9) by gelatin zymography, *Methods in Molecular Medicine,* 57. doi: 10.1385/1-59259-136-1:163

Twafra, S., Sokolik, C.G., Sneh, T., Srikanth, K.D., Meirson, T., Genna, A., Chill, J.H. and Gil-Henn, H., (2023), A novel Pyk2-derived peptide inhibits invadopodia-mediated breast cancer metastasis, *Oncogene,* 42: 278-292. doi: 10.1038/s41388-022-02481-w

Tynga I.M., Houreld N.N. and Abrahamse H., (2013), The primary subcellular localization of Zinc phthalocyanine and its cellular impact on viability, proliferation and structure of breast cancer cells (MCF-7), *Journal of Photochemistry and Photobiology B: Biology*, 120: 171-176. doi: 10.1016/j.jphotobiol.2012.11.009

Vicente-Manzanares, M. and Horwitz, A.R., (2011), Cell migration: an overview, In *Methods in Molecular Biology, vol 769: Cell Migration: Developmental Methods and Protocols,* Wells, C.M. and Parsons, M. (eds.), Springer Science + Business Media, Chapter 1. doi: 10.1007/978-1-61779-207-6_1

Vinci, M., Box, C. and Eccles, S.A., (2015), Three-dimensional (3D) tumor spheroid invasion assay, *Journal of Visualized Experiments,* 99: 52686. doi: 10.3791/52686

Voorwerk, L., Slagter, M., Horlings, H.M., Sikorska, K., van de Vijver, K.K., de Maaker, M., Nederlof, I., Kluin, R.J.C., Warren, S., Ong, S. Wiersma, T.G., Russell, N.S., Lalezari, F., Schouten, P.C., Bakker, N.A.M., Ketelaars, S.L.C., Peters, D., Lange, C.A.H., van WerkhovenE., van Tinteren, H., Mandjes, I.A.M., Kemper, I., Onderwater, S., Chalabi, M., Wilgenhof, S., Haanen, J.B.A.G., Salgado, R., de Visser, K.E., Sonke, G.S., Wessels, L.F.A., Linn, S.C., Schumacher, T.N., Blank, C.U. and Kok, M., (2019), Immune induction strategies in metastatic triple-negative breast cancer to enhance the sensitivity to PD-1 blockade: the TONIC trial, *Nature Medicine,* 25(6): 920-928. doi: 10.1038/s41591-019-0432-4

Wang, H., Guo, S., Kim, S-J., Shao, F., Ho, J.W.K., Wong, K.U., Miao, Z., Hao, D., Zhao, M., Xu, J., Zeng, J., Wong, K.H., Di, L., Wong, A.H-H., Xu, X. and Deng, C-X., (2021), Cisplatin prevents breast cancer metastasis through blocking early EMT and retards cancer growth together with paclitaxel, *Theranostics,* 11(5): 2442-2459. doi: 10.7150/thno.46460

Wang, C. and Huang, S., (2017). Drug development against metastatic cancers, *Yale Journal of Biology and Medicine*, 90: 119-123. PMID: 28356899

Wang, C-C., Lin, S-Y., Lai, Y-H., Liu, Y-J., Hsu, Y-L. and Chen, J.J.W., (2012), Dimethyl sulfoxide promotes the multiple functions of the tumor suppressor HLJ1 through activator protein-1 activation in NSCLC cells, *PLoS ONE,* 7(4): e33772. doi: 10.1371/journal.pone.0033772

Wang, D., Naydenov, N.G., Dozmorov, M.G., Koblinski, J.E. and Ivanov, A.I., (2020), Anillin regulates breast cancer cell migration, growth, and metastasis by non-canonical mechanisms involving control of cell stemness and differentiation, *Breast Cancer Research,* 22(3). doi: 10.1186/s13058-019-1241-x

Weber, G.F., (2013), Why does cancer therapy lack effective anti-metastasis drugs?, *Cancer Letters,* 328: 207-211. doi: 10.1016/j.canlet.2012.09.025

Weiskirchen, S., Schröder, S.K., Buhl, E.M. and Weiskirchen, R., (2023), A beginner's guide to cell culture: practical advice for preventing needless problems, *Cells,* 12(5): 682. PMID: 36899818

Welch, D.R. and Hurst, D.R., (2019), Defining the hallmarks of metastasis, *Cancer Research,* 79: 3011-3027. doi: 10.1158/0008-5472.CAN-19-0458

Wu, X-X., Yue, G.G-L., Dong, J-R., Lam, C.W-K., Wong, C-K., Qiu, M-H. and Lau, C.B-S., (2018), Actein inhibits the proliferation and adhesion of human breast cancer cells and suppresses migration *in vivo*, *Frontiers In Pharmacology,* 9(1466). doi: 10.3389/fphar.2018.01466

Xie, M., Vesuna, F., Botlagunta, M., Bol, G.M., Irving, A., Bergman, Y., Hosmane, R.S., Kato, Y., Winnard Jr., P.T and Raman, V., (2015), NZ51, a ring-expanded nucleoside analog, inhibits motility and viability of breast cancer cells by targeting the RNA helicase DDX3, *Oncotarget*. doi: 10.18632/oncotarget.4898

Yilmaz, V.T., Icsel, C., Batur, J., Aydinlik, S., Sahinturk, P. and Aygun, M., (2017), Structures and biochemical evaluation of silver(I) 5,5-diethylbarbiturate complexes with bis(diphenylphosphino)alkanes as potential antimicrobial and anticancer agents, *European Journal of Medicinal Chemistry,* 139: 901-916. doi: 10.1016/j.ejmech.2017.08.062

Yodkeeree, S., Ampasavate, C., Sung, B., Aggarwal, B.B. and Limtrakul, P., (2010), Demethoxycurcumin suppresses migration and invasion of MDA-MB-231 human breast cancer cell line, *European Journal of Pharmacology,* 627: 8-15. doi: 10.1016/j.ejphar.2009.09.052

Yu, M., Han, J., Cui, P., Dai, M., Li, H., Zhang, j. and Xiu, R., (2008), Cisplatin up-regulates ICAM-1 expression in endothelial cell via a NF-κB dependent pathway, *Cancer science,* 99(2): 391-397. doi: 10.1111/j.1349-7006.2008.00696.x

Yu, J., Mu, Q., Fung, M., Xu, X., Zhu, L. and Ho, R.J.Y., (2022), Challenges and opportunities in metastatic breast cancer treatments: nano-drug combinations delivered preferentially to metastatic cells may enhance therapeutic response, *Pharmacology and Therapeutics,* 236: 108108. doi: 10.1016/j.pharmthera.2022.108108

Zacharakis, N., Huq, L.M., Seitter, S.J., Kim, S.P., Gartner, J.J., Sindiri, S., Hill, V.K., Li, Y.F., Paria, B.C., Ray, S., Gasmi, B., Lee, C., Prickett, T.D., Parkhurst, M.R., Robbins, P.F., Langhan, M.M., Shelton, T.E., Parikh, A.Y., Levi, S.T., Hernandez, J.M., Hoang, C.D., Sherry, R.M., Yang, J.C., Feldman, S.A., Goff, S.L. and Rosenberg, S.A., (2022), Breast cancers are immunogenic: immunologic analyses and a phase II pilot clinical trial using mutation-reactive autologous lymphocytes, *Journal of Clinical Oncology,* 40(16): 1741-1754. doi: 10.1200/JCO.21.02170

Zhang, J., Wei, Y., Min, J., Wang, Y., Yin, L., Cao, G. and Shen, H., (2020), Knockdown of RAP2A gene expression suppresses cisplatin resistance in gastric cancer cells, *Oncology Letters,* 19: 350-358. doi: 10.3892/ol.2019.11086

Zheng, M-H., Bigdeli, F., Gao, L-X., Wu, D-Z., Yan, X-W., Hu, M-L. and Morsali, A., (2020), Synthesis, characterization and DNA binding investigations of a new binuclear Ag(I) complex and evaluation of its anticancer property, *International Journal of Nanomedicine,* 15: 953-964. doi: 10.2147/IJN.S225038

Zhou, R., Xu, L., Ye, M., Liao, M., Du, H. and Chen, H., (2014), Formononetin inhibits migration and invasion of MDA-MB-231 and 4T1 breast cancer cells by suppressing MMP-2 and MMP-9 through PI3K/AKT signalling pathways, *Hormone and Metabolic Research,* 46: 753-760. doi: 10.1055/s-0034-1376977

Zhu, X., Feng, J., Fu, W., Shu, X., Wan, X. and Liu, J., (2020), Effects of cisplatin on the proliferation, invasion and apoptosis of breast cancer cells following β-catenin silencing, *International Journal of Molecular Medicine,* 45: 1838-1850. doi: 10.3892/ijmm.2020.4543

Zimmer, A.J. and Freifeld, A.G., (2019), Optimal management of neutropenic fever in patients with cancer, *Journal of Oncology Practice,* 15: 19-24. doi: 10.1200/JOP.18.00269

Appendix A: Metastasis-related genes down-regulated by silver(I) phosphine complexes

Table A1 Names, symbols and relevant function in study of adhesion, invasion and other metastasis-related genes down-regulated in A375, SNO and MCF-7 cells treated with UJ1, UJ2 and UJ3, respectively. The relevant function was obtained from the GeneCards® Human Gene database.

Pathway	Gene name	Gene symbol	Relevant function in study
Adhesion	Integrin, alpha 1	*ITGA1*	Integrins consist of alpha and beta subunits with around 18 alpha subunits and 8 beta subunits present in mammals. These proteins are membrane receptors participating in cell adhesion in embryogenesis, haemostasis, immune function, tissue repair, and tumour metastasis.
	Integrin, alpha 3 (antigen CD49C, alpha 3 subunit of VLA-3 receptor)	*ITGA3*	See *ITGA1*
	Integrin, alpha 4 (antigen CD49D, alpha 4 subunit of VLA-4 receptor)	*ITGA4*	See *ITGA1*
	Integrin, alpha V (vitronectin receptor, alpha polypeptide, antigen CD51)	*ITGAV*	Integrin receptor for ligands of the ECM that facilitate adhesion and signal transduction. Also see *ITGA1*

	Integrin, beta 1 (fibronectin receptor, beta polypeptide, antigen CD29 includes MDF2, MSK12)	*ITGB1*	See *ITGA1*
	Pinin, desmosome associated protein	*PNN*	Among its related pathways are RNA transport and mRNA surveillance pathways
Invasion and Metastasis	Metastasis associated 1	*MTA1*	*MTA1* encodes a protein present in metastatic cells, and specifically found in mammary adenocarcinoma cell lines. Gene expression is strongly correlated with metastatic potential.
	Metastasis associated 1 family, member 2	*MTA2*	*MTA2* encodes a protein that forms part of NuRD, a nucleosome remodelling deacetylase complex found in the nucleus. It forms part of a small family of genes that encode proteins involved in transcriptional regulation. Also see *MTA1*
	Plasminogen activator, urokinase receptor	*PLAUR*	*PLAUR* encodes the receptor for uPA which may influence many normal and pathological processes related to the activation of plasminogen and degradation of the ECM.
	Twist homolog 1 (*Drosophila*)	*TWIST1*	Acts as a transcriptional regulator.

Engelbrecht, Z., (2017), Novel Anticancer silver(I) phosphines proven to target the mitochondrial-mediated cell death pathway in malignant cells, Ph.D. Thesis, University of Johannesburg, South Africa

Ferreria E. (2015) Silver(I) phosphine compounds selectively induce apoptosis in MCF-7 breast cancer cells, Ph.D. Thesis, University of Johannesburg, South Africa

Jenkins, S.R., (2015), Insights into the mechanisms of drug action of a novel silver(I) chemotherapeutic against malignant melanoma cell line, M.Sc. Dissertation, University of Johannesburg, South Africa

Appendix B: List of manufacturers, materials and apparatus

B1 Reagent manufacturers

β-mercaptoethanol – Sigma-Aldrich, USA

Acetic acid – Sigma-Aldrich, USA

Acrylamide – Sigma-Aldrich, USA

Agarose – Sigma-Aldrich, USA

alamarBlue™ - Bio-Rad, UK

Amido black – Sigma-Aldrich, USA

Antibodies – **Anti-Rabbit IgG (whole molecule) Peroxidase antibody produced in goat (Product no. A 0545)** - Sigma-Aldrich Chemical Co., USA

Goat Anti-Mouse IgG (H + L) - HRP Conjugate - Bio-Rad, USA

MMP-2 antibody produced in rabbit (#4022) - Cell Signalling Technologies, USA

MMP-9 antibody produced in rabbit (#3852) - Cell Signalling Technologies, USA

Monoclonal anti-β-actin antibody produced in mouse (Clone AC-74) - Sigma-Aldrich Chemical Co., USA

APS – Bio-Rad, Japan

Bis-acrylamide – Sigma-Aldrich, USA

Bromophenol blue – Merck, Germany

BSA – Santa Cruz Biotechnology, USA

Calcium chloride ($CaCl_2$) – Saarchem, SA

CDDP – Molekula, UK

Clarity™ western ECL Substrate – Bio-Rad, USA

Collagen type I from rat tail tendon – Sigma-Aldrich, USA

Coomassie brilliant blue – Saarchem, SA

Crystal violet – The Local Choice, SA

DMEM (with L-glutamine) – Sigma-Aldrich, UK
DMSO – Applichem GmbH, Germany

Ethanol – PE Chemicals, SA

FCS – Capricorn Scientific GmbH, South America
FluoroTrans® PVDF membrane (0.2 µm) – PALL LifeSciences, USA
Formaldehyde – Sigma-Aldrich, USA

Gelatin from bovine skin – Sigma-Aldrich, USA
Glycerol – Rochelle Chemicals, SA
Glycine – Sigma-Aldrich, USA

HBSS – Gibco, UK
Hydrogen chloride (HCl) – Saarchem, SA

Isopropanol – Associated Chemical Enterprises, SA

Laemmli buffer – Bio-Rad, USA

Methanol – Sigma-Aldrich, SA

Nitrocellulose membrane – Bio-Rad, Germany

PageRuler Plus Prestige protein marker – Thermo Scientific, Lithuania
PBS – Sigma-Aldrich, USA
Pen/Strep/Fungizone antibiotics – Lonza, USA
Protease inhibitor cocktail (SIGMAFAST™), EDTA free – Sigma-Aldrich, USA

RIPA – Thermo Scientific, USA

Skimmed milk powder – SPAR, SA
Sodium chloride (NaCl) – Associated Chemical Enterprises, SA
Sodium dodecyl sulphate (SDS) – Merck, Germany
Sodium hydrogen carbonate ($NaHCO_3$) – Melford Biolaboratories Ltd., UK
Sodium hydroxide (NaOH) – Associated Chemical Enterprises, SA

TEMED – MP Biomedicals Inc., France

Tris – Melford Biolaboratories Ltd., UK

Triton X-100 – BDH Labaratory Supplies, UK

Trypan blue dye (0.4%) / NaCl (0.81%) – Sigma-Aldrich, UK

Trypsin (0.25%) / Versene (0.1%) solution – Lonza, Belgium

Tween-20 – Sigma-Aldrich, USA

Zinc chloride ($ZnCl_2$) – Associated Chemical Enterprises, SA

B2 Materials

35 mm sterile cell culture dishes – Nest, USA

6, 24 and 96 well sterile cell culture plates – Nest, USA

75 cm^3 sterile cell culture flasks – Nest, USA

8 µm PET 24-well Transwell inserts – Merck Millipore, Germany

Cell scraper – JET-BIOFIL, Europe

B3 Apparatus

Bio-Rad Mini Protean® Tetra Cell electrophoresis system – Bio-Rad, USA

Countess™ automated cell counter – Invitrogen, USA

Counting slides – Bio-Rad, USA

NUVE EC 160 CO_2 incubator – Separations, SA

NUVE MN 120 Laminar flow cabinet – Separations, SA

NUVE NF 400R swing bucket centrifuge – Separations, SA

Microcentrifuge – Merck Millipore, SA

VICTOR® Nivo™ multimode plate reader – PerkinElmer, USA

ZEISS Primovert microscope equipped with ZEISS Axiocam ERc 5s and ZEN software (v2.6, blue edition) – ZEISS, Germany

Appendix C: Complexes

UJ1	UJ2	UJ3
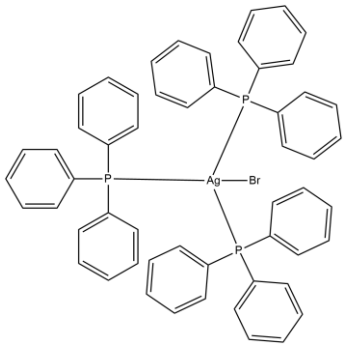	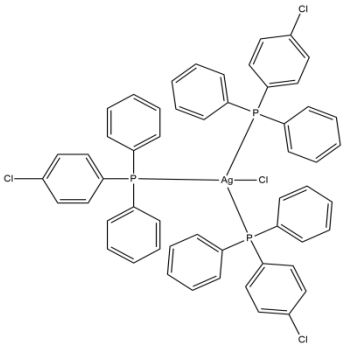	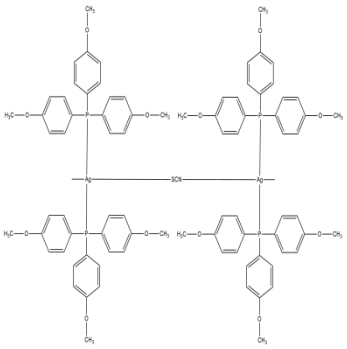
UJ50	**UJ92**	**UJ102**
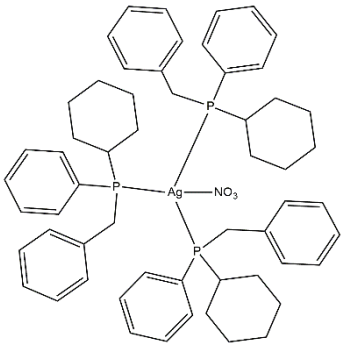	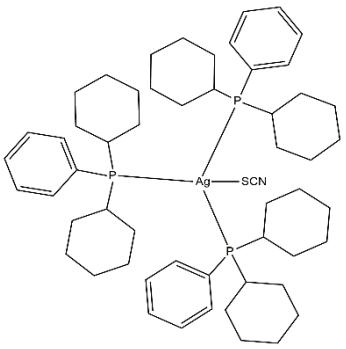	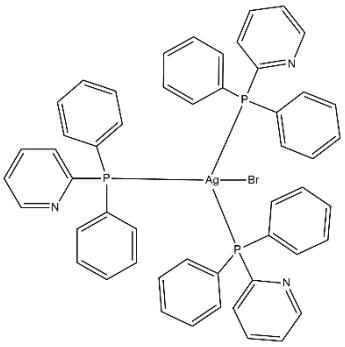
UJ115	**UJ116**	**UJ118**
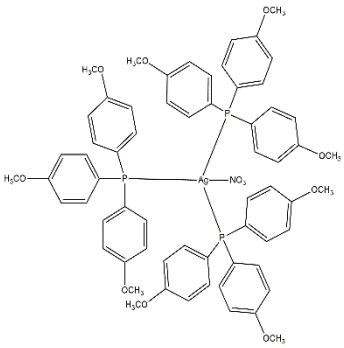	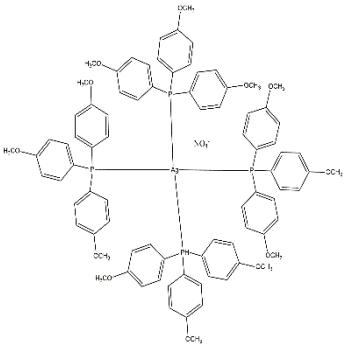	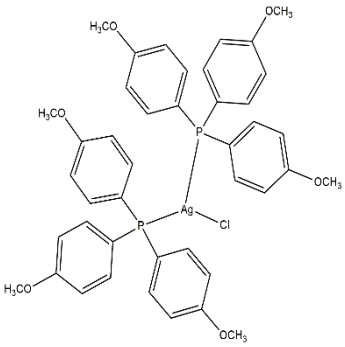

Figure C1 Chemical structure of the nine silver(I) phosphine complexes used in this study. The structure of UJ3 was obtained from Engelbrecht *et al.*, (2018).

C1 Synthesis of silver(I) phosphine complexes

The silver(I) phosphine complexes were synthesized by either Dr. Kariska Potgieter or Dr. Gouda Naganagowda from UJ at the Department of Chemical Sciences.

C2 Complex characterization

The silver(I) complexes were fully characterized in terms of melting point, Fourier transform infrared (FT-IR) spectra, nuclear magnetic resonance (NMR) spectra and elemental analysis, before being used for biological studies. Melting points were measured using a Stuart Scientific SMP10 Melting Point instrument or a melting point apparatus with a microscope. FT-IR spectra were captured using a PIKE MIRacle™ Gate attenuated total reflectance (ATR) attachment on a Bruker Tensor 27 FT-IR spectrometer. A Bruker Ultrashield Avance III 400 MHz spectrometer was used to measure and record NMR spectra. ^{1}H-NMR, ^{13}C{H}-NMR and ^{31}P{H}-NMR spectra were obtained in DMSO-d6 at 400 MHz for ^{1}H nuclei, 75 MHz for ^{13}C{H} nuclei and 161 MHz for ^{31}P{H} nuclei. All chemical shifts were reported in parts per million (ppm), with residual H or C serving as internal references. All ^{31}P{H} NMR chemical shifts were compared to an external standard, H_3PO_4. Dr. Edith Antunes performed the elemental analysis at Rhodes University's Department of Chemical Sciences (SA) utilizing a Thermo Flash 2000 series CHNS/O, Organic Elemental Analyzer.

Synthesis of 1:3 [Silver(I) bromide triphenylphosphine [AgBr {(PPh_3)$_3$}$_3$]] **(UJ1)**

This complex was synthesised and analysed according to literature procedures (Barron *et al.*, 1986; Berners-Price and Sadler, 1988). Solid AgBr (0.0582 g, 0.31 mmol) was added to a solution of triphenylphosphine (PPh_3) (0.2439 g, 0.93 mmol) in acetonitrile (50 mL). This mixture was heated under reflux overnight. The solution was then filtered while hot, followed by reducing the solvent to ±10 mL. The solution was left to cool to Rt. After cooling, colourless needles were obtained.

Melting point: 160-162 °C. ***IR (ν/cm^{-})^{1}:*** 3046.79(ν (=C-H), w), 2573.82 (ν (alkane, C-H, stretch), asymm, w), 1674.27, 1584.64, 1572.53 (ν (C=C aromatic), m), 1479.35, 1434.12 (ν (C=C aromatic), m), 1382.60 (s), 1315.99, 1285.57 (s), 1184.52-843.55 (ν (aromatic, C-H bend, meta), s), 740.73, 690.76 (ν (aromatic, C-H bend, ortho),m***). ^{1}H NMR ($CDCl_3$, 400 MHz) δ (ppm):*** 7.293-7.105 (m, 45H, Ar-H). ***^{13}C NMR ($CDCl_3$, 100 MHz) δ (ppm):*** 134.08 (d), 133.92 (d), 133.54 (d), 133.37 (d), 129.61 (s), 128.64 (d), 128.55 (d, aromatic carbon).

^{31}P NMR (161 MHz, $CDCl_3$) δ (ppm): 2.40 (single peak). ***Elemental analysis:*** $C_{54}H_{45}AgBrP_3$: Calculated: C, 66.55%; H, 4.65%. Found: C, 66.41%; H, 4.50%.

Synthesis of 1:3 [Silver(I) chloride tris(4-chlorophenyl) phosphine [AgCl {$(pClC_6H_4)_3P$}$_3$]] **(UJ2)**

AgCl salt (0.0444 g, 0.31 mmol) was added to a solution of tris(4-chlorophenyl)phosphine (0.340 g, 0.93 mmol) in acetonitrile (50 mL). The solution was heated under reflux overnight. The hot solution was filtered and evaporated to ±10 mL. Thereafter, the solution was left to crystallize at Rt for 24 hr. The supernatant was discarded, and the crystals were washed twice with 2 mL acetonitrile followed by drying under a vacuum. ***Melting Point:*** 264-266 °C. ***IR (v/cm^{-1}):*** 3050.52(ν (=C-H), w), 1896.66 (ν (alkane, C-H, stretch), asymm, w), 1477.07, 1384.33 (ν (C=C aromatic), m), 1178.84 (s), 1179.19 (s), 1011.60-810.96 (ν (aromatic, C-H bend, meta), s), 744.28, 703.09 (ν (aromatic, C-H bend, ortho),m). ***^{1}H NMR ($CDCl_3$, 400 MHz) δ (ppm):*** 7.281-7.228 (m, 36H, Ar-H). ***^{13}C-NMR ($CDCl_3$, 100 MHz) δ (ppm):*** 136.65 (s), 135.01 (d) 134.83 (d), 131.74 (d), 131.32 (d), 129.26 (d), 129.17 (d, aromatic carbon). ***^{31}P NMR ($CDCl_3$, 161 MHz) δ (ppm):*** -1.39 (single peak). ***Elemental analysis:*** $C_{55}H_{36}AgCl_{10}P_3$: Calculated: C, 52.3%; H, 2.93%. Found: C, 52.10%; H, 2.82%.

Synthesis of 1:2 [Silver(I) thiocyanate 4-methoxyphenyl phosphine [AgSCN{P(4-$MeOC_6H_4)_3$}$_2$]$_2$] **(UJ3)**

Synthesis and characterisation of UJ3 have been reported previously (Ferreira *et al.*, 2015).

Synthesis of 1:3 [Silver(I) benzyldiphenylphosphine]NO_3 (**UJ50**)

Solid $AgNO_3$ (0.1207 g; 0.71 mmol) was added to a solution of benzyldiphenylphosphine (0.5885 g and 2.13 mmol) in acetonitrile (50 mL). The solution was heated under reflux overnight, then filtered and allowed to reduce until approximately 10 mL. This solution was left to crystallize for 24 hr at Rt, from which small white needle crystals were isolated.

Melting point: 232 - 234°C. ***IR (v/cm^{-1}):*** 3049.09 (ν (=C-H),w), 2360.48, 2342.81 (ν (alkane, C-H, stretch), asymm, w), 1734.12, 1700.27, 1684.27, 1653.02, 1635.50 (w), 1558.54, 1539.52, 1506.83, (ν (aromatic, C=C aromatic, m), 1495.87, 1453.32, 1436.07, 1387.21, 1304.37 (ν (C=C aromatic), m), 1219.11 (s), 1182.54 - 833.31 (ν (aromatic, C-H bend, meta), s), 771.37, 752.84, 743.27, 692.76 (ν (aromatic, C-H bend, ortho), m). ***^{1}H-NMR (400 MHz, $CDCl_3$) δ ppm:*** 3.57 (s, 6H, CH_2), 6.953 - 7.423 (m, 54H, Ar-H). ***^{13}C{H}-NMR (100 MHz, $CDCl_3$) δ ppm:*** 135.09, 133.25, 133.09, 132.48, 132.29, 131.83, 131.23, 131.14,

130.29, 129.60, 129.54, 128.83, 128.74, 128.56, 128.54, 128.43, 126.66, 126.63 (s, Aromatic Carbon), 35.31, 35.24 (s, 6-CH_2). ***^{31}P{H} NMR (161 MHz, $CDCl_3$) δ ppm:*** 9.24 (Single Peak). ***Elemental Analysis*:** Calculated for $C_{57}H_{51}AgNO_3P_3$: C, 68.54%; H, 5.15%; Ag, 10.80%; N, 1.40%; O, 4.81%; P, 9.30%. Found: C, 68.34%; H, 4.88%; N, 1.71%.

Synthesis of 1:3 [Silver(I)dicyclohexylphenylphosphine]SCN (**UJ92**)

AgSCN salt (0.1014 g; 0.611 mmol) was added to dicyclohexylphenylphosphine (0.503 g and 1.833 mmol) in acetonitrile (50 mL). The solution was heated under reflux overnight, then filtered and reduced to ±10 mL and left to crystalize from which small white needles were isolated.

Melting point*:** 188 - 191˚C. ***IR (v/cm^{-1}): 2923.11, 2845.75 (ν (=C-H), w), 2063.40 (ν(SCN), s), 1481.50, 1445.47, 1432.88 (ν (aromatic, C-H bend, meta), s), 1000.16, 916.63, 886.47, 848.80, 817.80 (ν (aromatic, C-H bend, meta), s), 746.09, 728.52, 696.77 (ν (aromatic, C-H bend, ortho), m). ***^{1}H-NMR (400 MHz, $CDCl_3$) δ ppm:*** 1.079 – 1.451 (m, cyclohexyl H), 1.615 (s, cyclohexyl H), 1.705 (d, cyclohexyl H), 1.836 (d, cyclohexyl H), 2.053 (d, cyclohexyl H), 2.317 (t, cyclohexyl H), 7.369 (t, aromatic H), 7.388 (d, aromatic H), 7.405 (s, aromatic H), 7.439 (t, aromatic H), 7.457 (t, aromatic H), 7.569 (d, aromatic H). ***^{13}C{H}-NMR (100 MHz, $CDCl_3$) δ ppm:*** 25.88 – 32.50 (s, cyclohexyl C), 128.5 – 135 (3 singlets, aromatic C). ***^{31}P{H} NMR (161 MHz, $CDCl_3$) δ ppm:*** 24.58 (s). ***Elemental Analysis*:** Calculated for $C_{55}H_{81}AgNP_3S$: C, 66.79%; H, 8.25%; Ag, 10.91%; N, 1.42%; P, 9.39%; S, 3.24%. Found: C, 62.50%; H, 7.87%; N, 1.93%; S, 4.63%.

Synthesis of 1:3 [Silver(I) diphenyl-2-pyridylphosphine]Br (**UJ102**)

AgBr salt (0.1333 g; 0.71 mmol) was added to diphenyl-2-pyridyl phosphine (0.561 g and 2.13 mmol) in acetonitrile (50 mL). The solution was heated under reflux overnight. The hot solution was filtered, and the solvent was reduced to ±10 mL and left to crystalize from which small white needles were isolated.

Melting point*:** 183 - 186˚C. ***IR (v/cm^{-1}): 1569.99, 1479.34, 1448.83, 1433.24, 1417.92 (ν (aromatic, C-H bend, meta), s), 1277.34, 1151.29, (ν, C-N), 1092.28, 1046.53, 1028.20, 997.43, 987.26 (ν (aromatic, C-H bend, meta), s), 742.47, 720.25, 691.33, 617.77, 521.03 (ν (aromatic, C-H bend, ortho), m). ***^{1}H-NMR (400 MHz, $CDCl_3$)* δ ppm:** 7.140 – 7.183 (m, aromatic H), 7.251 – 7.295 (m, aromatic H), 7.337 – 7.377 (m, aromatic H), 7.476 – 7.548 (m, aromatic H). ***^{13}C{H}-NMR (100 MHz, $CDCl_3$) δ ppm:*** 123.100 (s, aromatic C), 128.589 (d, aromatic C), 129.507 (s, aromatic C), 129.731 (d, aromatic C), 133.245 (d, aromatic C),

134.331 (d, aromatic C), 135.872 (d, aromatic C), 150.377 (d, pyridyl C), 159.800 (s, pyridyl C), 160.106 (pyridyl C). ***^{31}P{H} NMR (161 MHz, CDCl$_3$) δ ppm:*** 3.63 (s). ***Elemental Analysis*:** Calculated for $C_{51}H_{42}AgBrN_3P_3$: C, 62.66%; H, 4.33%; Ag, 11.03%; Br, 8.17%; N, 4.30%; P, 9.51%. Found: C, 62.84%; H, 4.37%; N, 4.42%.

Synthesis of 1:3 [Sliver(I) tris-(4-methoxyphenyl)phosphine]AgNO$_3$ (**UJ115**)

$AgNO_3$ (0.0527 g; 0.31 mmol) was added to tris-(4-methoxyphenyl)phosphine (0.3277 g and 0.93 mmol) in acetonitrile (50 mL). The solution was heated under reflux overnight, then filtered and reduced to ±10 mL and left to crystalize from which small white needles were isolated.

Melting point*:** 208 - 209°C. ***IR (ν/cm^{-1}): 2837.16 (ν (=C-H),w), 1592.55, 1567.65, 1498.15, 1457.54, 1405.13 (ν (C=C aromatic), s), 1286.17, 1247.93, 1176.58, 1095.68, 1021.68 (ν (aromatic, C-H bend, meta), s), 819.17, 797.05, 772.48, 720.04 (ν (aromatic, C-H bend, ortho), s***). ^{1}H-NMR (400 MHz, CDCl$_3$) δ ppm:*** 3.789 (s, OCH_3), 6.719 (d, aromatic H), 7.106-7.153 (m, aromatic H). ***^{13}C{H}-NMR (100 MHz, CDCl$_3$) δ ppm:,*** 55.25 (s, OCH_3), 113.96 (d, aromatic), 114.45 (d, aromatic), 123.78 (d, aromatic), 133.88 (d, aromatic), 135.19 (d, aromatic), 161.04 (s, aromatic). ***^{31}P{H} NMR (161 MHz, CDCl$_3$) δ ppm:*** 3.75 (s). ***Elemental Analysis*:** Calculated for $C_{18}H_{21}AgNO_3P$: C, 61.67%; H, 5.18%; N, 1.14%. Found: C, 61.88%; H, 5.38%; N, 1.15%.

Synthesis of 1:4 [Sliver(I) tris-(4-methoxyphenyl)phosphine]AgNO$_3$ (**UJ116**)

$AgNO_3$ (0.0527 g; 0.31 mmol) was added to tris-(4-methoxyphenyl)phosphine (0.4369 g and 1.24 mmol) in acetonitrile (50 mL). The solution was heated under reflux overnight, then filtered and reduced to ±10 mL and left to crystalize from which small white needles were isolated.

Melting point: 161-163°C. ***IR (ν/cm^{-1}):*** 2836.33 (ν (=C-H),w), 1591.04, 1566.53, 1497.40, 1456.31, 1440.70, 1401.98, 1339.82 (ν (C=C aromatic), s), 1284.40, 1250.69, 1220.82, 1174.80, 1094.88, 1018.82 (ν (aromatic, C-H bend, meta), s), 826.83, 797.08, 772.21 (ν (aromatic, C-H bend, ortho), s). ***^{1}H-NMR (400 MHz, CDCl$_3$) δ ppm:*** 3.783 (s, OCH_3), 6.672 (d, aromatic H), 7.029-7.075 (m, aromatic H). ***^{13}C{H}-NMR (100 MHz, CDCl3) δ ppm:*** 55.42 (s, OCH3), 114.10 (d, aromatic C), 114.56 (d, aromatic C), 116.33 (d, aromatic C), 124.13 (t, aromatic C), 125.23 (s, aromatic C), 134.00 (d, aromatic C), 135.36 (d, aromatic C), 136.09 (d, aromatic C), 161.14 (s, aromatic C), 162.44 (d, aromatic C). ***^{31}P{H} NMR (161***

MHz, $CDCl_3$) δ ppm: 1.51 (s). ***Elemental Analysis*:** Calculated for $C_{18}H_{21}AgNO_3P$: C, 63.88%; H, 5.36%; N, 0.89%. Found: C, 62.79%; H, 5.46%; N, 094%.

Synthesis of 1:2 [Sliver(I) tris-(4-methoxyphenyl)phosphine]Cl (**UJ118**)

AgCl (0.0444 g; 0.31 mmol) was added to tris-(4-methoxyphenyl)phosphine (0.2184 g and 0.62 mmol) in acetonitrile (50 mL). The solution was heated under reflux overnight, then filtered and reduced to ±10 mL and left to crystalize from which small white needles were isolated.

Melting point*:** 183-185°C. ***IR (v/cm^{-1}): 2834.73 (ν (=C-H), w), 1590.65, 1568.30, 1496.78, 1457.17, 1440.32, 1403.07 (ν (C=C aromatic), s), 1283.37, 1245.25, 1175.79, 1097.94, 1025.18 (ν (aromatic, C-H bend, meta), s), 822.75, 769.67, 772.44 (ν (aromatic, C-H bend, ortho), s). ***^{1}H-NMR (400 MHz, $CDCl_3$) δ ppm:*** 3.798 (s, OCH_3), 6.829 (dd, aromatic H), 7.332-7.380 (m, aromatic H). ***^{13}C{H}-NMR (100 MHz, $CDCl_3$) δ ppm:*** 55.24 (s, OCH_3), 114.44 (d, aromatic), 123.72 (d, aromatic), 135.35 (d, aromatic), 161.10 (s, aromatic). ***^{31}P{H} NMR (161 MHz, $CDCl_3$) δ ppm:*** 4.75 (s). ***Elemental Analysis*:** Calculated for $C_{18}H_{21}AgNO_3P$: C, 59.48%; H, 4.99%. Found: C, 59.44%; H, 4.91%.

Appendix D: Toxicity of silver(I) phosphine complexes on BC and non-malignant cell lines

Table D1 Percentage viability of BC (MCF-7 and MDA-MB-231) and non-malignant (HDF-a, MRHF-1 and HEK-293) cell lines treated with 10 µM of silver(I) phosphine complexes for 24 hr. Values were calculated as a percentage of the VC (1% DMSO, set at 100%).

Treatment	Viability (%)				
	Cell line				
	MCF-7	MDA-MB-231	HDF-a	MRHF-1	HEK-293
UJ1	±25[a]	55.82	±90[a]	-	±45[a]
UJ2	±40[a]	115.07	±100[a]	-	±65[a]
UJ3	36.01[b]	89.44[b]	-	86.57[b]	61.94[b]
UJ50	6.82[c]	52.13[c]	-	108.73[c]	94.13[c]
UJ92	14.70[c]	32.21[c]	-	95.79[c]	92.03[c]
UJ102	42.21[c]	38.88[c]	-	93.94[c]	85.89[c]
UJ115	37.68[d]	48.59[d]	-	105.98[d]	93.27[d]
UJ116	32[d]	48.42[d]	-	95.67[d]	95.62[d]
UJ118	28[d]	50.82[d]	-	97.06[d]	75.12[d]

[a] Ferreria E., (2015), Silver(I) phosphine compounds selectively induce apoptosis in MCF-7 breast cancer cells, Ph.D. Thesis, University of Johannesburg, South Africa

[b] Badal, A., (2022), The mechanistic action of silver(I) thiocyanate 4-methoxyphenyl phosphine promoting apoptosis in MCF-7 and MDA-MB-231 breast cancer cell lines, M.Sc. Dissertation, University of the Witwatersrand, South Africa

[c] Roberts K.E., (2023), Insights into silver(I) phosphine complexes in targeting cell death and metastatic mechanisms in malignant cell lines, Ph.D. Thesis, University of the Witwatersrand, South Africa

[d] Engelbrecht Z., (20 July, 2023), Personal communication